POLYCISTRONIC HSV VECTORS FOR THE DIFFERENTIATION OF EMBRYONIC STEM CELLS TOWARD A CARDIAC LINEAGE

by

Lillian Louise Laemmle

Bachelor of Science, Pennsylvania State University, 2000

Submitted to the Graduate Faculty of

The School of Medicine in partial fulfillment

of the requirements for the degree of

Doctor of Philosophy

University of Pittsburgh

2015

UNIVERSITY OF PITTSBURGH

SCHOOL OF MEDICINE

This dissertation was presented

by

Lillian Louise Laemmle

It was defended on

April 20, 2015

and approved by

J. Richard Chaillet, MD, PhD Associate Professor, Microbiology and Molecular Genetics

Neal A. DeLuca, PhD, Professor, Microbiology and Molecular Genetics

Thomas E. Smithgall, PhD, Professor and Chair, Microbiology and Molecular Genetics

Michael Tsang, PhD, Associate Professor, Developmental Biology

Dissertation Advisor: Joseph C. Glorioso III, PhD, Professor, Microbiology and Molecular Genetics

POLYCISTRONIC HSV VECTORS FOR THE DIFFERENTIATION OF EMBRYONIC STEM CELLS TOWARD A CARDIAC LINEAGE

Lillian Laemmle, PhD

University of Pittsburgh, 2015

Cardiovascular disease is the leading cause of death in developed countries, but we lack the ability to regenerate cardiac tissue. Cell-based therapy holds promise to repopulate a damaged heart with functional cardiomyocytes. Developing technologies to produce cells for transplantation is key to the success of this approach. Pluripotent stem cells (PSC) are an ideal starting material for cell-based therapies because they can be expanded indefinitely in culture and their plasticity gives them the potential to regenerate any tissue or organ. The issue of teratoma formation in the host may be avoided by devising methods to differentiate PSC toward a desired lineage before transplantation. Because the heart is vital for life, and the biggest source of human morbidity and mortality, in vitro differentiation of PSC into cardiomyocytes for cell-based treatment of heart disease is an area of intense research.

Exogenous expression of vital cardiogenic genes in PSC can be a powerful tool. Transduction of PSC with recombinant viral vectors can deliver genes to activate cardiac programming and drive differentiation toward a cardiac lineage. Replication defective HSV vectors efficiently transduce PSC and can be engineered to express genes that alter the cellular differentiation program. The goal of this research was to develop highly defective HSV vectors to express multiple cardiac transcription factors in embryonic stem cells to increase their cardiogenic potential. Vectors vββG4Nk, vG4Nk, and vGTM were engineered to express *GATA4 and NKX2.5 or GATA4, TBX5, and MEF2c* in PSC with high efficiency and low toxicity.

Transduction of mESC with these vectors induced the expression of endogenous genes that are vital for cardiogenesis. Differentiation of mESC transduced with cardiogenic HSV vectors had a positive impact on terminal cardiomyocyte differentiation, producing many more embryoid bodies with beating cardiomyocytes than those transduced with control vectors. In addition, we found that delaying the drastic dilution of viral genomes that occurs over the time interval to terminal differentiation could enhance the outcome. Our results indicate that infection of mESC with cardiogenic HSV vectors has long reaching effects on mESC differentiation, supporting the suggestion that HSV vectors can be a useful tool for producing lineage related changes in differentiating PSC to generate specialized cell types.

TABLE OF CONTENTS

LIST OF TABLES

LIST OF FIGURES

PREFACE

The work presented in this dissertation would not have been possible without the support of my mentor Dr. Joseph Glorioso. His passion for translational science and the use of HSV as a multifunctional gene delivery tool inspired me throughout my graduate career and I would like to express my deepest gratitude to him for his consistent encouragement and optimism. I am also profoundly thankful to members of the Glorioso lab, past and present. Dr. April Craft shared with me all of her knowledge about growing HSV vectors, cell culture, and how to maintain and differentiate embryonic stem cells during my first months in the Glorioso lab. Dr. Justus Cohen taught me so much about designing vectors and experiments, interpreting data, and writing more effectively and precisely. I am certainly a better scientist due in no small part to his encouragement and guidance. I thank Drs. Bonnie Reinhart, Marco Marzulli, Daniela Leronni, and Yoshitaka Miyagawa for answering all of my many questions, helping me when my experiments went wrong or I needed to learn a new technique, or for giving me a shoulder to cry on or a good laugh when I was having a bad day. I would also like to thank Dr. William Goins who is an encyclopedia of knowledge about HSV and many of the materials and techniques used in the Glorioso lab. He is extraordinarily generous with his time and always made himself available to help me and answer my questions.

I want to offer my most sincere gratitude to my family for everything they have done to make it possible for me to achieve my dream of completing graduate school. My mom is one of

the best people I know and has spent countless hours watching my boys when they were sick or their schools were closed so that I could go to the lab without worry. She has been the perfect mom to me in every way and an excellent role model as a strong, intelligent, and generous woman and mother as well as the most wonderful Granny to my sons. My dad, Dr. Joseph Laemmle, was the first and only person in our family to earn a PhD, and has always supported me and strongly encouraged me to complete graduate school. When I decided that I needed a break from academia after finishing my BS, he told me that once I had a good career and a nice home, I would never be able to give that up to go back to school full time. I am happy to prove him wrong! Finally and most importantly, I want to express my profound appreciation and gratitude to my husband Peter. He and our sons Erik and Finn have enriched my life in more ways than I can say or understand. Peter has wholeheartedly supported me from the moment I applied to graduate school, through the ups and downs of laboratory research, and the intense focus of my final months preparing for graduation. I am so grateful for his patience and dedication in taking care of our children to give me the time I needed, day, night, or weekend, so that I could do my best to succeed.

ABBREVIATIONS

2A	ribosomal skipping sequence
4BLA	Vero cells that express ICP4 upon HSV infection
7B	Vero cells that express ICP4 and ICP27 upon HSV infection
AAV	adeno-associated virus
ACE	angiotensin-converting enzyme
ara-c	cytosine β-D-arabinofuranoside
bFGF	basic fibroblast growth factor
bGHpA	bovine growth hormone polyadenylation signal
BMMNC	bone marrow mononuclear cells
BMP	bone morphogenetic protein
bp	base pairs
CAGp	CMV early enhancer/chicken β actin promoter
cm^R	chloramphenicol resistance gene
CPE	cytopathic effects
cTnI	cardiac troponin I
cTnT	cardiac troponin T
CVD	cardiovascular disease
EB	embryoid body
EF1αp	elongation factor-1 alpha promoter
ESC	embryonic stem cells
FHF	first heart field
FIGE	field inversion gel electrophoresis
G4	GATA4
G4Nk	GATA4 and Nkx2.5
GTM	GATA4, Tbx5, and Mef2c
gc	genome copies
hESC	human embryonic stem cells
HSC	hematopoietic stem cells
HSV-1	herpes simplex virus type 1
ICP	infected cell protein
iPSC	induced pluripotent stem cells
JΔNI8eGFP	JΔNI8GFPΔcherry
kan^R	kanamycin resistance gene
kb	kilobase
kDa	kilodalton
LAT	latency associated transcript

LIF	leukemia inhibitory factor
LV	left ventricle
LVAD	left ventricular assist device
LVEF	left ventricular ejection fraction
mESC	mouse embryonic stem cells
MI	myocardial infarction
MLC2a	myosin light chain 2a
MOI	multiplicity of infection
MSC	mesenchymal stem cells
Nk	Nkx2.5
Ø	mock/control
Ø EB	embryoid bodies made from mock infected mESC
ORF	open reading frame
PCR	polymerase chain reaction
pfu	plaque forming units
PS	primitive streak
PSC	pluripotent stem cells
qRT-PCR	quantitative real time polymerase chain reaction
rbGpA	rabbit beta globin polyadenylation signal
SDS-PAGE	sodium dodecyl sulfate poly-acrylamide gel electrophoresis
SHF	second heart field
U2OS	human osteosarcoma cells
U2OS-ICP4/27	U2OS cells that express ICP4 and ICP27 upon HSV infection
UbCp	ubiquitin C promoter
U_L	unique long segment of HSV-1 genome
U_S	unique short segment of HSV-1 genome
vG4Nk	HSV vector JΔNI8G4NkeGFP
vG4Nk EB	embryoid bodies made from JΔNI8G4NkeGFP-infected mESC
vGFP	HSV vector JΔNI8eGFPΔcherry
vGFP EB	embryoid bodies made from JΔNI8eGFP-infected mESC
vGTM	HSV vector JΔNI8GTMeGFP
vGTM EB	embryoid bodies made from JΔNI8GTMeGFP-infected mESC
α/IE	HSV-1 immediate early gene
α-MHC	alpha myosin heavy chain
β/E	HSV-1 early gene
vββG4Nk	HSV vector JDββG4NkmCh
vββG4Nk EB	embryoid bodies made from JDββG4NkmCh-infected mESC
JDββHE EB	embryoid bodies made from JDββHE-infected mESC
Δ	deleted

1.0 INTRODUCTION

1.1 CARDIAC DEVELOPMENT

The heart is the first organ to function during embryonic development. From the earliest stages of embryogenesis through adulthood, the life of all animals depends on uninterrupted cardiac function. The cellular and molecular events that occur during heart development, and its function and gene expression through adulthood, are highly conserved among mammals. Specific manipulations in mice, including gene knockouts, reporter genes to define differentiation related events, cell grafts to evaluate cellular function, and explant cultures to examine molecular genetics, are used to elucidate the events involved in mammalian cardiogenesis. Understanding the development and operation of the heart is vital for learning about the pathology of and devising treatments for congenital and acquired cardiac diseases. Following gene expression and cell signaling patterns through the earliest stages of embryonic cardiogenesis all the way to committed heart cell types in vivo enables us to influence these events in vitro to generate cardiomyocytes from pluripotent stem cells or, more recently, to transdifferentiate other committed cell types into cardiomyocytes both in vitro and in vivo.

1.1.1 Embryonic cardiogenesis

Commitment of a subset of embryonic cells to cardiogenesis is one of the earliest events to occur in a developing embryo. Cell fate mapping experiments in mouse embryos demonstrated that cardiac precursor cells are found prior to gastrulation, a process that begins with the appearance of the primitive streak (PS) around mouse embryonic day E5 (*1*). Brachyury expression marks PS formation (*2*), which establishes bilateral symmetry in the embryo and determines the site of gastrulation, the formation of the three germ layers (endoderm, mesoderm, and ectoderm). Timing and location of cellular ingression through the PS determines the fate of gastrulating cells. A subset of epiblast cells moves as a sheet through the PS, undergoing epithelial-to-mesenchymal transition and forming the mesendoderm. Cardiac mesoderm progenitors migrate to an anterior lateral region relative to the PS to form the splanchnic mesoderm. At mouse embryonic day E7.5 (roughly week 2 of human gestation), these mesodermal cells underlying the head folds, called the first heart field (FHF), form the cardiac crescent (*3*). The crescent fuses at the midline on E8 (3 weeks human gestation) to form the beating cardiac tube, which then undergoes a rightward looping and rapid growth to form an S-shaped structure. The cardiac crescent grows through cell proliferation and recruitment of additional cells called the secondary heart field (SHF) (*4*), and undergoes a series of rearrangements that ultimately leads to the formation of the recognizable four-chambered septated heart by E14.5 (approximately 7 weeks human gestation).

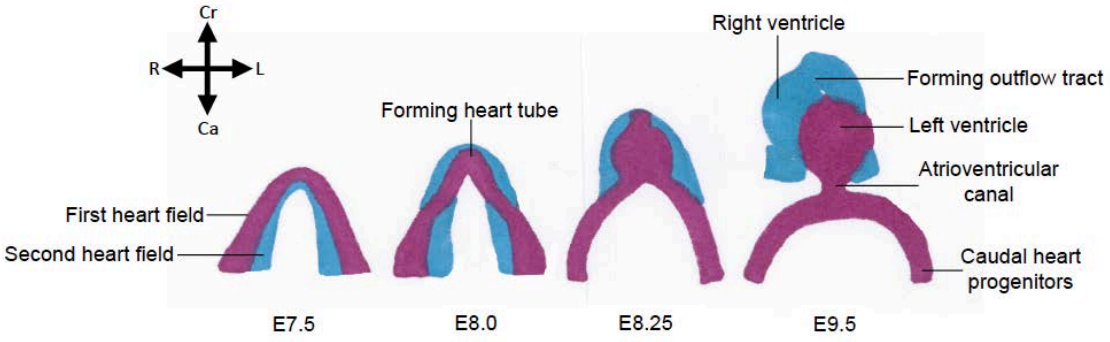

Figure 1. Formation of the cardiac crescent and rearrangements to form the embryonic heart
The cardiac crescent forms at the cranial side of the 7.5 day old mouse embryo. Contributions from the first heart field are shown in red and the second heart field in blue. Cr – cranial; Ca – caudal; R – right; L – left.

Following septation, the heart chambers continue to grow while complex differentiation programs take place to generate the additional smooth muscle cells, pacemakers, fibroblasts, cardiomyocytes, endothelial cells, and conducting cells that compose the mature heart (*5*).

1.1.2 Molecular events driving cardiogenesis

Cardiac lineage specification is initially driven largely by a gradient of signaling molecules established very early during embryogenesis. Transforming growth factor (TGF)β family members Nodal and Activin work together with the Wnt/β-catenin pathway to specify the formation of the mesendoderm in developing embryos (*6*). Bone morphogenetic protein (BMP)2,

another TGFβ family member, is vital for the induction of cardiac mesoderm (*7*), and BMP2-deficient mice are non-viable, suffering from severe cardiac defects (*8*). The critical balance between BMP2 and Nodal is tightly regulated by Wnt/β-catenin signaling in the PS (Figure 2). Dysregulation of the BMP/Smad vs. Nodal balance causes a defect in the laterality in the heart-forming region (*9*).

Figure 2. BMP and Wnt expression in the early embryo
Around mouse embryonic day E5, gradients of BMP, Wnt, and Wnt inhibitors form to create the primitive streak (PS) and initiate cardiogenesis in the correct location of the developing embryo. BMP induces formation of the precardiac mesoderm while Wnt inhibits cardiac formation in other parts of the embryo.

The proximal-distal gradient of Nodal/Smad plays a vital role in the segregation of the endoderm and mesoderm and regulates expression of the transcription factors *OCT4* and *EOMES* (*10*). *OCT4* is vital for cardiac specification and targets *SOX17*, another transcription factor required in early cardiogenesis (*11*). The first mesodermal lineage to emerge expresses the transmembrane

receptor VEGF-R2 (mouse gene *Flk-1*, human gene *KDR*) in response to BMP4 signaling, which also induces expression of the zinc finger transcription factors *GATA4/5/6* in the precardiac mesoderm (*12*). GATA4 is widely regarded as the master regulator of cardiogenesis, binding to the promoters of many cardiac-specific genes to switch on their expression, and *GATA4* null mice do not develop a heart and die in utero (*13*). GATA4 is expressed in the embryonic myocardium throughout development and into adulthood (Figure 4) (*14*). GATA sites are frequently present along with Smad sites on the enhancers of cardiac genes, including the early expressed *NKX2.5*, underscoring the vital role of BMP signaling in embryonic cardiac development (Figure 3) (*15*). Introduction of the BMP antagonist Noggin to pre-cardiac mesoderm inhibits cardiomyogenesis and expression of cardiac marker genes *GATA4, NKX2.5, MEF2A, eHAND,* and *VMHC1* (*7*).

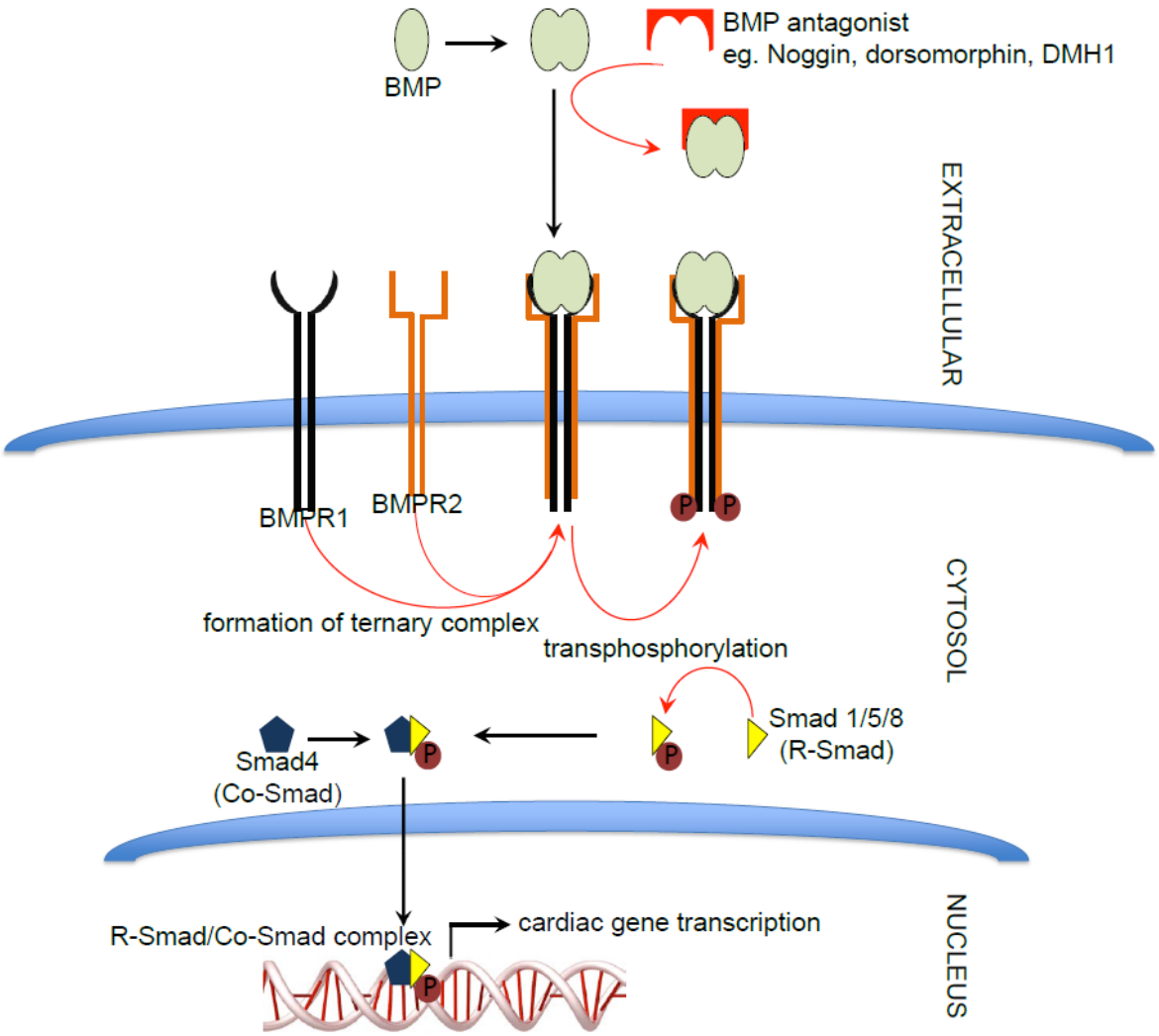

Figure 3. Cardiac gene transcription is activated through BMP/Smad signaling
BMP expression and signaling in the developing embryo is vital for embryonic patterning and formation of the heart. BMPs form active dimers and bind to BMP receptors (BMPR), driving the formation of the ternary complex consisting of two type 1 and two type 2 BMP receptor subunits and their bound BMPs. Type 2 BMPRs phosphorylate type 1 BMPRs, which in turn phosphorylate and activate R-Smad. Phosphorylated R-Smad forms a complex with Co-Smad that is transported to the nucleus where it binds to promoters/enhancers and activates the transcription of cardiogenic genes.

As *Flk-1/KDR* expression decreases, the mesoderm is patterned into distinct subsets and mesoderm posterior 1 (Mesp1) is expressed. Mesp1 functions to promote activation of the cardiogenic transcriptional network as mesodermal cells ingress through the PS (*16*). The cardiac crescent begins to organize and FHF progenitors begin to differentiate into committed myocardial cell types through their exposure to cytokines of the BMP (*17*) and FGF (*18*) families and inhibitors of the Wnt pathway (*19*). Expression of T-box transcription factor 5 (Tbx5) and contractile proteins like myosin light chain-2a (MLC2a) follows as the linear heart tube forms and begins to beat.

The SHF, marked by expression of the LIM-homeodomain transcription factor ISL1, is activated through FGF, SHH, and canonical Wnt signaling (*20*). ISL1 function is required for proliferation and migration of SHF cells to the primitive heart tube, and its expression is suppressed as the cardiac progenitor cells reach the developing heart and begin to differentiate in response to BMP, Notch, and non-canonical Wnt signaling (*21*).

As the heart tube begins to loop and rearrange to form its four septated chambers, transcription of a whole host of other transcription factors and cardiac-specific genes is initiated by GATA4, MESP1, HAND2, NKX2.5, MEF2C, MYOCD, and TBX5 among others. These transcription factors give rise to the expression of all of the structural and functional cardiac proteins, including cardiac troponin T, α-myosin heavy chain (α-MHC), myosin light chain 2a and 2v, and α-actinin.

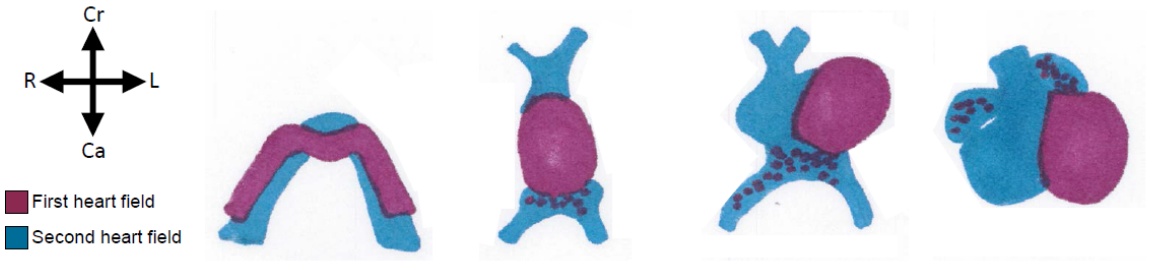

Stage	Cardiac Crescent	Linear Heart Tube	Looping Heart	Chamber Specialization/ Septation
Mouse Embryo Stage	E7.5	E8	E9-12	E10+
Human Embryo Stage	Day 15	Day 20	Day 28-30	Day 32+
Key Regulators	GATA4 NKX2.5 MESP1/2 ISL1 BAF60C MEF2C	GATA4 NKX2.5 TBX5 TBX20 MEF2C	GATA4 NKX2.5 TBX5 MEF2C HAND1/2	GATA4 NKX2.5 TBX5 PITX2 TBX1

Figure 4. Key regulators of embryonic cardiomyogenesis
Expression of cardiac transcription factors at different times throughout heart formation guide the differentiation of cardiac progenitors into specialized cardiac cell types. Cr – cranial; Ca – caudal; R – right; L – left.

1.2 CARDIOVASCULAR DISEASE

Cardiovascular disease (CVD) remains the largest cause of global morbidity and mortality, particularly in developed nations. One American dies from CVD every 40 seconds with a total annual cost in the United States of an estimated $315.4 billion, over $100 billion more than all cancers and benign neoplasms combined (*22*). While CVD encompasses a wide range of medical problems relating to the cardiovascular system, ischemic heart disease, a restriction of blood flow to the heart, is by far the most pervasive (*22*). Myocardial infarction (MI) is typically a result of atherosclerosis, the build-up of plaque, causing blockage of the coronary arteries. The

resulting loss of blood flow permanently damages the patient's heart, leading to arrhythmia, chronic heart disease, and sometimes death. Unlike many organs, the adult mammalian heart lacks significant inherent regenerative capacity (*23*). During a large MI, 10^8 to 10^9 functional cardiomyocytes are lost to apoptosis or necrosis (*24*) and the function of the post-infarcted heart deteriorates over time (*25*). The lost cells are replaced by scar tissue consisting mainly of fibroblasts that do not contribute to and further inhibit cardiac function. Advances have been made in the treatment of ischemic heart disease, including the use of angiotensin-converting enzyme (ACE) inhibitors and β-adrenergic blockers to improve cardiac function (*26*). Left ventricular assist devices (LVAD) can act as a bridge treatment to heart transplant, or as a destination treatment in patients who are terminally ill and/or do not qualify for transplantation, by pumping blood out of the left ventricle to support normal circulation (*27*). While currently available treatments improve the prognosis and quality of life for patients suffering from heart disease, they lack the ability to regenerate the functional cardiac tissue that has been damaged or lost. The only currently established method to cure a patient with severe heart damage is heart transplantation, an option that is not viable in most cases due to poor overall health of the patient, the extremely limited availability of donor organs, and the requirement for lifelong intense immunosuppressive therapy following transplant. Cell-based therapy for the treatment of CVD is a promising alternative, and has become an increasingly popular area of study in recent years. Cell-based therapy aims to repopulate a damaged heart with functional cardiomyocytes to physically heal the heart instead of merely alleviating the symptoms of CVD. Laboratories have published data on transplantation of numerous different cell types into animal models and later humans who have suffered myocardial infarction (MI) with mixed and often conflicting results. There are many variables that must be considered before cell-based therapy can become a

standard treatment for diseased and damaged hearts, and careful consideration of the data with longer-term follow-up is an absolute necessity. For example, Laflamme et al. reported significant improvement in cardiac function after four weeks in a rat model of MI upon injection of hESC-derived cardiomyocytes (*28*), but Mummery et al. followed a similar protocol in mice with a three month follow-up, and found that while at four weeks the transplanted cells survived and significantly improved cardiac function, by three months there was no significant functional improvement (*29*).

The type of cells transplanted is a critical factor in the ultimate success of the cell-based approach to treatment of CVD. Early studies focused on transplantation of committed cells with promising results, including skeletal myoblasts (*30*) and fetal cardiomyoblasts (*31*), but these types of cells are limited in availability and not practical for extensive clinical use, leading focus to shift towards stem cells and their derivatives.

1.3 STEM CELLS

Stem cells possess two defining characteristics: the ability to self renew, or divide symmetrically to create new stem cells, and the ability to divide asymmetrically to differentiate into other cell types, either into further lineage committed progenitor cells or into terminally differentiated mature cell types. Stem cells can be derived from embryonic tissue (embryonic stem cells, ESC), created through reprogramming of differentiated cell types (induced pluripotent stem cells, iPSC), and found in many organs throughout the adult body. While ESC and iPSC are pluripotent, or able to differentiate into any cell type in the body, adult stem cells are more lineage restricted and considered to be multipotent. More recently, the considerable plasticity of

adult stem cells has been recognized as they are transplanted into other niches and give rise to cell types beyond their perceived lineage restriction (*32-35*).

1.3.1 Adult stem cells and cardiac regenerative therapy

Also known as somatic stem cells, adult stem or progenitor cells are a small sub-population of cells that reside in many tissues and organs throughout the body. They collectively give rise to a large family of descendants with many types of specialized phenotypes that are capable of renewing and repairing organs and tissues. These cells are an attractive option for use in cell-based therapies because they can be autologously derived and have the potential to differentiate into many lineages when transplanted outside of their niche. Bone marrow in particular contains a relatively large reservoir of both hematopoietic stem cells (HSC) and mesenchymal stem cells (MSC). MSC are a useful cell type for regenerative medicine because they are easily expanded in vitro and can form bone, cartilage, tendon, muscle, and fat cells (*36*). MSC have been shown to transdifferentiate into cardiomyocytes in culture in the presence of 5-azacytidine (*37*) or when co-cultured with cardiomyocytes (*38, 39*). Other types of adult stem cells include satellite cells that are responsible for the maintenance of muscle fibers (*40*), epidermal and follicular stem cells that reside in the apical portion of hair follicles and give rise to skin, hair, sebaceous glands, and sweat glands (*41, 42*), and several types of endodermal stem cells that reside near the bottom of each gut crypt and give rise to specialized Paneth, enteroendocrine, goblet, and columnar cells (*43*), among many others.

The presence of cardiac-specific stem cells in the adult mammalian heart remains controversial. While lower vertebrates such as teleosts and amphibians are able to regenerate large parts of their myocardium throughout adulthood (*44*), most mammals, including humans,

cannot. Until recently it was thought that mammalian cardiomyocytes lose the ability to regenerate shortly after birth, but it was discovered that a small portion of these cells can re-enter the cell cycle and divide in adulthood (*45, 46*). Other more recent studies have confirmed that cardiomyocyte turnover occurs throughout the life of mammals, but rate estimates are mostly low and vary widely. One clever study took advantage of the spike of carbon-14 (^{14}C) levels in the atmosphere in the 1950s and 1960s from above ground nuclear testing. The investigators used ^{14}C levels to determine the birth date of cardiomyocytes and showed that at age 25, new cardiomyocytes form in the human heart at a rate of about 1.5% per year, but this rate drops dramatically as we age (*47*). Another group also measured ^{14}C levels to estimate that the rate of cardiomyocyte turnover in adult humans is much higher, between 7-23% per year (*48*), while other groups estimated that the actual value is between 1-2% per year in both adult mice and humans using [^{3}H]thymidine (*49*) and imaging assays (*50*). The fact that terminally differentiated cardiomyocytes can regenerate at all led some to hypothesize that there are resident cardiac stem cells in the adult mammalian heart that give rise to the majority of new cardiomyocytes, although others argue that these regenerated cells are derived solely from mature cardiomyocytes re-entering the mitotic cell cycle. Several groups have identified cells that express c-kit as adult cardiac progenitors (*51, 52*), others claim that expression of just SCA can be used to identify cardiac stem cells (*53*), and still others believe that CD31-/SCA1+ side population cells obtained from FACS analysis of adult heart tissue are the true cardiac stem cells (*54*). Whether or not the adult human heart actually holds a population of stem cells able to regenerate functional cardiomyocytes, it is obvious that the presence of these cells alone is not enough to replenish all of the cells that are lost to apoptosis or necrosis during a cardiac event. Isolating these purported cardiac stem cells and expanding them in vitro to sufficient numbers for clinical trials has proven

difficult, making them impractical as a therapy for mending a wounded heart. Taking this into consideration, along with the apparent safety of transplanted adult progenitor cells, there has been much focus on using other adult stem cells, primarily those derived from bone marrow, for clinical trials of cell-based therapy for the heart.

1.3.2 Adult stem cells and cardiac ischemia: Clinical trials

In an early study, bone marrow mononuclear cells (BMMNC) were injected into the area bordering the site of MI in mice. Visual tracking of the eGFP-expressing BMMNC led to the conclusion that the cells differentiated into functional cardiomyocytes and improved left ventricular (LV) function (*55*). These results were so convincing that very soon after, a similar therapy was attempted with autologously derived BMMNC on a 46 year old human male who had sustained an acute MI, with a significant improvement in cardiac function (*56*). However subsequent studies employing extensive fate tracking of transplanted cells in mice demonstrated that HSC derived from BMMNC do not acquire a cardiac phenotype, suggesting a more cautious interpretation. The eGFP+ cardiomyocytes observed in the Orlic study (*55*) were likely due to autofluorescence, which is common in injured cardiac tissue following MI, or fusion of eGFP+ BMMNC with endogenous cardiomyocytes (*57, 58*). Multiple clinical trials have delivered BMMNC to almost 2000 patients for cardiac repair, and meta-analyses of the data clearly demonstrate that while it is a safe treatment for MI, it is not particularly effective, with only modest clinical improvements and no significant improvement in LV function (*59-61*).

Trials with MSC have also had inconsistent but more positive results. Pre-clinical studies in large animals (swine) showed that autologously-derived MSC robustly engraft in the infarcted heart with modest improvements in cardiac function (*62, 63*). In phase 1/2 clinical trials,

treatment of MI with MSC improved LV function at 3 but not 6 months after MI (*64*), and documented the overall safety of this approach (*65*). Other clinical trials demonstrated that patients injected locally or percutaneously with MSC after MI had global reduction in scarring (*66, 67*). In a clinical trial comparing the efficacy of MSC with BMMNC for treatment of ischemic cardiomyopathy, MSC but not BMMNC reduced infarct size and improved regional myocardial function (*68*). In the PROMETHEUS study, six patients with CVD received injections of autologous MSC and MRI was used to measure scar size, perfusion, wall thickness, and contractility after 0, 3, 6, and 18 months (*69*). While patients showed reduced scar size, contractile improvement, and improved LV function, the results are inconclusive because there was no placebo group, but the improvements observed were very promising. Another interesting approach taken by Bartunek et al. cultured autologously derived MSC with a cytokine cocktail to induce partial cardiogenic differentiation, and delivered these cells by transendocardial injection to more than 30 patients with ischemic heart failure (*70*). LV function was significantly improved in the cell therapy group compared to the placebo group, and patients receiving the primed MSC experienced overall higher scores on numerous clinical parameters. The safety of this approach was also demonstrated by a two year follow-up period with no negative effects from MSC transplantation.

While the use of bone marrow derived adult stem cells appears to be clinically safe in treating cardiac ischemia, the long-term success of this approach is questionable. Some trials describe modest improvements in cardiac function while others do not, but the consensus is that neither HSC derived BMMNC nor MSC transdifferentiate into cardiomyocytes in vivo. Observed clinical improvements in patients receiving these cells are most likely due to indirect mechanisms such as delivery of paracrine factors to improve angiogenesis and vascularization,

and potentially the mobilization of resident cardiac stem cells or cardiomyocytes to partially regenerate damaged cardiac tissue. There is little convincing evidence that adult stem cells can actually differentiate into functional cardiomyocytes in vitro (*66, 71, 72*). Paracrine factors alone are unlikely to be sufficient to restore function to extensively scarred myocardium and diseased cardiac tissue. As an alternative, because ESC and iPSC (collectively pluripotent stem cells, PSC) can differentiate into any cell type, considerable time and effort have been put forth to devise ways to utilize these cells to develop safe and effective clinical therapies for ischemic cardiac disease.

1.3.3 Pluripotent stem cells and cardiac therapy

Embryonic stem cells are derived from the inner cell mass of the blastocyst and are able to grow indefinitely in culture and give rise to cells of all of the three germ layers, endoderm, ectoderm, and mesoderm (*73*). Mouse (murine) ESC (mESC) were first derived by Evans and Martin in 1981 (*74, 75*) and are the best characterized of the PSC. Human ESC (hESC) were first isolated in 1998 (*76*) and have since been at the center of great scientific interest as well as ethical controversy. In 2006, a group in Japan led by Shinya Yamanaka reported that mouse fibroblasts could be reprogrammed to adopt a pluripotent state similar to ESC through the introduction by retroviral transduction of the genes Oct4, Sox2, c-Myc, and Klf4 (*77*). These cells, called induced pluripotent stem cells (iPSC), are functionally identical to mESC with similar morphology, gene expression patterns, capacity for proliferation, and ability to form teratomas. Moreover, mouse iPSC are competent for germline transmission, giving rise to adult chimeras (*78-80*). In 2007, the mouse studies were replicated by expressing the same four factors in human fibroblasts, successfully enabling for the first time the ability to derive autologous

pluripotent stem cells that can be used similarly to hESC without the ethical concerns (*81*). The generation of pluripotent stem cells from somatic cells offers great potential for disease-specific model systems, drug discovery, and the production of individualized regenerative therapeutics (*82*). While c-Myc is linked to cardiovascular gene expression (*83*), strategies to eliminate this proto-oncogene from the original reprogramming Yamanaka factors were immediately explored in order to reduce the oncogenic potential of the reprogramming approach and make iPSC safer for future human therapies. Reprogramming has since been achieved by safer means, without the use of c-Myc (*84*) and through the introduction of the reprogramming factors using non-integrative technologies (*85-88*).

The morphology of PSC is distinct from differentiated cell types. PSC colonies are very round with a well-defined border and appear glassy under the microscope. They express high levels of alkaline phosphatase (*89*) and telomerase (*90*) activity, both of which are downregulated in differentiated cell types. A complicated network of transcription factors regulates pluripotency in PSC. Oct4, Sox2, and Nanog are key factors at the core of the regulatory network that maintains the pluripotency of stem cells (*91, 92*). Oct4 is a POU family transcription factor that is specifically expressed in the ICM of the blastocyst and acts as a gatekeeper to prevent stem cell differentiation (*93*). Oct4 forms heterodimers with Sox2, an SRY-related HMG box (Sox) family member, to bind to and regulate a set of downstream targets (*94*), including the respective regulatory regions of their own genes (*95*). Pluripotency is also regulated through complex epigenetic mechanisms such as histone modification, DNA demethylation, chromatin remodeling, and microRNAs (reviewed in (*96*)).

Because they have been studied extensively for more than three decades, more is known about mESC than any other type of PSC. mESC can be maintained in culture in an

undifferentiated state with a normal karyotype for long periods of time with relative ease. Culturing mESC on a feeder layer of irradiated or mitotically inactivated mouse embryonic fibroblasts (MEF) effectively inhibits spontaneous differentiation (*74*). mESC can be maintained in a pluripotent state without feeder cells by using the cytokine leukemia inhibitory factor (LIF) in media containing fetal calf serum, which effectively inhibits their differentiation and supports proliferation (*97*). LIF-mediated signaling occurs via heterodimerization of two class I cytokine receptors, the low-affinity LIF receptor and gp130 (*98*), activating the latent transcription factor STAT3 by phosphorylation (*99*). While maintenance of pluripotency through the canonical Jak/STAT pathway via LIF requires the inclusion of serum in the mESC media, addition of TGFβ superfamily member BMP4 along with LIF can be sufficient to maintain self-renewal in the absence of serum through phosphorylation of Smad1 and activation of the Id (inhibitor of differentiation) family (*100*).

The maintenance of pluripotency of human PSC (both hESC and hiPSC) is regulated through different mechanisms than that of mouse PSC. Unlike murine ESC and iPSC, the presence of LIF cannot maintain human PSC in a self-renewing state. Human PSC are more challenging to culture than their murine counterparts because they are more prone to spontaneous differentiation and exhibit poor survival when passaged as single cells upon enzymatic dissociation. Experiments using human PSC often produce inconsistent results due to variability in media, matrix, and culture conditions (*101*). They require expensive specialized media containing basic fibroblast growth factor (bFGF) (*102*). Yet like murine PSC, human PSC can be cultured nearly indefinitely while retaining their ability for self-renewal and differentiation, and are similarly often grown on fibroblast feeder cells. However the addition of BMP4 to the media of human PSC induces their differentiation into trophoblast or primitive endoderm-like cells

(*103*). Inhibition of BMP signaling by addition of BMP4 antagonist Noggin can contribute to the maintenance of pluripotency of human PSC (*104*). Because human PSC are more clinically relevant than murine PSC, there has been a great deal of effort focused on moving from a culture system dependent on serum-rich media and a MEF feeder matrix toward a system using defined media (*105*). Even more recently, chemically defined xeno-free media and matrices have been developed for the derivation and culture of human iPSC for potential clinical translation (*106, 107*).

Pluripotent stem cells offer great promise for cell-based treatment of ischemic heart disease. Because of their characteristic plasticity and self-renewal, they can proliferate indefinitely in culture, enabling them to be grown in large numbers for use in research. In theory, PSC are ideal for cell-based therapies because they can differentiate into any cell type in an adult organism, enabling them to regenerate any tissue or organ.

Transplantation of undifferentiated or partially differentiated human and mouse embryonic stem cells into animal models of myocardial infarction have produced some promising results, including in vivo differentiation of ESC into cardiomyocytes and significant improvement in heart function. Tomescot et al. primed hESC with BMP2 and fibroblast growth inhibitor SU5402 so that they expressed mesoderm and cardiac genes *ISL1, NKX2.5, MEF2C,* and *α-ACTININ*. These primed hESC were injected into a rat MI model, and two months after transplant, functional human cardiomyocytes were detected in the injected animals (*108*). However the potential for the formation of teratomas, rapidly proliferating tumors containing cell types from all three germ layers, remains an important concern in the use of undifferentiated embryonic stem cells from mouse or human origin (*109, 110*). Nelson et al. reported that injection of even small numbers of undifferentiated mouse ESCs into an infarcted mouse heart

resulted in significant improvement in heart function, including increases in ejection fraction and peak mitral blood flow velocity, and showed evidence that some of the transplanted cells differentiated into functional cardiomyocytes. Unfortunately more than 20% of the animals developed ESC-derived teratomas in the pericardium (*111*). One way to avoid the issue of teratoma formation is to differentiate ESC toward a desired cell type in vitro prior to transplant. Both mouse and human PSC can be differentiated into cardiomyocytes in vitro through a variety of mechanisms (*112-115*), though the safest and most efficient ways to accomplish this fate specification are still being investigated. While directed differentiation of PSC is an area of intense study, no current differentiation protocols can produce 100% of the cell type of interest, and lingering pluripotent cells is always a major concern. Removal of undifferentiated cells can be achieved through mechanisms described in section 1.3.5. As we begin to understand more about fate determination in pluripotent cells, we are discovering ways to use culture conditions, cell sorting, and other techniques to manipulate them.

1.3.4 Cardiac differentiation of murine PSC

The potential of mouse embryonic stem cells to form spontaneously beating cardiac cells in vitro was first reported in 1985 (*116*), and efforts to understand and control this process have continued since. While numerous techniques have been described to produce cardiomyocytes from mouse embryonic stem cells, most begin with the aggregation in suspension of ESCs to form embryoid bodies, structures containing a mixture of differentiating cells with derivatives from the three germ layers which resemble the structure of a mouse embryo (*117*). To create embryoid bodies, mESC are trypsinized and resuspended at a low concentration in media devoid of LIF (*118*). The cells are then aggregated either through the use of plates with low attachment

surface coatings, swirling plates, or by creating hanging drops of cells on the tops of bacterial petri dishes. After several days, the embryoid bodies can be plated on gelatin coated plates for further outgrowth and differentiation, or dissociated and subjected to sorting or various treatments. Embryoid bodies allowed to attach and continue to differentiate will typically form spontaneously contracting areas indicative of cardiomyocyte formation at a low frequency, influenced by a number of factors including cell line and culture conditions (*116*). The difficulty has been unraveling the events that result in cardiomyogenesis and intervening to create a highly enriched population of cardiac cells.

Kouskoff et al. have described an elegant method to generate cardiomyocytes from transgenic mouse embryoid bodies. They engineered a line of mESC from mice with the GFP gene integrated in the *Brachyury* locus under the control of the *Brachyury* promoter (*119*). Brachyury is a member of the T-box family of transcription factors and the earliest marker of the mesoderm, the germ layer that gives rise to tissues such as skeletal muscle, bone, blood, and heart (*120*). Using embryoid bodies created from this cell line, they were able to sort for cells of mesodermal lineage based on GFP expression. They additionally sorted based on expression of vascular endothelial growth factor receptor 2 (VEGFR2, Flk-1). Flk-1 is vital for vascular endothelial and hematopoietic differentiation, and is transiently expressed during the formation of cardiac tissue (*121*). Their experiments showed that only the day 3.25 GFP^+ ($Brachyury^+$)/$Flk\text{-}1^-$ population contained cells with cardiogenic potential. In subsequent experiments, they determined that stage-specific expression of Flk-1 in embryoid body differentiation marks pre-cardiac mesoderm. They found that by sorting and reaggregating GFP^+/$Flk\text{-}1^-$ cells after 3.25 days of embryoid body differentiation, and resorting at day 4.25, the population that is GFP^+/$Flk\text{-}1^+$ is highly enriched for cardiac progenitors (*122*). They were able to produce a population

containing greater than 50% cardiomyocytes as determined by cardiac-specific gene expression, a vast improvement over the 1 – 5% that form from unmanipulated embryoid bodies (Figure 5).

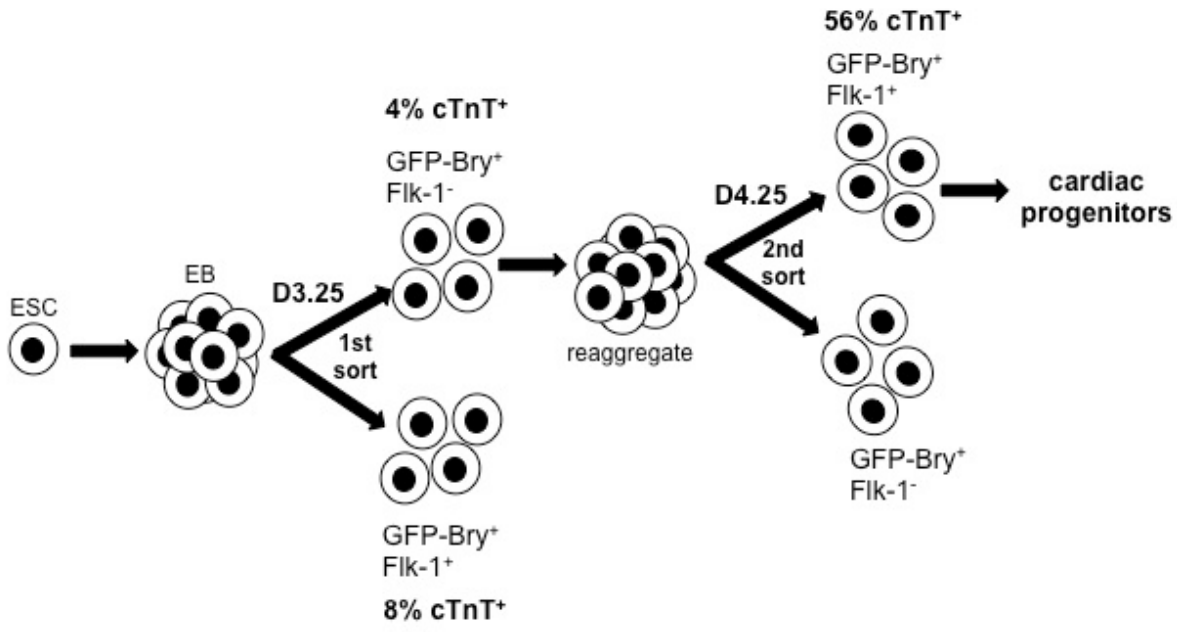

Figure 5. Sorting strategy to enrich EB cells for cardiac precursors.
Mouse ESC were differentiated in EB then sorted after 3.25 days based on GFP-Bry and Flk-1 expression. GFP-Bry$^+$/Flk-1$^-$ cells were reaggregated and sorted again on day 4.25. This later emerging Flk-1$^+$ population is distinct from the earliest Flk-1$^+$ population and is highly enriched for cardiac progenitor cells. (*119, 122*)

These studies highlight the tight temporal control of cardiogenesis, but more recent findings by Gordon Keller's group show that restriction of cardiac potential to this day 4.25 Flk-1^+ population is not absolute (*123*). These investigators found that only sorted cells with cardiac potential express Notch4, and they describe the generation of an ES cell line with tet-inducible Notch4 expression. By inducing Notch4 signaling, they were able to respecify the day 3.25 GFP^+/Flk-1^+ population to a cardiac fate, generating greater than 60% cardiomyocytes. This procedure represents a significant improvement over their previously described method as it eliminates one sorting step and provides greater efficiency of cardiomyocyte generation from a potentially larger pool of starting material.

Another strategy that incorporates cell sorting to enrich for cardiac progenitors was described by Nelson et al (*124*). They used systems-expression profiling along with bioinformatic network analysis to screen for cell surface proteins expressed at distinct stages of embryoid body formation from mESC, and identified the chemokine receptor CXCR4 as highly over-represented during cardiac induction (*124*). After five days of in vitro differentiation as EB in hanging drops, sorting for cells co-expressing CXCR4 and Flk-1 produced a population highly enriched for cardiac progenitors. Following sorting and reaggregation, further differentiation of these cells into spontaneously beating cardiac tissue expressing cardiac transcription factors was observed. The advantage of this approach is that it does not require the generation or acquisition of a transgenic mESC line, making it more immediately and widely useful to others in the field.

An alternative approach to sorting for cardiac progenitors from partially differentiated embryoid body cells is to use culture conditions, gene transfer, or treatment with small molecules to drive pluripotent stem cells toward a cardiac lineage. Perhaps the most straightforward approach is to modify the differentiation media to contain growth factors or drugs capable of

altering cell signaling and influencing cells to adopt a cardiac fate. Addition of VEGF to embryoid body differentiation media has been shown to significantly enhance the differentiation of mESC into cardiomyocytes (*125*). Bone morphogenetic proteins (BMP) are a group of secreted signaling proteins that are widely expressed during embryogenesis and development. Expression of BMP2 has been shown to be vital at certain stages in cardiogenesis (*8*), while its suppression can enhance cardiac development in a context dependent fashion (*126, 127*). Treatment of mESC with Noggin, a BMP antagonist, for three days prior to the onset of differentiation resulted in the formation of large numbers of beating embryoid bodies (*126*), while treatment during the first 24 hours of differentiation with small molecules dorsomorphin (*128*) or DMH1 (*129*), specific inhibitors of BMP signaling, leads to a significant expansion of the cardiomyogenic lineage.

Since iPSC were first derived in 2006, generating cardiomyocytes from iPSC for patient-specific regenerative cardiac therapy has been a major focus. Because they are nearly identical to mESC, murine iPSC are differentiated into cardiomyocytes in vitro utilizing many of the same techniques. Mauritz et al. described the cardiac differentiation of murine iPSC generated through retroviral transduction with Oct4, Sox2, Klf4, and c-Myc. They compared the efficiency, gene expression, and functional characteristics of cardiomyocytes created from spontaneously differentiating EB cells between mESC and iPSC. While the cardiac differentiation of iPSC was less efficient than mESC, the derived cardiomyocytes were functionally identical (*130*).

Murine iPSC generated without c-Myc were differentiated via EB formation in hanging drops. Cardiomyocytes were isolated from the EB using Percoll gradient centrifugation and characterized. Murine iPSC-derived cardiomyocytes performed similarly to those derived from

mESC in kinetic and gene expression assays, and these iPS progeny cells were detected with successful engraftment and functional contribution in the hearts of healthy chimeric mice (*131*).

Exogenous expression of genes known to be involved in cardiogenesis can be a powerful tool to influence the fate of PSC. Techniques such as infection with recombinant viral vectors and transfection can be used to deliver genes to PSC at specific times before and during differentiation. Craft et al. described the use of the replication defective HSV vector, JDββHE, to infect mESC and embryoid body cells and deliver the myogenic transcription factors Pax3 and MyoD (*132*). They used microarray analysis to determine that infection with these vectors augmented expression of genes involved in muscle lineage determination, demonstrating that gene transfer from an HSV vector has the potential to alter the fate of differentiating pluripotent cells.

GATA4, NKX2.5, and TBX5 are cardiac-specific transcription factors co-expressed in the precardiac mesoderm, and are among the earliest and most vital factors active during cardiac induction (*133*). Together with myocardin (MYOCD), they are considered to be the master regulators of heart development (*134*). Experimental disruption of GATA4, NKX2.5, or TBX5 leads to failure of normal heart development and cardiomyocyte maintenance, and embryonic death in mice (*135-140*). GATA4 and NKX2.5 are concurrently expressed and have been shown to physically interact in vitro and in vivo to synergistically transactivate expression of genes involved in cardiac differentiation, including atrial natriuretic factor, alpha myosin heavy chain (*α-MHC*), and cardiac troponin T (*cTnT*) (*141*). Yamada et al. have used retroviral transduction of mesenchymal stem cells with *GATA4* and *NKX2.5* to produce a population of cells with cardiomyocyte properties and expression profiles (*142*). Recently, strides have been made in completely bypassing a pluripotent intermediate by transdifferenting fibroblasts and other

somatic cells directly into cardiomyocytes (induced cardiomyocytes, iCM) with several different combinations of cardiac transcription factors. Ieda et al. used a combination of *GATA4*, *TBX5*, and *MEF2C* (GTM) to directly reprogram cardiac and dermal fibroblasts into cardiomyocytes in vitro (*143*). Qian et al. used the same GTM combination to transdifferentiate cardiac fibroblasts in vivo into cardiomyocytes (*144*). Also in 2012, Song et al. included *HAND2* into the GMT mixture to achieve more efficient transdifferentiation of adult mouse tail-tip fibroblasts in vitro and cardiac fibroblasts in vivo, and reported moderate improvements in cardiac function following surgically induced MI (*145*). However other reports (*146*) have failed to repeat the success of these initial experiments, leaving a lot of questions unanswered. Is the activation of a cardiac reporter gene (eg. *α-MHC* promoter driving eGFP expression as in (*143*)) sufficient to conclude that transdifferentiation into true cardiomyocytes was achieved? There are a number of criteria used (*147*), but there is currently no clear consensus about the characteristics required for a cell to be considered an iCM. Still this is an exciting area of research for cardiac regenerative medicine because the lack of a PSC intermediate removes the risk of teratoma formation in patients transplanted with iCM.

1.3.5 PSC-derived cardiomyocytes for cardiac regeneration

Most of the recent pre-clinical studies with PSC for cardiac regenerative therapy have focused on utilizing human PSC in vitro-derived cardiomyocytes to treat animal models of MI. Because of the risk of teratoma formation in recipients of PSC-derived cell types, they have not yet been used in clinical trials in humans.

It is physiologically more meaningful to use mouse PSC and their derivatives for cell-based therapy in mouse models due to the small size of mice and their faster heart rate compared

to larger mammals. Human cardiomyocytes may survive and electrically couple in rodent hearts, but they cause arrhythmias and are not necessarily the best model for human CVD therapy. However because the ultimate goal is to regenerate the human heart, animal models including mice, rats, guinea pigs, monkeys, sheep, and pigs have been implanted with hESC-derived cardiomyocytes with generally favorable results. A 2009 preclinical study by Menard et al. did use cardiac committed mESC in a sheep model of MI. Mouse ESC were cultured for 36 hours with BMP2 prior to transplantation, and these cells were able to engraft and fully differentiate into cardiomyocytes, significantly increasing LV ejection fraction (LVEF), the amount of blood pumped from the LV with each heartbeat, a typical measure of cardiac functionality (*148*). Human ESC-derived cardiomyocytes were transplanted into rat (*149*) and pig (*150*) models of MI and found to interact normally with endogenous cardiomyocytes to form new myocardium. They expressed cardiomyocyte genes *α-MHC*, *MLC-2v*, and *ANF*, and the graft sizes increased over time indicating that the implanted cells proliferated in vivo. Electrophysiological mapping and histopathological examination were used by Kehat et al. and Xue et al. to demonstrate that hESC-derived cardiomyocytes can form pacemaker cells and electrically couple to the host myocardium in pigs (*150*) and guinea pigs (*151*). A number of other studies showed improved function of the post-MI heart upon implantation of hESC-derived cardiomyocytes into animal models including mouse (*152*), rat (*153*), and monkey (*154*) models. Human iPSC-derived cardiomyocytes have been used similarly in pre-clinical studies with largely positive results. For a comprehensive review of these experiments, see Lalit et al. (*155*).

All of this data taken together hints at the promise of PSC-derived cells for cardiac regenerative therapy, but there is still much to be learned before it can be translated to the clinic. Most importantly, we must develop methods to ensure that any remaining undifferentiated cells

are completely removed from the culture to remove the risk of teratoma formation in patients. This can be accomplished in a number of ways, including using antibodies against stem cell-specific surface antigens such as SSEA-5 (*156*) and certain lectins (*157*) to deplete undifferentiated cells. Other questions remain, such as what is the ideal cell type for transplant into the injured heart? Would a more or less committed cell type survive and function effectively, or is a mixture of cell types that provide mutual support for growth and vascularization a better choice since the heart itself is made of several different types of cells? How can enough cells be safely and efficiently produced to meet the overwhelming demand? When is the optimal time to treat patients with cell-based therapies following a cardiac event, and how should the cells be delivered?

The answer to the latter has been the subject of much research in recent years. In most pre-clinical studies, cells have been injected directly into the myocardium along the site of scar formed from infarction. While the cells do engraft and function, the survival of the donor cells is often poor. Strategies to improve graft survival and the outcome for the host, such as the use of PSC-based biomimetic materials (*158*), cardiopatches (*159*), and other mechanisms, are currently being investigated.

1.4 HERPES SIMPLEX VIRUS TYPE 1 (HSV-1)

1.4.1 HSV-1 genome structure

Herpes simplex virus type 1 (HSV-1) is a double stranded DNA virus with a broad host cell range. It is well suited for use as a gene delivery vector for PSC due to its ability to infect many

cell types, including PSC and their derivatives (*132*). Unlike retroviruses, HSV-1 remains episomal so that genomes are lost over time as host cells divide, and host chromosomes are not disrupted by integration of the viral genome. HSV-1 has a large ~152 kb genome that encodes over 80 proteins. Approximately half of these are not essential for viral replication in cell culture, and deletion of their genes through genetic recombination makes it possible to insert large and multiple transgenes. The HSV genome is segmented into unique long (U_L) and unique short (U_S) sequences connected by inverted repeat elements called the joint.

1.4.2 HSV-1 gene expression cascade

HSV-1 initiates a temporal cascade of gene expression following infection and entry into a host cell, involving the sequential expression of immediate early (α), early (β), and late (γ) genes (*160*). Five immediate early genes are expressed upon viral genome entry into the host cell nucleus, infected cell protein (ICP) 0, ICP4, ICP22, ICP27, and ICP47. The promoters of the immediate early genes contain an enhancer element that is responsive to VP16, an HSV structural protein that is transported into the nucleus along with the viral DNA (*161*). The primary function of the immediate early genes, particularly ICP4, is to activate expression of the early genes that encode viral proteins necessary for DNA replication. Late genes are transcribed following DNA replication and primarily encode virion structural proteins (*160*). Of the five immediate early genes, only ICP4 and ICP27 are absolutely required for expression of early and late genes and DNA synthesis (*162*). ICP4 serves as a transactivator of viral genes, while ICP27 is vital for processing and transport of viral mRNAs. ICP0 and ICP22 are not required for HSV replication in vitro, but also play a role in the transactivation of viral genes and improve gene expression and replication efficiency of the virus (*163*).

1.4.3 Replication defective HSV-1 vectors

The rigid sequence of HSV gene expression makes generation of replication defective mutants for use as vectors relatively straightforward. By eliminating one or more immediate early genes required for activation of the gene expression cascade, the virus cannot express early or late genes, replicate its DNA, or produce infectious progeny. Replication and production of these defective vectors can be achieved through the use of a complementing cell line that provides the missing gene functions in trans (*164*). However simply eliminating the replication competence of HSV does not make it a suitable vector. Even in the absence of lytic viral replication, ICP0, ICP4, ICP22, and ICP27 are toxic to cells (*165*). Elimination of ICP0 enhances the survival of infected cells (*166*), but also drastically reduces transgene expression (*167*) as well as early and late viral gene expression (*168*). Achieving a balance between toxicity and robust transgene expression is vital in the design and construction of replication defective HSV vectors. With this in mind, vectors JDββHE (*132*) and JΔNI8GFP (*169*) were developed in our lab.

1.4.4 HSV-1 vector JDββHE

Vector JDββHE (*132*) contains deletions of two immediate early genes, ICP4 and ICP22, as well as the internal repeated sequences (JD, joint deleted). Immediate early genes ICP0 and ICP27 were placed under the control of the promoter of β gene thymidine kinase and are expressed with early gene kinetics. This genome design results in a vector that can replicate only in the presence of ICP4, which is supplied in trans by the Vero cell line derivatives 4BLA or 7b in response to infection with HSV. The 4BLA cell line expresses ICP4 under the control of the ICP4 promoter (*132*), and the 7b cell line in addition expresses ICP27 under the control of the ICP27 promoter

(*170*). JDββHE also contains a copy of the ICP0 promoter driving expression of lacZ in the U_L41 locus, disrupting the virion host shutoff function that shuts down host protein synthesis (*171*) and allowing expression of lacZ to monitor transgene expression. JDββHE in addition was engineered to express GFP under the control of the HCMV IE promoter in the deleted ICP4 locus so that infected cells can be easily visualized by fluorescence microscopy. These modifications together provided a vector with abundant room for insertion of foreign sequences and low toxicity to host cells. RNA analyses have shown that expression of the ICP0 gene is up to 100-fold lower in JDββHE-infected cells than in cells infected with an ICP0+ reference virus (*132*). This low level of ICP0 gene expression provides enough ICP0 function to allow complete transduction in an MOI-dependent manner and robust transgene expression in both embryonic stem cells and embryoid body cells, but minimizes ICP0-mediated toxicity. Infection of embryonic stem cells with JDββHE does not interfere with self-renewal or mesoderm formation, as evidenced by normal expression of early mesoderm markers Brachyury and Flk-1 in embryoid bodies derived from embryonic stem cells infected at MOIs of up to 100 (*132*).

1.4.5 HSV-1 vector JΔNI8GFP

The design of vector JΔNI8GFP was conceived to improve upon JDββHE by eliminating all residual ICP0- and ICP27-mediated toxicity without abolishing robust transgene expression in dividing and non-dividing cells. All manipulations to engineer JΔNI8GFP were carried out in bacteria utilizing an HSV-bacterial artificial chromosome (BAC) as described in detail for a very similar vector, JΔNI7GFP, by Miyagawa et al. (*169*). JΔNI8GFP differs from JΔNI7GFP (*169*) only by the additional deletion of U_L41, making it more similar to JDββHE.

Deletion of ICP0 expression leads to global silencing of the viral genome in infected host

cells, resulting in a complete loss of transgene expression (*172*). However, it was found that transgene(s) placed within the latency-associated transcript (LAT) locus were selectively protected from epigenetic silencing, resulting in robust expression even in the absence of any immediate early gene expression (*169*). Latency is a quiescent state in which expression of viral lytic genes has been extinguished. However, during latency, HSV persistently expresses a latency-associated non-coding RNA (LAT). The presence of LAT RNA, a stable 2 kb intron spliced from an 8.3 kb LAT mRNA, is the hallmark of latency. Elements of the latency promoter have been shown to promote gene expression from HSV vectors. LAT expression during latency is controlled by latency associated promoters (LAP) 1 and 2 (*173, 174*). LAP2 can act as a long-term enhancer element for transgene expression. A region known as LATP2 contains the LAP2 element and extends further into the 2 kb intron region (*175*). The LAT locus is also protected from viral genome silencing during latency by regions rich in CTCF binding sites called CTRLs, with CTRL1 located upstream of LAP1 and CTRL2 in the intron just downstream of LATP2 (*176*).

2.0 RATIONALE AND SIGNIFICANCE

2.1 SIGNIFICANCE

Cardiovascular disease remains a leading cause of death in developed countries, killing one in five Americans and adversely affecting the health of at least one in three (*177*). Advances have been made in the treatment of ischemic heart disease, including the use of drugs such as angiotensin-converting enzyme (ACE) inhibitors and β-adrenergic blockers to improve cardiac function (*178, 179*). Currently available treatments can improve the prognosis and quality of life for patients suffering from heart disease, but they lack the ability to replace cardiac tissue lost to the disease. The only established method to cure a patient whose heart has been injured by myocardial infarction or damaged by other diseases is heart transplantation, an option that is only rarely available.

2.2 CELL-BASED THERAPY FOR CARDIAC DISEASES

Cell-based therapy for the treatment of cardiac diseases has the potential to replace lost cardiomyocytes and therefore has become an area of intense study. While many laboratories have published encouraging results of transplantation of different cell types into animal models of myocardial infarction, the type of cells transplanted is a key factor in the ultimate success of

this approach. Transplantation of fully committed cells into animal models of infarcted hearts has had mixed results, and these cells are of limited availability and not practical for clinical use. Adult progenitor cells can be autologously derived and studies have shown moderately improved outcomes in patients receiving these cells, but they do not differentiate in vivo into cardiomyocytes. Any improvements observed upon adult stem cell therapy in the heart are due to paracrine effects or increased vascularization in the damaged area, neither of which is sufficient to replace lost cardiac function. Pluripotent stem cells (ESC and iPSC) can differentiate into functional cardiomyocytes, but teratoma formation in the host is an important hurdle that must be overcome before PSC or their derivatives can be transplanted into patients.

Much effort is currently devoted to determining the best procedures to achieve in vitro differentiation of PSC into cardiomyocytes. Induced expression of one or more genes vital to cardiac programming of PSC is a logical strategy to influence PSC differentiation, but until recently, gene transfer methods for PSC have been limited by inefficiency, vector toxicity, and concerns regarding vector integration into the host-cell genome.

2.3 REPLICATION DEFECTIVE HSV VECTORS FOR PLURIPOTENT STEM CELLS

Replication defective HSV vector JDββHE was designed to be non-toxic, yet capable of efficient transgene delivery to and expression in pluripotent stem cells and their derivatives without compromising the cell's ability to self-renew and differentiate along the mesodermal lineage. Experiments involving infection of mESCs with JDββHE and subsequent formation of embryoid bodies have demonstrated that the vector does not have a significant effect on the expression of

the mesoderm marker Brachyury or the hemangioblast marker Flk-1. JDββHE-based vectors containing the myogenic genes *Pax3* and *MyoD* have been shown to alter gene expression profiles of embryoid body cells such that target genes relevant to muscle development were upregulated, indicating that genes expressed from this vector have the potential to influence lineage determination in pluripotent stem cells (*132*). We engineered the JDββHE vector, as well as a similar but yet further crippled vector, JΔNI8, to deliver vital early cardiac transcription factors to mESC. Initially JDββHE-based vectors seemed ideal, but when the new JΔNI8-based vectors were tested, it became clear that they were better suited for our purposes because of their reduced toxicity and strong expression of transgenes from the protected LAT locus. Both vector types expressing cardiogenic transgenes were used to enhance cardiac differentiation of mESC signified by increased upregulation of genes involved in cardiomyogenesis (Table 1) as measured by qRT-PCR, and by increases in spontaneously contracting cardiomyocytes in EB cultures derived from experimental compared to control vector-transduced mESC.

Table 1. Genes involved in cardiac differentiation used for qRT-PCR experiments

	Gene	Function in cardiomyogenesis
Differentiated cardiomyoctyes ← Precardiac mesoderm	*Foxa2*	Expressed in mesoderm-committed cells With Mef2c, activates *Myocd* transcription Upregulated with induced Gata4 expression
	Gata6	Disruption leads to congenital heart malformations *Gata4* and *Gata6* are highly conserved and have partially redundant roles, but each is required for maintenance of heart health Upregulated with induced Gata4 expression
	Tbx20	Essential for embryonic heart development Physically interacts with Gata4 and Nkx2.5
	Myocd	Cardiac transcriptional regulator of SRF Transcription activated by Mef2c and Foxa2 Expressed from E7.5+ in the cardiac crescent and activates its own enhancer
	Sox17	Upregulates genes related to heart development *Sox17* null embryos show defective heart development and loss of Myocd+ cardiogenic precursors Upregulated with induced Gata4 expression
	Mlc2a	Vital for formation of atrial chambers Expressed from E9+
	Myo5b	Unconventional myosin motor expressed in the heart Controls ion channel recycling Upregulated with induced Gata4 expression
	cTnI/cTnT	Cardiac-specific troponins that physically interact with each other Involved in Ca2+-regulated contraction of cardiac muscle

References: *Foxa2* (*180, 181*), *Gata6* (*181-184*), *Tbx20* (*185-187*), *Myocd* (*140, 188*), *Sox17* (*181, 189*), *Mlc2a* (*190*), *Myo5b* (*181, 191*), *cTnI/cTnT* (*192*).

3.0 CONSTITUTIVE EXPRESSION OF GATA4 IN D3 EMBRYONIC STEM CELLS

3.1 INTRODUCTION

The temporospatial expression pattern of transcription factors plays a vital role in cell lineage determination in a developing embryo. Commitment of a subset of embryonic cells to adopt a cardiac fate is one of the earliest events to occur in embryogenesis, and GATA4 is a key regulator of cardiogenesis that is expressed from the earliest stages of cardiac commitment, through development, and into adulthood (*14*). GATA4 is considered to be the master transcriptional regulator of cardiac development, and loss of GATA4 function is incompatible with life (*13*).

GATA4 is a zinc finger transcription factor that binds to the promoters of many cardiac-specific genes to switch on their expression and drive the ordered proliferation, migration, and differentiation of cells in the precardiac mesoderm to form the embryonic heart. GATA4 has a C-terminal zinc finger to facilitate DNA binding at (a/t)GATAA(g) residues, and an N-terminal zinc finger that stabilizes protein-DNA interactions and participates in specific protein-protein interactions (*193*). The GATA4 sequence is highly conserved among mammals, underscoring its essential role in the development and function of the heart.

Cardiovascular disease is the leading cause of morbidity and mortality across the globe. The adult mammalian heart lacks significant regenerative capacity, and currently no therapies

exist to replace damaged heart tissue. Cell-based treatment for cardiac ischemia offers great promise, but much needs to be learned before it can become clinically relevant. Pluripotent stem cells are theoretically ideal for cell-based therapies because they can differentiate into any cell type in an adult organism, enabling them to regenerate any tissue or organ. However transplantation of undifferentiated pluripotent stem cells carries the potential for the formation of teratomas, rapidly proliferating tumors containing cell types from all three germ layers (*109*). It should be possible to avoid the issue of teratoma formation by differentiating stem cells into a desired lineage in vitro prior to transplantation. Directed differentiation of pluripotent stem cells is an area of intense study as a deeper understanding of fate determination and ways to intervene to produce specific cell types are revealed.

We are interested in using expression of essential cardiac transcription factors to influence embryonic stem cell fate and enhance their differentiation into cardiomyocytes. Because *GATA4* sits atop the hierarchy of the cardiac gene transcriptional network, it is a logical target for cardiomyocyte differentiation. In this study, we describe the creation of D3 mESC lines that constitutively express GATA4. By using nucleofection and selection with puromycin, we generated lines that constitutively expressed varying levels of GATA4. These GATA4-expressing mESC lines displayed significantly greater cardiogenic potential than their eGFP-expressing counterpart. One line produced 80% more contracting embryoid bodies than the control eGFP-expressing line. Constitutive GATA4 expression in differentiating EB also dramatically enhanced the expression of other cardiac genes, including endogenous *Gata4*, *Nkx2.5*, cardiac troponin I (*cTnI*), and *Mlc2a*.

3.2 MATERIALS AND METHODS

3.2.1 Cells and culture conditions

D3 mouse embryonic stem cells (a gift from T.E. Smithgall, University of Pittsburgh) were cultured in Dulbecco's modified Eagle's medium (DMEM, Corning) supplemented with 15% fetal bovine serum (FBS, GIBCO), 1% non-essential amino acids (GIBCO), 1 mM sodium pyruvate (GIBCO), 100 U/ml penicillin (Cellgro), 100 μg/ml streptomycin (Cellgro), 0.1 mM 2-mercaptoethanol (GIBCO), and 1000 U/ml mouse leukemia inhibitory factor (LIF, Millipore) on 10 centimeter dishes coated with 0.2% gelatin (Sigma). Media was exchanged daily and cells were passaged with trypsin every 2-3 days to maintain a state of self-renewal and minimize spontaneous differentiation.

3.2.2 Construction of GATA4 expression cassette

A cassette containing the CAG promoter, GATA4 coding sequence, and SV40 polyadenylation signal was constructed as follows. Plasmid pCDH (System Biosciences) was modified to replace the CMV promoter with the CAG promoter and then human GATA4 cDNA (Open Biosystems) was ligated into the plasmid. The CAG promoter was derived from plasmid pPEP100 (kindly provided by P. Spear, Northwestern University) (*194*) as a 1.7 kb SpeI to EcoRI fragment and cloned between the SpeI and EcoRI sites of plasmid pCDH as a SpeI to produce plasmid pCDH-CAG. The 1.4 kb fragment containing the human *GATA4* cDNA in pTopo-GATA4 (Open Biosystems) was excised using EcoRI and cloned into the EcoRI site of pCDH-CAG to create CAGp-GATA4-SV40pA-EF1p-Puro^{R}. The correct orientation of the GATA4 fragment was

verified with diagnostic digests. Plasmid CAGp-eGFP-SV40pA-EF1p-Puro^R was created as a control, and both plasmids were linearized with SpeI prior to Nucleofection.

3.2.3 Generation of D3 mES cell lines expressing GATA4 and eGFP

Linearized plasmids CAGp-GATA4-SV40pA-EF1p-Puro^R and CAGp-eGFP-SV40pA-EF1p-Puro^R were introduced into D3 mESC via nucleofection. First the plasmids were linearized by digestion with SpeI and the DNA was purified from an agarose gel. D3 mES cells were fed four hours prior to nucleofection. Cells were prepared for nucleofection by detaching them with trypsin, pelleting the cells and washing them with PBS, and resuspension in 90 µl Ingenio Electroporation Solution (Mirus). 10 µg linearized DNA was diluted into 10 µl Ingenio Electroporation Solution, and mixed with the cells in an electroporation cuvette. The DNA was nucleofected into the cells using an Amaxa Nucleofector I set on program A-13. Immediately after nucleofection, 500 µl warm media was added to the cells in the cuvette, and the cells were plated in gelatin coated 10 cm dishes containing warm ES media with LIF. Media was changed 24 h after plating. 48 h after nucleofection, 2 µg/ml puromycin was added to the media for selection. Resistant colonies began to appear 24 h after the onset of selection, and were picked from 10 cm dishes under a microscope in a hood one week after nucleofection. Each colony was placed in one well of a 24 well plate for expansion. At least ten clones were expanded for each cell line. Cell lines were characterized by observation of eGFP expression (D3-eGPF), Western blotting (D3-GATA4), EB assay, and reverse transcriptase (RT) quantitative real time (q) polymerase chain reaction (PCR).

3.2.4 Western blot analysis

Cell lysates were collected from undifferentiated D3-eGFP and D3-GATA4 mESC lines as well as from d12 EB in RIPA lysis buffer supplemented with protease inhibitors (Roche). Proteins were separated on a 10% polyacrylamide gel and transferred by semi-dry transfer onto PVDF membranes. The membranes were washed in Tris-buffered saline (TBS) and blocked for 1 h at room temperature in TBS-T (20 mM Tris, 0.5 M NaCl [pH 7.5] plus 0.5% Tween 20) supplemented with 10% nonfat dry milk. Primary antibodies were diluted in blocking buffer. Diluted antibody was reacted with the blocked PVDF overnight at 4°C, washed 3 times for 10 min each in TBS-T, and reacted with horseradish peroxidase-conjugated secondary antibody diluted in blocking buffer for 1 h at room temperature. The bound Igs were revealed by enhanced chemiluminescence (Thermo Scientific). Antibody information can be found in Table 2.

Table 2. Primary and secondary antibodies used for Western blotting

Antibody	Vendor	Cat. Number	Dilution
Primary			
GATA4	Santa Cruz	sc-25310	1:100
GATA4	abcam	ab84593	1:100
Nkx2.5	Santa Cruz	sc-81973	1:200
Nkx2.5	abcam	ab91196	1:500
TBX5	Santa Cruz	sc-17866	1:200
MEF2C	Santa Cruz	sc-13268	1:200
2A peptide	Millipore	ABS31	1:1000
Secondary			
anti-mouse HRP	Sigma	RABHRP2	1:10000
anti-rabbit HRP	Sigma	RABHRP1	1:2000

3.2.5 Embryoid body assay

Cells were suspended in mESC media without LIF at a concentration of $4x10^4$ cells/ml. 20 µl drops of cells were pipetted onto the lid of a petri dish, and the lid was inverted over the dish that contained 30 ml sterile water to prevent the drops from evaporating. The cells were incubated at 37°C with 5% CO_2 and allowed to aggregate to form embryoid bodies (EB) and differentiate for two days in hanging drops. After 48 h in hanging drops, the EB were pipetted one per well into 48 well plates, each well containing 500 µl mESC media without LIF. The EB were observed daily for the appearance of spontaneously contracting cells, and the number of wells containing these cells was recorded each day.

3.2.6 RNA extraction and qRT-PCR analysis

Total RNA was extracted from D3 mES cell lines and embryoid bodies using Qiagen RNeasy Plus mini kit with gDNA eliminator columns (Qiagen). Reverse transcription was performed on 1-2 µg RNA in 20 µl final volume using random decamers as first strand primers with Ambion's RETROscript Kit (Ambion), and the resulting cDNA was diluted 1:10 for qPCR analysis.

Primers were obtained from Invitrogen. Primer sequences and references for qPCR are listed in Table 3. qPCR was performed using LightCycler SYBRgreen Master Mix (Roche) and a Step One Plus Real-Time PCR System (Applied Biosystems). Cycling conditions were 95°C for 10 min followed by 40 cycles of 95°C for 15 sec and then 60°C for 1 min. Each cDNA was

analyzed in triplicate, and the results for the three wells were averaged. Threshold cycle (Ct) values were used to calculate changes in gene expression using the $2^{-\Delta\Delta Ct}$ method (*195*). Expression levels were normalized to HPRT and mRNA expressed relative to uninfected D3 mESC.

Table 3. Primer sequences used for qRT-PCR

Gene	Forward Primer	Reverse Primer	Product Length (bp)	Reference
GATA4 (human)	TTCCAGCAACTCCAGCAACG	GCTGCTGTGCCCGTAGTGAG	97	Zhu et al. (*196*)
Gata4	GCCCAAGAACCTGAATAAAT	CGGACACAGTACTGAATGTCT	195	So et al. (*197*)
NKX2.5 (human)	CTTCAAGCCAGAGGCCTACG	CCGCCTCTGTCTTCTCCAGC	210	Zhu et al. (*196*)
Nkx2.5	CAGTGGAGCTGGACAAAGCC	TAGCGACGGTTCTGGAACCA	217	Lakshmipathy et al. (*198*)
Mlc2a	TCAGCTGCATTGACCAGAAC	AAGACGGTGAAGTTGATGGG	148	Yamashita et al. (*199*)
cTnI	ACGTGGAAGCAAAAGTCACC	CCTTCTTCACCTGCTTGAGG	189	So et al. (*197*)
anf	CTGTTTAAAGATTCTGCTCACC	GAGAGACCAGTGAAGAACTAGC	151	So et al. (*197*)
HPRT	GCTGGTGAAAAGGACCTCT	CACAGGACTAGAACACCTGC	249	Anton et al. (*200*)
Oct4	TGTTCCCGTCACTGCTCTGG	TTGCCTTGGCTCACAGCATC	82	Greber et al. (*201*)
Foxa2	CCCTACGCCAACATGAACTCG	GTTCTGCCGGTAGAAAGGGA	222	Oda et al. (*181*)
Gata6	GCAATGCATGCGGTCTCTAC	CATATAGAGCCCGCAAGCAT	185	Oda et al. (*181*)
Sox17	CTCGGGGATGTAAAGGTGAA	CTTAGCTCTGCGTTGTGCAG	182	Primer3 (*202*)
Myo5b	ACACTATGTCCGGTGCATCA	CCGGTTGAAGAAGTCATGGT	163	Primer3 (*202*)

3.3 RESULTS

3.3.1 mESC lines constitutively expressing GATA4 and eGFP

In order to determine whether expression of GATA4 increases the cardiogenic potential of D3 mESCs, cell lines were created to constitutively express human GATA4. An eGFP-expressing mESC line was similarly generated for use as an experimental control. Dual gene expression

cassettes were constructed with the CAG promoter driving expression of either human *GATA4* or eGFP and the EF1α promoter driving expression of the puromycin resistance gene (Figure 6A). Following linearization, the plasmids were introduced into D3 mESCs by nucleofection and transduced colonies were identified by selection for resistance to puromycin. Several individual colonies were isolated and expanded.

mESC expressing eGFP were readily identified by fluorescence microscopy. D3-eGFP clonal lines retained normal stem cell morphology and every colony formed by these cells robustly expressed eGFP (Figure 6B). Cell lysates were collected from three D3G4 lines (A, B, and C), and equal amounts of protein from each line were separated by gel electrophoresis. Western blotting demonstrated that the three lines varied widely in their expression of GATA4 protein (Figure 6C). D3G4-B expressed a high level of GATA4, D3G4-C appeared to express no GATA4, and D3G4-A expressed an intermediate level of the protein. No GATA4 expression was observed in unmodified D3 mESC or D3-eGFP (data not shown).

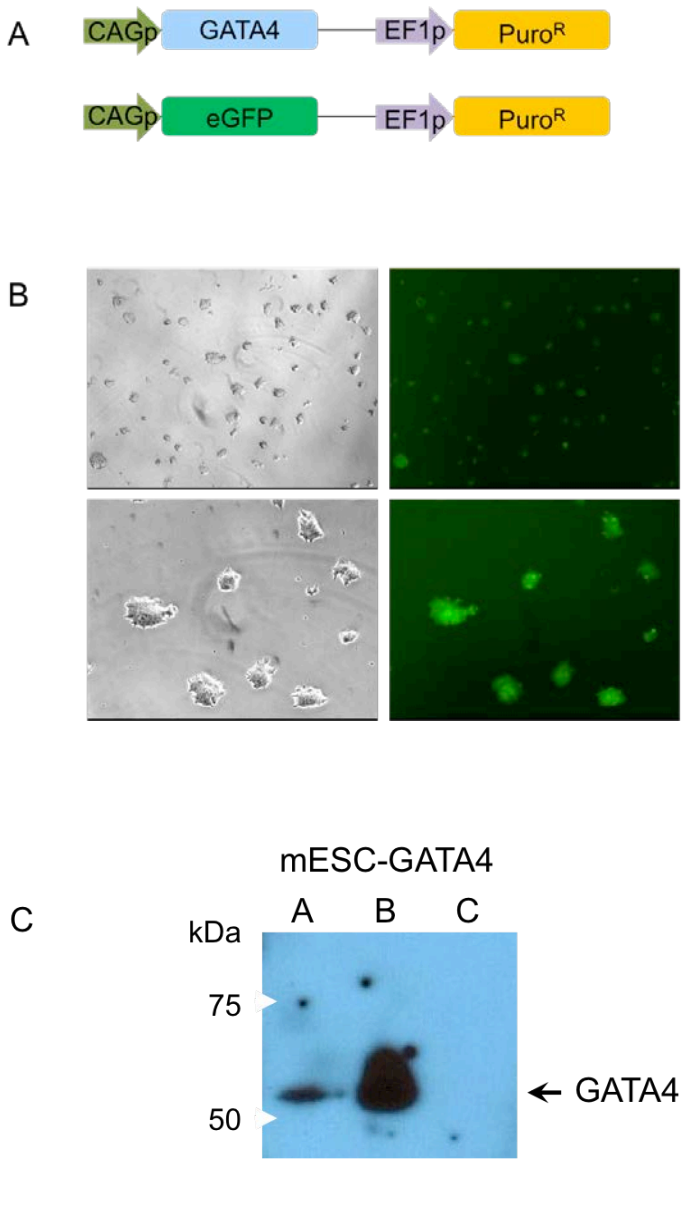

Figure 6. D3 mESC cell lines for constitutive expression of eGFP or GATA4
(A) Schematics of the DNA fragments used for nucleofection of mESC to generate eGFP- and GATA4-expressing cell lines. (B) eGFP expression in undifferentiated cells from an mESC-eGFP clone at low (upper panels) and high (lower panels) magnification. Cells are shown from left to right in brightfield, fluorescence, and overlay. (C) Western blot showing expression of GATA4 in three mESC-GATA4 clonal cell lines.

3.3.2 Constitutive GATA4 expression enhances cardiac differentiation in EB

To determine whether constitutive expression of GATA4 affects mESC differentiation, EB were generated from unmodified D3 mESC, D3-eGFP, and D3G4 lines B and C by the hanging drop procedure and then plated one per well in 48 well plates. The EB were monitored daily from days 8 – 14 after the onset of differentiation for the appearance of spontaneously contracting cells, indicative of the presence of mature cardiomyocytes. While unmodified mESC and D3-eGFP exhibited very low levels of cardiac differentiation, the two D3G4 lines produced many more EB with large areas of contracting cells (Figure 7). D3G4-B, the line that expressed the highest level of GATA4 protein, had the largest percentage of EB with contracting cells (>90% on day 12). Although it appeared from the Western blot of Figure 6C that D3G4-C expressed little or no GATA4 protein, these cells also demonstrated dramatically more cardiogenic potential than the unmodified mESC or the D3-eGFP line. Almost 65% of D3G4-C EB contained visible cardiomyocytes on day 14 compared to a maximum of 17% of control EB.

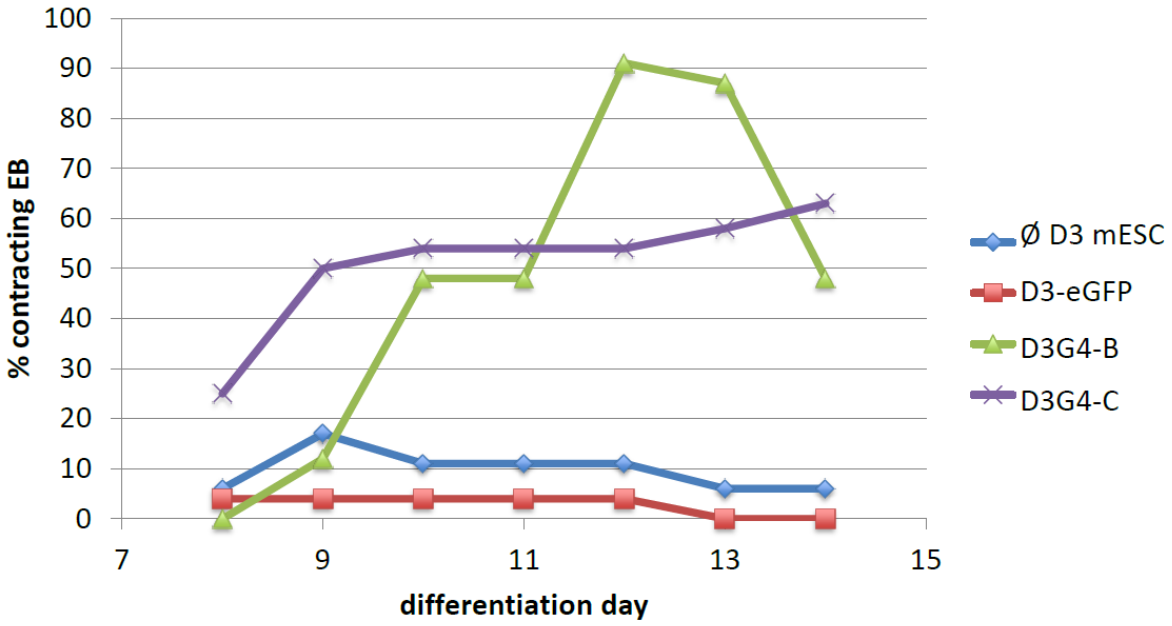

Figure 7. Cardiomyocyte differentiation of modified mESC lines
Control mESC, D3-eGFP, and D3G4 lines B and C were differentiated in EB. EB with visible contracting patches of cells were counted daily from 8 – 14 d after the onset of differentiation.

3.3.3 Differentiating D3G4 mESCs express higher levels of cardiac-specific genes than control D3-eGFP cells

We examined the expression of selected cardiac genes in late-stage EB derived from D3-eGFP and D3G4-B. RNA was extracted on day 12, the day when EB display the greatest cardiomyocyte activity as determined in Figure 7. In this experiment, 74% of D3G4-B EB contained contracting foci on day 12 while none of the D3-eGFP EB did (Figure 8A). qRT-PCR with SYBR Green reagents was used to quantify relative cardiac-specific gene expression as well

as expression of *Oct4*, a pluripotency marker. We examined expression of *Nkx2.5*, a gene expressed in some of the earliest cardiac progenitors through fully differentiated cardiomyocytes, as well as *cTnI* and *Mlc2a*, genes expressed only in more committed cardiac cell types (see Table 1). Mouse heart cDNA was included as a positive control for cardiac genes. Gene expression was normalized to *HPRT* cDNA and expressed relative to undifferentiated, unmodified mESC (Figure 8B). As expected, *Oct4* expression was dramatically downregulated in 12 day old EB and was undetectable in mouse heart cDNA. Species-specific primers were used to distinguish GATA4 expression from the human transgene and the endogenous murine gene. Although the human *GATA4*-specific primers showed some background amplification with D3-eGFP EB and mouse heart cDNAs, the signal from D3G4-B cDNA was more than 100-fold higher. Expression of the mouse *Gata4* gene, as well as the *Nkx2.5* and *cTnI* genes, was up to ~10-fold higher in D3G4-B EB than in D3-eGFP EB. D3G4-B EB also contained over 500-fold more *Mlc2a* mRNA than D3-eGFP EB. Overall, the expression levels of these genes in D3G4 EB more closely resembled those in mouse heart than in D3-eGFP EB (Figure 8C).

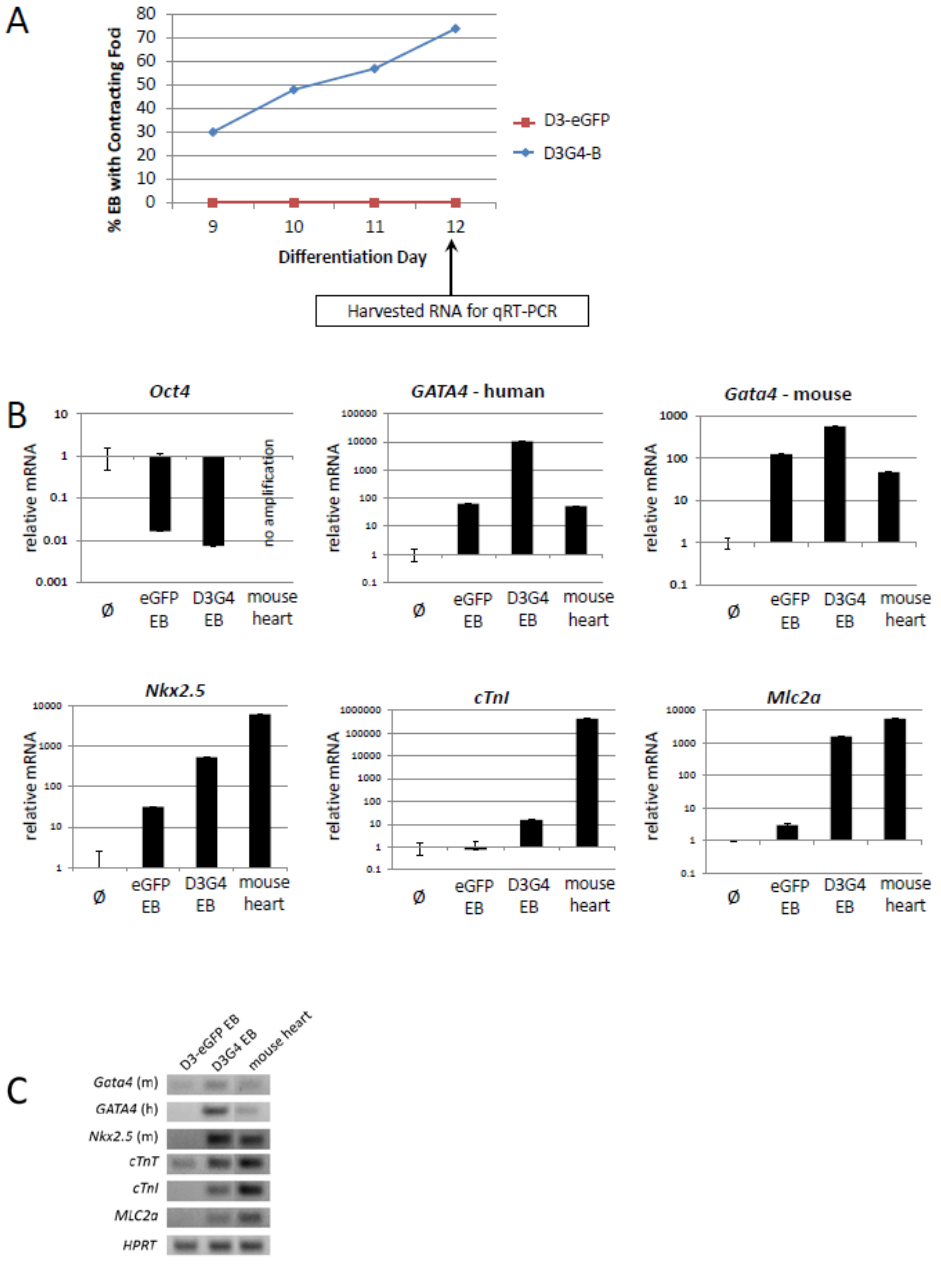

Figure 8. Comparison of gene expression in d12 EB made from D3-eGFP and D3G4-B by qRT-PCR

(A) mESC were differentiated for 12 d in EB. RNA was extracted and reverse transcribed. (B) qRT-PCR data for *Oct4* and cardiac-specific gene expression. Ø, unmodified undifferentiated mESC. Gene expression data was normalized to *HPRT* cDNA and expressed relative to unmodified undifferentiated mESC. (C) PCR products from reactions using cardiac gene-specific primers on cDNA from d 12 D3-eGFP EB, d 12 D3G4-B EB, and mouse heart run on an agarose gel for comparison of cardiac gene expression patterns.

3.4 DISCUSSION

The goal of this study was to determine whether continuous expression of high levels of GATA4 throughout differentiation in EB would increase the cardiogenic potential of mESC. We describe the creation of D3 mouse embryonic stem cell lines that constitutively express the early cardiac transcription factor (human) GATA4 or eGFP as a control. Differences in cardiogenic potential between the experimental and control lines were determined by recording the appearance of spontaneously contracting cardiomyocytes in EB cultured for two weeks following the onset of differentiation. In addition, we examined the expression of several cardiac-specific genes in 12 day old EB derived from the highest GATA4-expressing line compared to the eGFP control line.

Although all lines were maintained under puromycin selection, GATA4 protein levels in the three D3G4 lines described here varied widely. GATA4 protein was not detected in D3G4-C, while D3G4-B produced robust amounts of the protein and D3G4-A showed an intermediate level. Constitutive expression of ectopic GATA4 in differentiating EB from D3G4-B appeared to significantly increase the cardiogenic potential of these cells as greater than 90% of these EB contained large areas of spontaneously contracting cells, while fewer than 20% of EB derived from unmodified mESC or D3-eGFP cells displayed visible evidence of cardiomyocyte differentiation. Despite the absence of detectable GATA4 protein in D3G4-C, many more EB from this line developed areas of contracting cells compared to EB from either of the control cell lines (maximum 63% vs. 17% for the controls). This result may indicate that a small amount of

exogenous human GATA4 that is below the limit of detection by Western blot is sufficient to enhance cardiomyocyte differentiation from mESC. Alternatively, D3G4-C may have acquired other changes during its isolation and propagation that predisposed the cells to cardiomyogenesis, perhaps explaining the earlier appearance of contracting EB from this line than from D3G4-B (Figure 7).

We used qRT-PCR to identify differences between d12 EB derived from D3G4-B and D3-eGFP in the mRNA levels of four cardiac-specific genes that are expressed at different stages of cardiomyogenesis (Table1). High levels of human GATA4 expression were detected in D3G4-B EB compared to the D3-eGFP control EB. In addition, increases of up to two orders of magnitude were observed for endogenous cardiac genes in EB from D3G4-B compared to D3-eGFP EB and on balance, the expression pattern of these genes in D3G4-B EB was not unlike that in mouse heart.

Together, our data strongly indicate that constitutive GATA4 overexpression can be a powerful driver of in vitro cardiac differentiation of mESC. Our findings are consistent with previous studies that extol GATA4 as the master regulator of cardiogenesis (*13, 203*). Because GATA4 is known to be expressed in vivo throughout all developmental stages from precardiac mesoderm to the adult heart (*14*), it is not unexpected that constitutive overexpression of GATA4 can drive pluripotent stem cells toward a cardiac lineage without detrimental effects on terminally differentiated cardiomyocytes. However, the approach taken in this study involves permanent chromosomal modification of stably transfected stem cells, a system that is undesirable for the generation of clinically viable cardiomyocytes because of its oncogenic potential (*85*). Additionally, the use of a single D3G4 line for experimentation does not allow extrapolation to other *GATA4*-transduced pluripotent stem cell lines as each line divides at its

own pace and it is unclear how closely related different lines are to one another once they have been sufficiently expanded for differentiation and gene expression analyses. For example, we found that several lines, including D3G4-A, were much more prone to spontaneous differentiation than others. This may be due to differences in transgene integration sites that differentially affect transgene expression and may cause selection of different second-site events that in turn can lead to variations in growth rate and spontaneous differentiation between individual lines.

While our study demonstrates that forced expression of GATA4 enhances the cardiogenic potential of mESC, implementation of strategies to express this and other cardiogenic factors through non-integrative mechanisms will be essential to produce a clinically relevant product for the treatment of cardiac ischemia. Our observation that human GATA4 induces expression of its mouse counterpart as well as other cardiac genes, directly or indirectly, suggests that an early pulse of ectopic GATA4 expression may be sufficient to commit daughter cells to the cardiac lineage and thus it will be worthwhile to determine whether transient ectopic GATA4 expression from a replication-defective, non-integrating viral vector can enhance cardiomyocyte production from pluripotent stem cells. The work described in the next chapters was aimed at determining whether transient expression of a powerful cardiac transcription factor like GATA4 from our vectors is capable of initiating a cascade of cardiac gene expression, conferring enhanced mESC cardiogenic potential.

4.0 GENERATION OF A JDBB-BASED HSV VECTOR FOR THE DIFFERENTIATION OF EMBRYONIC STEM CELLS INTO CARDIOMYOCYTES

4.1 INTRODUCTION

Embryonic stem cells (ESC) are derived from the inner cell mass of the blastocyst-stage embryo and can grow indefinitely in culture. ESC possess two defining characteristics. They can self renew to produce identical daughter ESC, and they can differentiate to give rise to cells of all three germ layers, endoderm, ectoderm, and mesoderm, that are present from embryogenesis through adulthood. (*73*). Murine embryonic stem cells (mESC) are the best characterized of all pluripotent stem cells, and ever since their initial isolation in 1981 (*74*, *75*), ways have been sought to intervene in their complex differentiation processes to enrich for cells of a particular lineage. Because cardiovascular disease is the largest cause of global morbidity and mortality (*22*), and the adult heart lacks the ability to regenerate functional cardiomyocytes, there is much interest in developing the technology to generate cardiomyocytes from in vitro differentiated pluripotent stem cells for use in cell-based heart therapy.

Many different methods have been tested to enhance the cardiac differentiation of mESC. Most begin with the aggregation in suspension of ESCs to form embryoid bodies (EB), structures resembling a mouse embryo that contain a mixture of differentiating cells derived from the three germ layers (*117*). Upon attachment to gelatin-coated plates, EB maintained in differentiation

media will typically form spontaneously contracting areas indicative of cardiomyocyte formation at a low frequency, a process influenced by a number of factors including the specific mESC line and culture conditions (*116*). The difficulty has been unraveling the events that lead to cardiomyogenesis and intervening to create a population highly enriched for cells with cardiogenic potential.

Fluorescence-activated cell sorting (FACS) has been used successfully by a number of groups to sort EB cell populations for cardiac progenitor cells. Gordon Keller's lab elucidated some of the earliest events in cardiomyogenesis and discovered that the time-dependent coexpression of Flk-1 and Brachyury marks a cell population highly enriched for cardiac progenitors (*119, 122*). Another group used FACS to obtain a population of cells from 5 day old EB that co-express CXCR4 and Flk-1 and has a dramatically increased capacity for cardiomyocyte differentiation (*124*).

Culture conditions, gene transfer, and treatment with small molecules have also been used to drive pluripotent stem cells to differentiate toward a cardiac lineage. Induced Notch4 expression (*123*), addition of VEGF to culture media (*125*), and small-molecule modification of BMP signaling (*126-129*) all successfully enhanced cardiomyocyte development. Although some of the transcription factors vital to cardiomyocyte differentiation have been identified, commonly used methods for gene transfer to pluripotent stem cells have limitations. Non-viral gene transfer methods such as electroporation or nucleofection require high DNA concentrations and large numbers of cells, and cell viability and transduction efficiency are often poor (*204, 205*). The use of viral vectors for gene delivery to pluripotent stem cells has many advantages over other methods, including high efficiency and low toxicity to host cells. Lentiviruses and retroviruses efficiently infect stem cells and express transgenes with low toxicity, but the fact that they

integrate into the host cell genome is a major deterrent to their use in cells for clinical translation (*206, 207*). Adenovirus and adeno-associated viral vectors infect stem cells inefficiently and exhibit poor transgene expression (*208, 209*). AAV, lenti- and retroviral vectors in addition have limited transgene capacity, precluding the delivery of large or multiple transgenes from a single vector.

HSV vectors have many advantages for gene transfer to embryonic stem cells. They are easily rendered replication defective and strategic genome modifications can limit or prevent the expression of viral genes that are toxic to host cells. HSV has a large genome, much of which is not required for efficient infection or transgene expression, and therefore has ample room for large transgene cassettes. HSV vector JDββHE (*132*) is highly replication defective, containing deletions of two immediate early genes, ICP4 and ICP22, as well as a complete deletion of the internally repeated or "joint" sequences (JD, joint deleted). The promoters of the immediate early ICP0 and ICP27 genes are replaced with copies of the early (β) thymidine kinase gene promoter so that the toxic products of these genes are significantly expressed only in engineered cell lines that provide the essential ICP4 protein in trans for virus production. As a result of these and other modifications, the vector that has ample room for foreign sequences. ICP0 is a multi-functional protein with non-specific transactivating activity attributable to its ability to protect the viral genome against epigenetic silencing. The ICP0 promoter substitution in JDββHE reduces expression of the ICP0 100-fold in embryonic stem cells, limiting ICP0-mediated cytotoxicity, yet this low level generates enough ICP0 activity to support robust transgene expression (*132*). JDββHE transduction of mESC does not interfere with self renewal or mesoderm induction, as evidenced by normal expression of Brachyury and Flk-1 in EBs derived from mESC infected at MOIs of up to 100. Furthermore, expression of developmental transgenes from JDββHE

produced lineage-related gene expression changes in differentiating EB (*132*). For these reasons, we chose the JDββHE backbone for insertion of early cardiac transcription factors *GATA4* and *NKX2.5* in order to generate a vector that could drive mESC differentiation toward a cardiac lineage.

GATA4 is one of the key regulators of cardiogenesis that is expressed throughout cardiac development and in the adult heart. It is co-expressed with NKX2.5 in the precardiac mesoderm where these two proteins interact to synergistically activate the transcription of numerous other cardiac genes, such as the genes for *TBX5*, *α-MHC*, and *cTnT* (*141*). We generated vector vββG4Nk by homologous recombination between the JDββHE genome and a *GATA4-Nkx2.5* co-expression cassette. Transduction of mESC with vββG4Nk induced the expression of murine cardiac-related genes, enhancing the cardiogenic potential of the cells as evidenced by a greater proportion of EB containing contracting cardiomyocytes following mESC infection with vββG4Nk than with JDββHE or mock infection.

4.2 MATERIALS AND METHODS

4.2.1 Cells and culture conditions

ICP4 deficient HSV vectors were propagated on ICP4 complementing cells lines. 7b cells are Vero (African green monkey kidney) cells that contain the both the ICP4 and ICP27 coding sequences under control of their native promoters (*170*). U2OS-ICP4 cells are human osteosarcoma cells that contain the ICP4 coding sequence under control of its native promoter (*169*). 293T cells are a derivative of human embryonic kidney 293 cells that contain the SV40 T-

antigen. All three cell lines were cultured in DMEM (Corning) supplemented with 10% FBS (GIBCO), 100 U/ml penicillin (Cellgro), and 100 μg/ml streptomycin (Cellgro). U2OS-ICP4 cells were maintained under constant selection with 2 μg/ml puromycin (Sigma).

D3 mouse embryonic stem cells (a gift from T.E. Smithgall, University of Pittsburgh) were cultured in DMEM (Corning) supplemented with 15% FBS (GIBCO), 1% non-essential amino acids (GIBCO), 1 mM sodium pyruvate (GIBCO), 100 U/ml penicillin, 100 μg/mL streptomycin, 0.1 mM 2-mercaptoethanol (GIBCO), and 1000 U/ml mouse LIF (Millipore) on 10 centimeter dishes coated with 0.2% gelatin (Sigma). Media was exchanged daily and cells were passaged with trypsin every 2-3 days to maintain a state of self-renewal and minimize spontaneous differentiation.

4.2.2 G4NkmCh cassette construction

The G4NkmCh cassette was constructed in the commercially available pcDNA3.1(+)Hyg plasmid (Life Technologies). First, the 2.3 kb PvuII fragment was removed and the plasmid backbone self-ligated. Next, a PacI/NheI linker was added into the SapI site of the plasmid backbone to create additional unique sites for cloning. The CMV promoter was then replaced with the CAG promoter, which was derived from plasmid pPEP100 (kindly provided by P. Spear, Northwestern University) (*194*) as a 1.7 kb SpeI to EcoRI fragment. This fragment was inserted into the pcDNA plasmid that had been digested with the same enzymes. The resulting plasmid was called pcDNA-CAGp. Next human *GATA4*, human *NKX2.5*, and mCherry were PCR amplified with primers to add restriction sites and 2A sequences. Plasmids containing human *GATA4* and *NKX2.5* cDNAs were obtained from Open Biosystems. mCherry was derived from pEP-miR (Cell Biolabs). Briefly, *GATA4* was PCR amplified with primers forward (F/)

F/EcoRI-GATA4 and reverse (R/) R/GATA4-T2A and Nkx2.5 cDNA was amplified with primers F/T2A-Nkx and R/Nkx-Xho. The resulting two PCR products were then gel purified and amplified together with primers F/EcoRI-GATA4 and R/Nkx-Xho to give a fragment that begins with an EcoRI restriction site followed by a start codon, the *GATA4* coding sequence, the T2A sequence, the *NKX2.5* coding sequence, and ending with an XhoI restriction site (EcoRI-GATA4-T2A-Nkx2.5-XhoI) all in the same open reading frame (ORF). Plasmid pcDNA-CAGp and fragment EcoRI-GATA4-T2A-Nkx2.5-XhoI were each cut with EcoRI and XhoI and the fragment was ligated into the plasmid backbone to give rise to plasmid pG4Nk.

In the final step, mCherry was amplified with primers F/Xho-E2A-mCherry and R/mCherry-PmeI, resulting in a fragment beginning with an XhoI restriction site, followed by the E2A sequence, the mCherry coding sequence, and ending with a PmeI restriction site (XhoI-E2A-mCherry-PmeI). This fragment and plasmid pG4Nk were digested with XhoI and PmeI and the mCherry fragment was ligated into the plasmid, giving rise to plasmid pG4NkmCh, with *GATA4, NKX2.5*, and mCherry all in one continuous ORF. Sequences were obtained for all parts of the cassette (Genewiz) to verify that no errors occurred during PCR amplification.

Table 4. Primer sequences for construction of G4NkmCh cassette

F/EcoRI-GATA4	ccacaGAATTCGTAATAGGATAGCGACatgtatcagagcttggccatg
R/GATA4-T2A	*CCTCGACGTCACCGCATGTTAGCAGACTTC*CTCTGCCCTCTCCGGAGCCc gcagtgattatgtccccgtgac
F/T2A-Nkx	*GAAGTCTGCTAACATGCGGTGACGTCGAGG*AGAATCCTGGCCCAatgttcccc agccctgctctcacg
R/Nkx-Xho	CTGTAGCTCGAGccaggctcggataccatgcag

F/Xho-E2A-mCherry	CTGAGCCTCGAGGGTCAATGTACTAACTACGCTTTGTTGAAACTCGCTGG CGATGTTGAAAGTAACCCCGGTCCTatggtgagcaagggcgaggaggat
R/mCherry-PmeI	CTGTGGGTTTAAACctatcatgggtccttgtacagctcg

Underlined sequences are restriction sites, green designates start codons, blue designates 2A sequences (italics for partial 2A), and red designates stop codons.

4.2.3 Vector vββG4Nk construction

Vector JDββHE (*132*) was engineered to contain the G4NkmCh cassette via homologous recombination in ICP4/ICP27 complementing 7b cells through transfection and infection as previously described (*170*). The recombination plasmid was constructed as follows. The G4NkmCh cassette was isolated from pG4NkmCh by digestion with NheI, filling in of the 5' overhang, digestion with SpeI, and gel purification of the 5.2 kb band containing the cassette. In parallel, U_L41 targeting plasmid pH41 (*210*) was digested with BamHI, filling in of the 5' overhang, digestion with SpeI, and the G4NkmCh cassette was ligated into the pH41 backbone to generate U_L41 targeting plasmid pH41G4NkmCh. The plasmid was linearized by digestion with ClaI and gel purified for transfection. 7b cells that had been plated in 6 well plates 24 h prior and were approximately 75% confluent were transfected with 3µg linearized pH41G4NkmCh using Lipofectamine LTX (Invitrogen) according to the manufacturer's protocol. 24 h post transfection, the 7b cells were infected in a monolayer in 6 well plates with JDββHE at an MOI of 0.04 or 0.15 pfu/cell in 1 ml serum free DMEM at 37°C with 5% CO_2 for 2 h with occasional rocking. 2 ml serum free media was added to the wells and the plates were incubated at 33°C. The virus was allowed to replicate until nearly all of the cells in a well demonstrated cytopathic effects (CPE), and the cells and virus were collected in their media,

sonicated, aliquoted, and frozen at -80°C. Fresh 7b cells were plated in 6 well plates and infected at a range of concentrations with the virus collected from the transfection/infection. The virus was allowed to replicate for 48-72 h. Wells with widely spaced plaques were identified, and plaques that expressed both eGFP and mCherry were picked with a pipette under a fluorescence microscope and serially diluted on 7b cells in 96 well plates to obtain clones of vββG4Nk. These clones were plaque purified three times by choosing wells with a single $eGFP^{+}/mCherry^{+}$ recombinant, using the virus from the plaque to infect fresh cells in suspension, plating serial dilutions of these cells, and repeating until a clonal population of virus was obtained as indicated by 100% eGFP-mCherry co-expression.

4.2.4 Large scale production of vββG4Nk

To obtain a large quantity of high titer virus to complete these studies, vββG4Nk production was scaled up from a 96 well plate to 10-20 T150 tissue culture flasks. For large scale production, U2OS-ICP4 cells were plated in the desired number of T150 flasks and when the cells became confluent, they were infected in a monolayer with one isolate of the plaque purified virus at an MOI of 0.1 pfu/cell. The cells were infected in 10 ml serum free DMEM (Corning) per T150 flask with occasional gentle agitation for 2 h at 37°C. After two hours, 10 ml serum free DMEM was added to each flask, and the infected cells were incubated at 33°C to allow for maximum virus survival without cell overgrowth until the entire flask reached CPE, typically 7-10 days post infection (dpi). The media was then collected and the dead cells were spun out in a table top centrifuge at 3,000 rpm for 10 min at 4°C. The supernatant containing the virus was filtered through a 0.8 μm Versapor membrane (PALL Corporation), and then concentrated by multiple cycles of high speed centrifugation at 19,500 rpm for 45 min at 4°C. All of the supernatant was

spun down into two tubes, and the resulting viral pellets were each gently resuspended in 200 µl phosphate buffered saline (PBS) with 10% glycerol by gentle agitation at 4°C for 24-48 h. The resuspended pellets were combined, divided into 5-20 µl aliquots, and stored at -80°C. One aliquot was then titered by infecting U2OS-ICP4 cells with serial dilutions for 2 h at 37°C, overlaying with high density DMEM containing 5% methyl cellulose (Sigma), and incubating at 33°C until the plaques were large enough to count under the microscope, typically 48-72 hpi.

4.2.5 Western blot analysis

GATA4 and NKX2.5 expression from pG4NkmCh was confirmed by transfection of 293T cells with the plasmid using Lipofectamine LTX (Invitrogen) according to the manufacturer's protocol and collection of total cellular protein 24 h later. GATA4 and NKX2.5 expression from vββG4Nk was confirmed by infection of U2OS-ICP4 cells at a range of MOIs (0.005 – 0.5) and protein collection at 24 hpi. Cell lysates were harvested in RIPA lysis buffer supplemented with protease inhibitors (Roche). Proteins were separated on a 10% polyacrylamide-SDS gel and transferred by semi-dry transfer onto PVDF membranes. The membranes were washed in Tris-buffered saline (TBS) and blocked for 1 h at room temperature in TBS-T (20 mM Tris, 0.5 M NaCl [pH 7.5] plus 0.5% Tween 20) supplemented with 10% nonfat dry milk. Antibodies diluted in blocking buffer were reacted with the membranes overnight at 4°C, washed 3 times for 10 min each in TBS-T, and reacted with horseradish peroxidase-conjugated secondary antibody diluted 1:10,000 in blocking buffer for 1 h at room temperature. The bound Igs were revealed by enhanced chemiluminescence (Thermo Scientific). Antibodies are listed in Table 2.

4.2.6 Embryoid body assay

D3 mouse embryonic stem cells were infected in suspension with JDββHE or vββG4Nk or mock infected in a small volume in Eppendorf tubes at 37°C with continuous rotation for 1-2 hours. Infected cells were diluted in mESC media without LIF at a concentration of $4x10^4$ cells/ml. 20 µl drops of cells were pipetted onto the lid of a petri dish, and the lid was inverted over the dish that contained 30 ml sterile water to prevent the drops from evaporating. The cells were incubated at 37°C with 5% CO_2 and allowed to aggregate to form embryoid bodies (EB) and differentiate for two days in hanging drops. After 48 h in hanging drops, the EB were pipetted one per well into 48 well plates, each well containing 500 µl mESC media without LIF. The EB were observed daily for the appearance of spontaneously contracting cells, and the number of wells containing these cells was recorded each day.

4.2.7 RNA extraction and quantitative RT-PCR analysis

Total RNA was extracted from D3 mES cell lines and embryoid bodies using Qiagen RNeasy Plus mini kit (Qiagen) according to the manufacturer's protocol.

Total RNA was extracted from the heart of an adult mouse as follows. The mouse was humanely sacrificed and the heart dissected out and immediately placed into 2 ml RNAlater (Qiagen) to stabilize and protect RNA. The heart was then minced with two razor blades and transferred into a Dounce homogenizer in 2 ml TRIzol reagent (Life Technologies) and mechanically ground. Remaining solids were pelleted and discarded, and 200 µl chloroform was added to the supernatant. The solution was transferred into two 1.5 ml phase-lock tubes and centrifuged for 15 min at 14,000 rpm at 4°C. The aqueous phase was transferred into a gDNA

eliminator column and the RNA extracted using an RNeasy Plus mini kit (Qiagen) according to the manufacturer's protocol.

Reverse transcription was performed on 1-2 μg RNA in 20 μl final volume using random decamers as first strand primers with Ambion's RETROscript Kit (Ambion), and the resulting cDNA was diluted 1:10 for quantitative RT-PCR analysis.

Primers were obtained from Invitrogen. Primer sequences and references for qPCR are listed in Table 3. qPCR was performed using LightCycler SYBRgreen Master Mix (Roche) or TaqMan Gene Expression Assays (Invitrogen) and a Step One Plus Real-Time PCR System (Applied Biosystems). Cycling conditions were 95°C for 10 min followed by 40 cycles of 95°C for 15 sec and then 60°C for 1 min. Each cDNA was analyzed in triplicate, and the results for the three wells were averaged. Threshold cycle (C_t) values were used to calculate changes in gene expression using the $2^{-\Delta\Delta Ct}$ method (*195*). Expression levels were normalized to *HPRT* mRNA for SYBRgreen or 18S ribosomal RNA levels for TaqMan, and expressed relative to uninfected D3 mESC.

4.3 RESULTS

4.3.1 G4NkmCh cassette construction and confirmation

A cassette designed for recombination with the JDββHE vector genome in order to express human *GATA4*, *NKX2.5*, and mCherry as a marker for gene expression was constructed as detailed in Materials and Methods. The expression of these three genes is controlled by the CAG

promoter. *GATA4*, *NKX2.5*, and eGFP are translated from a single multigene ORF by the inclusion of in frame 2A sequences between genes (Table 5). 2A sequences are short, 18-22 amino acid sequences derived from small RNA viruses, and allow the generation of multiple proteins from a single transcript (*211*). They function through a "ribosomal skipping" mechanism between the highly conserved glycine and proline residues at the carboxyl terminus of the 2A sequence, leaving a tag at the carboxyl end of the upstream protein and adding the terminal proline residue to the downstream ("2B") sequence without impairing the 2B translation efficiency (*212*). In this construction, we took advantage of two known 2A sequences, T2A and E2A. Two distinct sequences were used to minimize the possibility of recombination. The advantage of using 2A sequences to form polycistronic transcripts is that they are highly efficient and allow for stoichiometric expression of individual transgene products while avoiding the need for separate promoters. This 2A system allows recombination of three separate transgenes into JDββHE through a single recombination event.

Table 5. 2A sequences used in HSV vectors and their 'skipping' sites.

Family	Example	Designation	Amino Acid Sequence
			2A "skipping" site ↓
Picornaviridae	FMDV	F2A	VKQTLNFDLLKLA**GDVE**S**NPG** **P**
	ERAV	E2A	QCTNYALLKLA**GDVE**S**NPG** **P**
Tetraviridae	TaV	T2A	EGRGSLLTC**GDVE**E**NPG** **P**

Following PCR amplification of human *GATA4* and *NKX2.5* cDNAs with primers to add the necessary 2A sequences and restriction sites, the cassette was assembled into a shuttle plasmid (Figure 9A) and sequenced. The sequences were verified and plasmid pG4NkmCh was transfected into 293T cells. Cell lysates were collected 24 h post transfection, and Western blotting was performed to confirm expression of the three proteins.

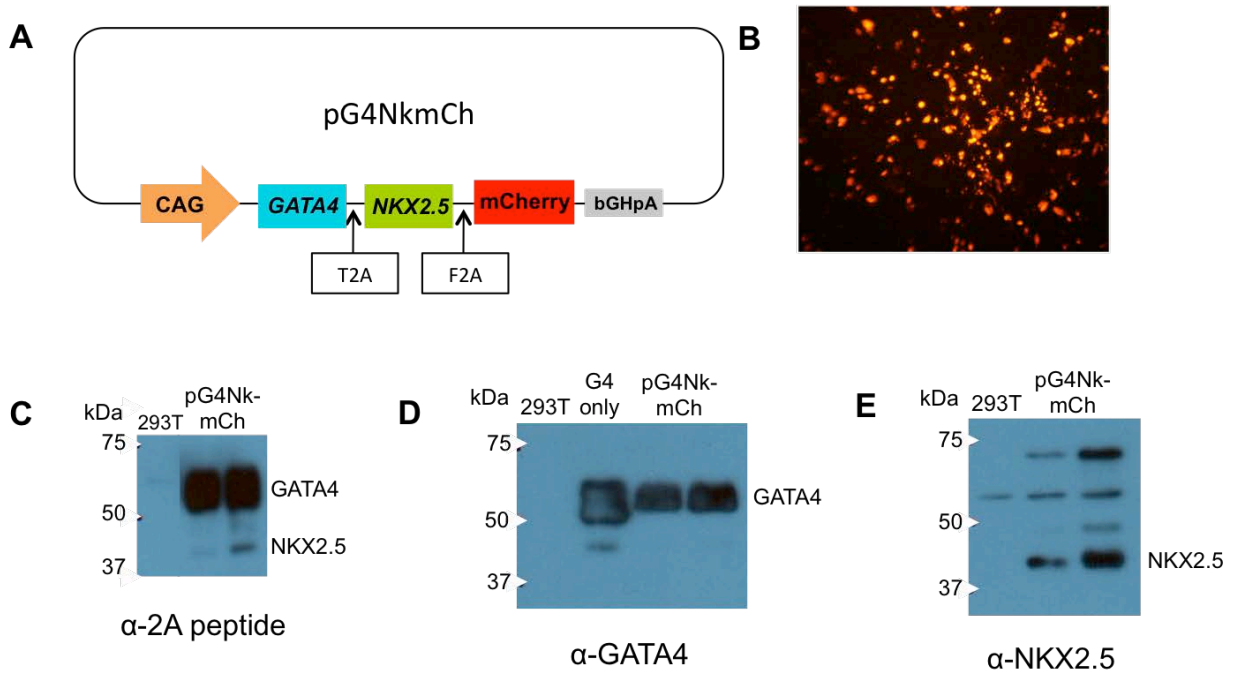

Figure 9. Plasmid pG4NkmCh and transgene expression upon transfection into 293T cells.
A schematic of the structure of the transgene cassette in plasmid pG4NkmCh is shown in (**A**). The CAG promoter drives expression of three transgenes, *GATA4*, *NKX2.5*, and mCherry, with T2A and F2A sequences separating them. (**B**) mCherry expression in 293T cells transfected with plasmid pG4NkmCh 24 h post transfection. (**C**) Expression of both GATA4 and NKX2.5 proteins from pG4NkmCh 24 h post transfection in 293T cells is revealed in a Western blot with a primary antibody against the 2A peptides. Expression of GATA4 and NKX2.5 was also demonstrated through Western blotting with specific GATA4 (**D**) and NKX2.5 (**E**) antibodies. The two lanes for pG4NkmCh in (C-E) represent two separate clones of pH41G4NkmCh transfected independently into 7b cells. G4 only (D) represents 293T cells transfected with a plasmid that expresses GATA4 but not NKX2.5 from the CMV promoter.

mCherry expression was readily observed by fluorescence microscopy in 293T cells transfected with pG4NkmCh (Figure 9B). Using an antibody against the carboxy-terminal 2A peptides, proteins of the expected size for GATA4 (~50 kDa) and NKX2.5 (~40 kDa) were detected in lysates of 293T cells transfected with pG4NkmCh (Figure 9C). Likewise, GATA4 (Figure 9D) and NKX2.5 (Figure 9E) were detected by their individual monoclonal antibodies on separate Western blots. The NKX2.5 antibody consistently detects additional larger proteins on Western blots aside from the ~40 kDa NKX2.5 protein. It is unlikely that these are fusion proteins between NKX2.5 and GATA4 or mCherry since no bands of the corresponding sizes were detected on the individual blots for GATA4 (Figure 9C, no ~70-kDa or ~45-kDa bands) or mCherry (data not shown), or the blot probed with the anti-2A peptide antibody.

4.3.2 Recombination of the G4NkmCh cassette into JDββHE and growth of vββG4Nk

The G4NkmCh cassette was cloned into the U_L41 targeting plasmid pH41 (*210*) to create plasmid pH41G4NkmCh (Figure 10A). This plasmid has long regions of homology ("homology arms") to the viral U_L41 locus on both ends of the transgene cassette. These homology arms contain the sequences flanking the U_L41 deletion in the JDββHE genome, 1.7 kb of the 5' flank and 1.5 kb of the 3' flank, to allow for homologous recombination of G4NkmCh into the vector. Plasmid pH41G4NkmCh was transfected into 7b cells and cell lysates were collected 48 h post transfection to verify that GATA4 and NKX2.5 proteins were expressed appropriately within the context of the surrounding U_L41 sequences.

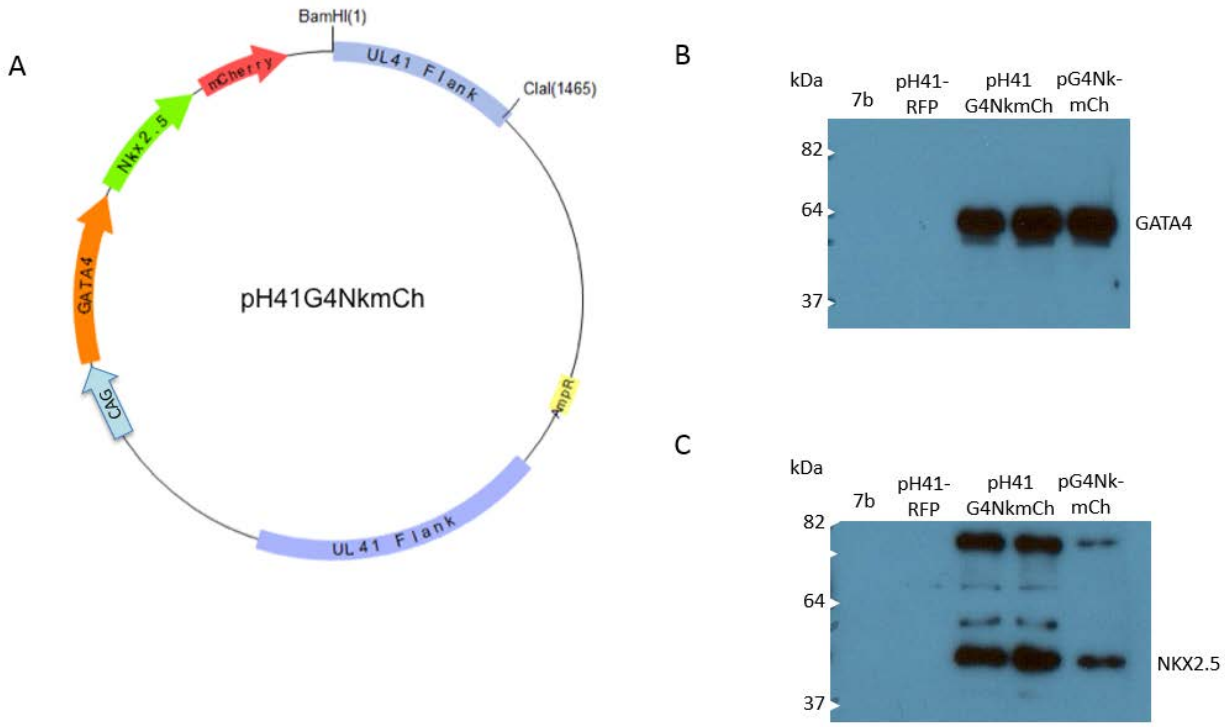

Figure 10. Schematic of and transgene expression from U_L41 targeting plasmid pH41G4NkmCh. 7b cells were transfected with pH41G4NkmCh (A), cell lysates collected, and Western blots were performed to demonstrate expression of GATA4 (B) and NKX2.5 (C) proteins. Lysates from untransfected 7b cells and 7b cells transfected with RFP expression plasmid pH41RFP were included as negative controls. 7b cells transfected with pG4NkmCh were included as positive controls for both GATA4 and NKX2.5 expression. The two lanes for pH41G4NkmCh in (B) and (C) represent two separate clones of pH41G4NkmCh transfected independently into 7b cells.

7b cells transfected with pH41G4NkmCh clearly expressed mCherry 24-48 h post transfection when examined by fluorescence microscopy, and red fluorescent protein (RFP) expression was evident in cells transfected with control plasmid pH41RFP containing the RFP gene under control of the CMV promoter in plasmid pH41 (not shown). Western blotting demonstrated that GATA4 (Figure 10B) and NKX2.5 (Figure 10C) were expressed in pH41G4NkmCh-transfected 7b cells at the correct sizes, co-migrating with their counterparts

from pG4NkmCh-transfected cells; no products were observed in untransfected or pH41RFP-transfected cells. With this verification completed, the G4NkmCh cassette was recombined into HSV vector JDββHE in ICP4/ICP27-complementing 7b cells using a transfection/infection protocol adapted from reference (*213*), as described below.

ClaI was used to linearize pH41G4NkmCh in the plasmid backbone outside of the insert (Figure 10A). Linearized pH41G4NkmCh was transfected into 7b cells, and 24 h post transfection the cells were infected with JDββHE. The transfected/infected 7b cells were incubated at 33°C to maximize virus yield. Once all of the cells showed signs of CPE (Figure 11A), the virus was collected and used to infect fresh 7b cells in 6 well plates at a range of dilutions to obtain large, widely spaced plaques in at least one well (Figure 11B, *left*). Approximately 20 well-isolated plaques that co-expressed eGFP (from the deleted ICP4 locus of JDββHE) and mCherry (from the G4NkmCh cassette) were picked under a fluorescence microscope and serial dilutions were used to infect 96 well plates of fresh 7b cells (Figure 11C). Many recombinant plaques were identified in this first round of limiting dilution and several were purified through two more rounds to obtain clonal populations of vββG4Nk (Figure 11D). One clonal isolate along with JDββHE was grown in multiple T150 flasks of 7b cells to produce enough virus for experimentation. Titers of both viruses were between $2x10^6$ and $8x10^6$ pfu/ml. Final vector configurations are shown in Figure 12.

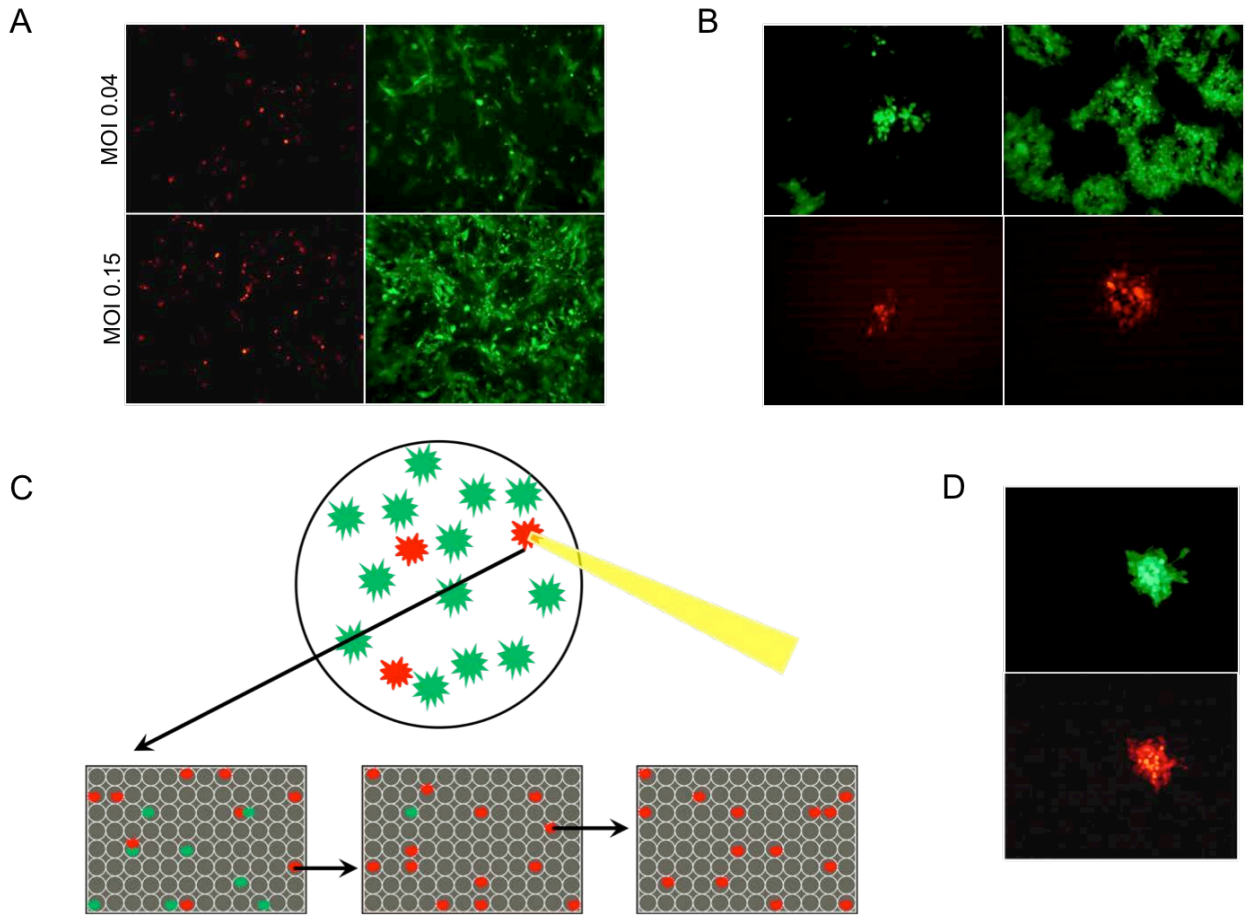

Figure 11. Recombination of the G4NkmCh cassette into JDββHE to form vββG4Nk
(A) 7b cells 48 h post pH41G4NkmCh transfection, 24 hpi with JDββHE at different MOIs. Expression of mCherry (left panels) and eGFP (right) was visualized by fluorescence microscopy. (B) After the cells from (A) were killed by the virus, fresh 7b cells were infected with dilutions of the virus from the transfection/infection, showing the presence of both recombinant (red + green) and non-recombinant (green only) viruses. (C) Schematic of the plaque purification protocol used to obtain clonal isolates of vββG4Nk. Red, recombinants (red + green); green, JDββHE. See text. (D) Plaque from a clonal isolate of vββG4Nk showing co-expression of eGFP and mCherry.

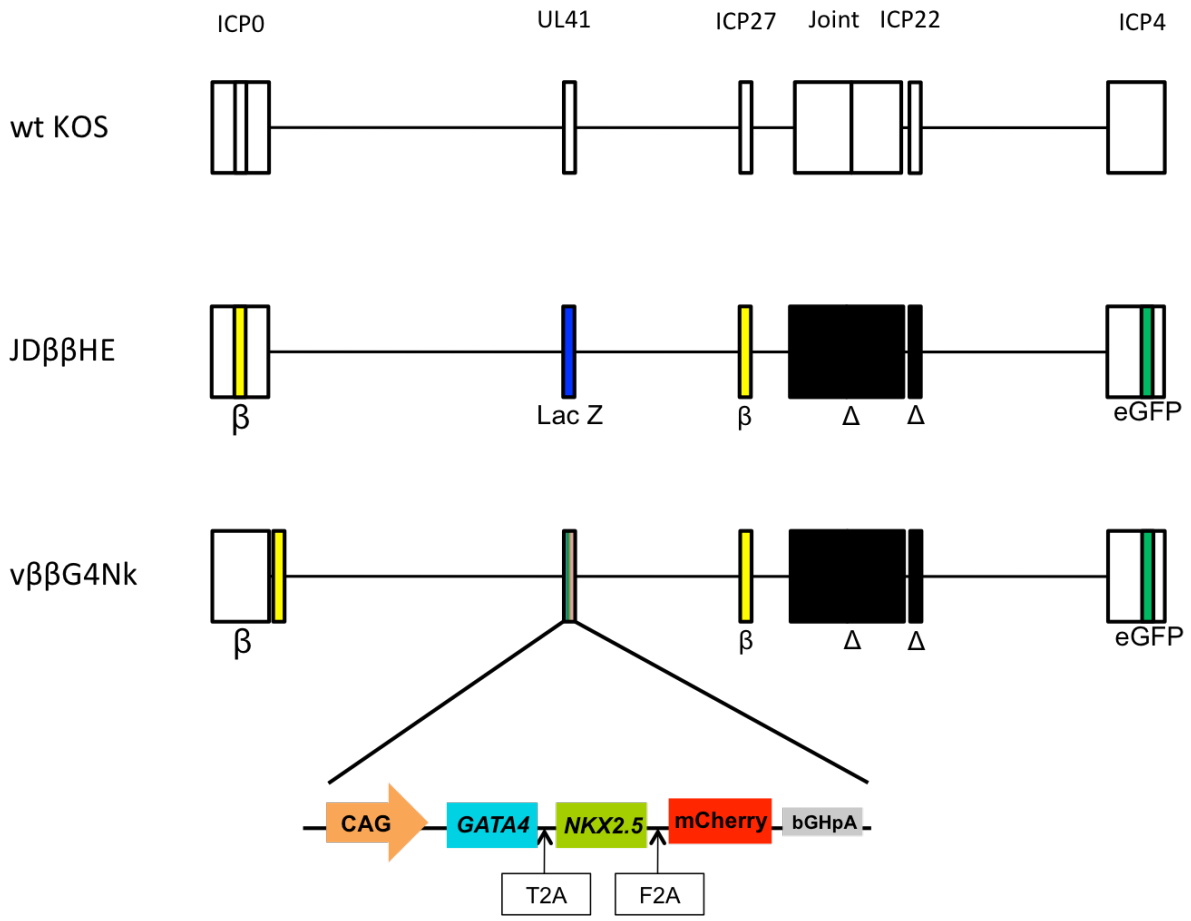

Figure 12. Description of recombinant HSV vectors
Virus genomes are shown schematically with genes labeled at the approximate location in the vectors (not to scale). Deletions in JDββHE are depicted in black, and IE to E gene promoter substitutions (β) in yellow (*132*). Transgenes are colored and labeled. For vector vββG4Nk, the entire transgene cassette shown below the vector diagram is located within the U_L41 locus.

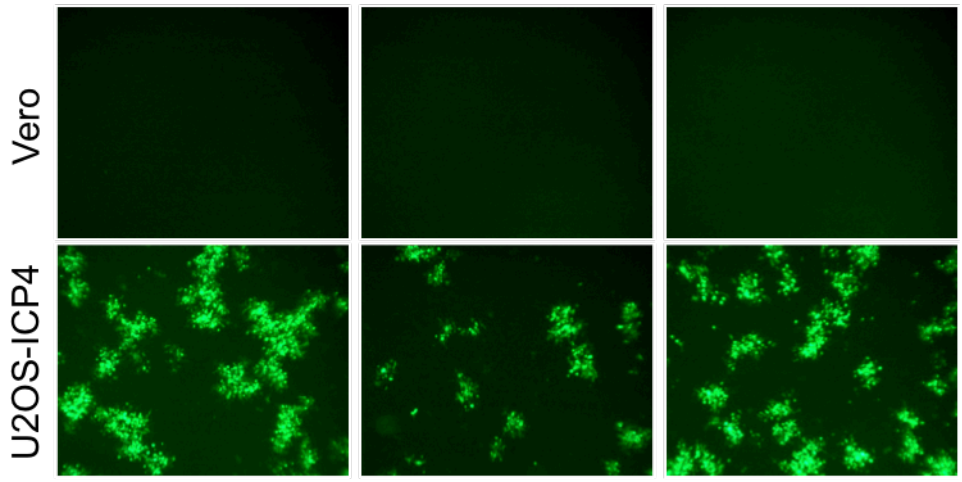

Figure 13. vββG4Nk replication on ICP4 complementing and non-complementing cells
Vero and U2OS-ICP4 cells were infected with three separate isolates of vββG4Nk and visualized at 6 dpi by fluorescence microscopy.

4.3.3 Characterization of vββG4Nk

To confirm that vββG4Nk does not replicate in non-complementing cells, both non-complementing Vero cells and ICP4-complementing U2OS-ICP4 cells were infected with three different vββG4Nk isolates. The infected cells were observed for 6 dpi. While vββG4Nk formed many plaques on ICP4-complementing cells, no plaques were observed on Vero cells (Figure 13).

Transgene expression from vββG4Nk was confirmed in ICP4 complementing U2OS cells by infecting the cells at three different MOIs (0.005 – 0.5 pfu/cell), collecting cell lysates 24 hpi, and performing a Western blot with primary antibodies against GATA4 and NKX2.5. The blots demonstrated that both GATA4 (Figure 14A) and NKX2.5 (Figure 14B) were expressed from

vββG4Nk in an MOI-dependent manner. The 2A sequences functioned correctly when expressed from the HSV vector, allowing translation of separate correctly sized proteins. A smaller product is always detected with the GATA4 antibody in Western blots of lysates from HSV-infected cells (Figure 14A). This product is independent of GATA4 expression. It is also seen in cells infected with HSV vectors that do not express GATA4 (data not shown). Thus this GATA4 antibody cross-reacts with a protein that is either expressed from HSV or induced by HSV infection.

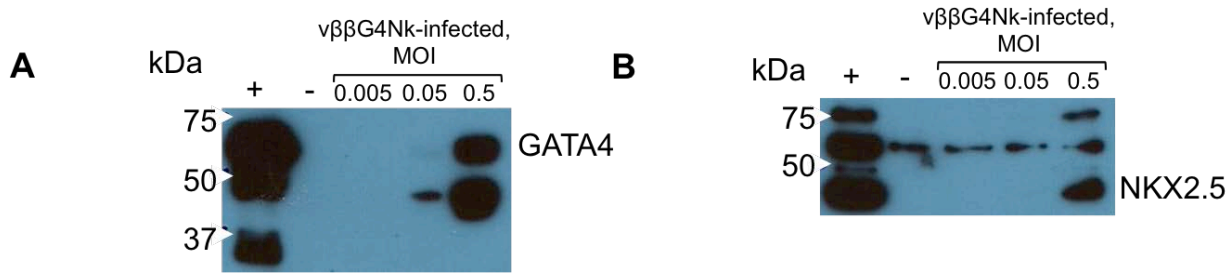

Figure 14. Expression of transgenes in U2OS-ICP4 cells infected with vββG4Nk at different MOIs
Western blots of lysates collected from ICP4-complementing U2OS cells infected with vββG4Nk and probed with GATA4 (A) and NKX2.5 (B) antibodies. Positive control in the first lane (+) is 293T cells transfected with pG4NkmCh, negative control in the second lane (-) is mock-infected U2OS-ICP4 cells.

Expression of GATA4 and NKX2.5 transgenic proteins was detected by Western blot lysates from mESC infected with vββG4Nk at MOIs of 3 and 10, but the GATA4 bands were less clear than for NKX2.5 on these blots (Figure 15). Although Western blots using this GATA4 antibody nearly always show bands with greater intensity than the antibody for NKX2.5 on the

same samples (see Figure 10 and Figure 14), in this blot the opposite is true. We are unsure of the cause of this anomaly. Transduction of mESC with vββG4Nk could be clearly observed by fluorescence microscopy as co-expression of eGFP and mCherry after infection with vββG4Nk at MOI=1 (Figure 16).

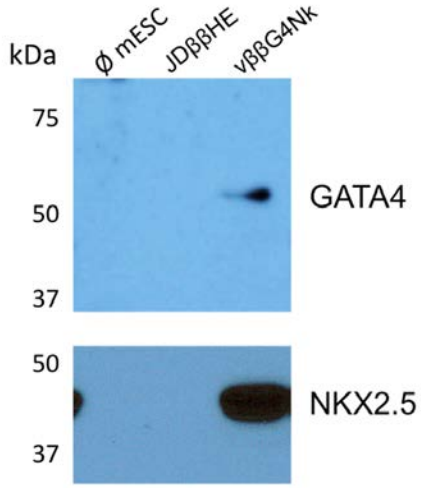

Figure 15. GATA4 and NKX2.5 transgene expression in mESC by Western blot
Lysates were collected from Ø-, JDββHE-, and vββG4Nk-infected mESC, proteins separated by SDS-PAGE, and blots probed with antibodies against GATA4 and Nkx2.5.

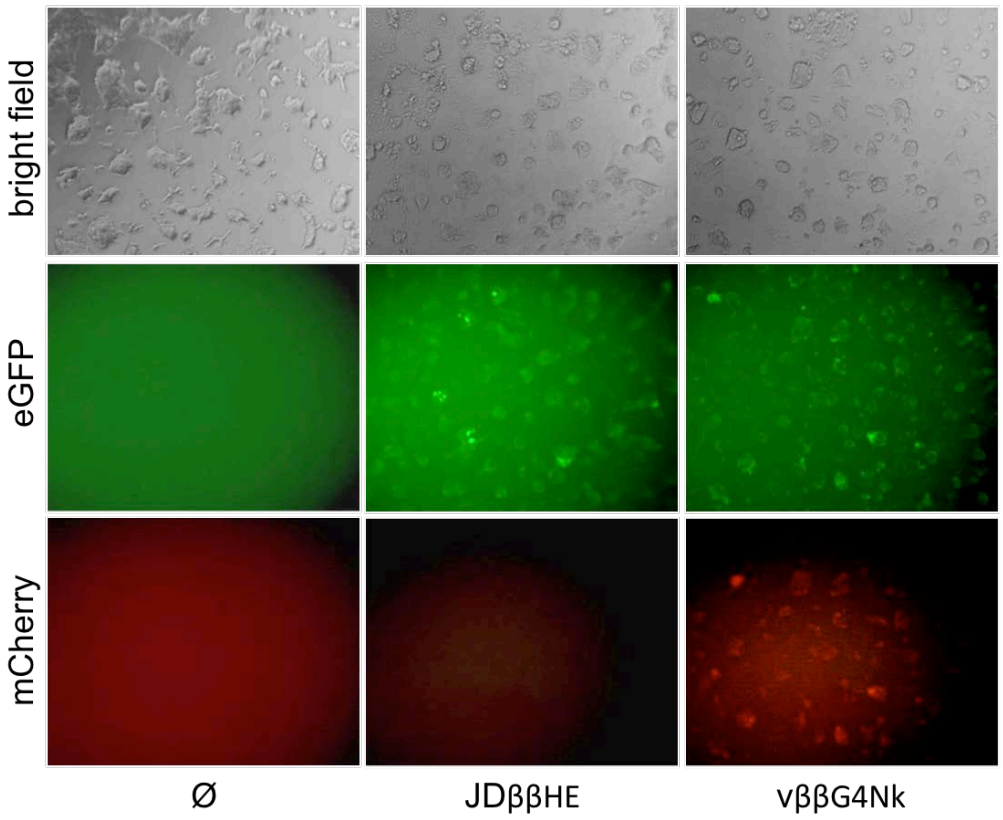

Figure 16. mESC infected at MOI=1 with vββG4Nk express eGFP and mCherry at 24 hpi
D3 mESC were infected in suspension at an MOI of 1 with JDββHE, vββG4Nk, or mock-infected and plated in gelatin-coated 6 well plates. The top row shows bright field pictures of the cells, the middle row is eGFP expression from the deleted ICP4 locus in JDββHE and vββG4Nk, and the bottom row is mCherry expression from the G4NkmCh cassette in vββG4Nk.

4.3.4 Transduction of mESC with vββG4Nk induces endogenous cardiac gene expression

In the preceding experiments, we demonstrated that vββG4Nk can efficiently transduce mESC and express transgenes GATA4, NKX2.5, mCherry, and eGFP. Next we investigated the duration of transgene expression and its effects on the expression of endogenous cardiac genes using RT-PCR and qRT-PCR.

First we checked the specificity of our human *GATA4* and *NKX2.5* PCR primers. U2OS-ICP4 cells were transfected with either pG4NkmCh or with plasmids that express *GATA4* or *NKX2.5* alone, were mock-infected or infected with vββG4Nk. RNA was collected 48 h post transfection or infection, reverse transcribed, and the cDNA used for PCR with the human-specific *GATA4* and *NKX2.5* primers. The PCR products were run on a 2% agarose gel. The primers for each transgene amplified a product of the expected size only in cells treated with the corresponding gene. A PCR-amplified *GATA4* product was detected only in cDNA from pG4NkmCh-transfected cells, cells transfected with the plasmid that expressed GATA4 alone, and cells infected with vββG4Nk. An *NKX2.5* product was only amplified from cDNA of cells transfected with pG4NkmCh, the plasmid that expressed *NKX2.5* alone, and cells infected with vββG4Nk (Figure 17A).

Mouse-specific primer sets were used for semi-quantitative RT-PCR on RNA collected from mESC, vββG4Nk-infected mESC, and d11 EB with many spontaneously contracting foci as a positive control for cardiac-specific genes. mESC infected with vββG4Nk were allowed to grow in a 6 well plate for 48 h in media containing LIF to inhibit spontaneous differentiation prior to RNA collection. The RT-PCR results demonstrated that human *GATA4* and *NKX2.5*

transgene RNA could only be detected from vββG4Nk-infected mESC, and indicated that expression of endogenous cardiac genes, including mouse *Gata4* and *Nkx2.5*, *cTnI*, and *Mlc2a*, were upregulated in vββG4Nk-transduced mESC compared to control mESC (Figure 17B). Since *cTnI* and *Mlc2a* are typically expressed in more mature cardiac cell types (Table 1), the data indicated that even when cultured with LIF, cardiac programming may begin in mESC immediately following infection with vββG4Nk. They also confirmed that the primers for human *GATA4* and *NKX2.5* were specific as no product was detected in d11 EB while the primers for mouse *Gata4* and *Nkx2.5* did amplify a product.

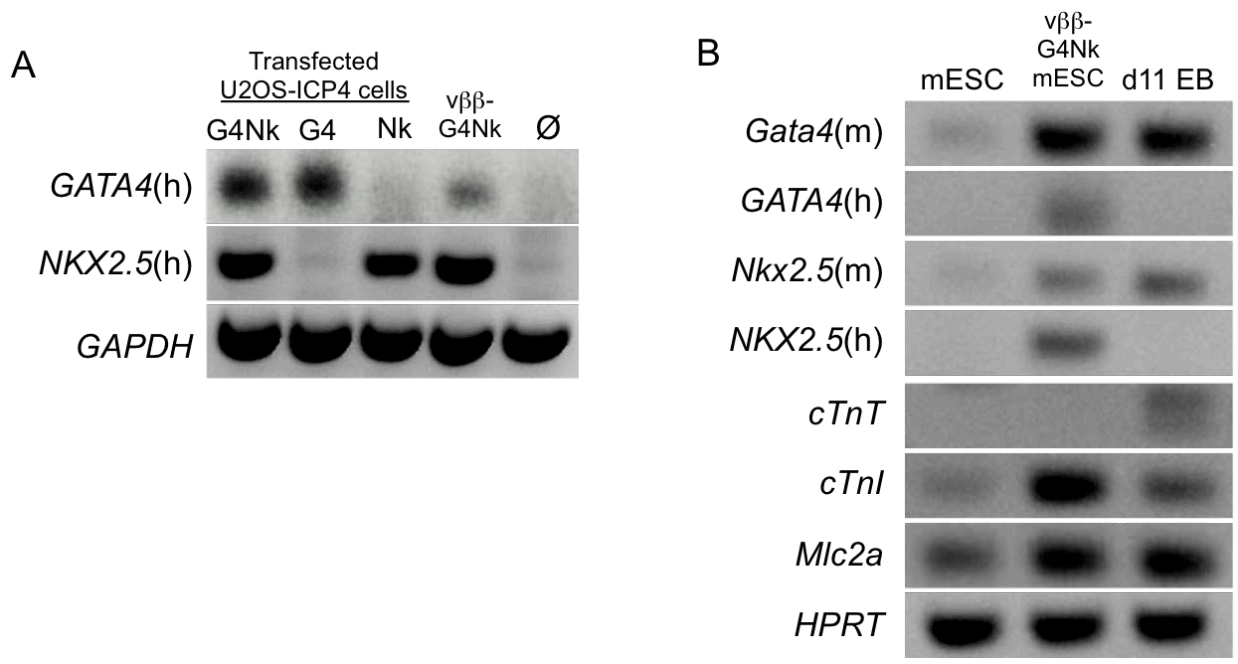

Figure 17. Semi-quantitative RT-PCR for cardiac-specific genes
Products from semi-quantitative RT-PCR run on 2% agarose gels. (A) U2OS cells were transfected with plasmids expressing both *GATA4* and *NKX2.5* (G4Nk), *GATA4* alone (G4), or *NKX2.5* alone (Nk), or 48 hpi with vββG4Nk. Products from RT-PCR with human-specific *GATA4* and *NKX2.5* primers were run on a 2% agarose gel. (B) Endogenous cardiac gene expression was examined by RT-PCR in vββG4Nk-infected mESC 48 hpi and compared to undifferentiated mESC and 11 d old EB containing many mature cardiomyocytes. RT-PCR products were amplified with cardiac gene-specific primers and run on a 2% agarose gel.

To quantitatively assess changes in gene expression, quantitative RT-PCR (qRT-PCR) was used to compare transgene and endogenous RNA expression in mESC that were mock-infected, infected with JDββHE, or infected with vββG4Nk at MOI=1. Cells were maintained in 6 well plates with mESC media plus LIF. RNA was collected 48 hpi and reverse transcribed. Mouse heart cDNA was included as a control for cardiac gene expression. Each sample was

measured in triplicate, and the C_t values were averaged. Relative mRNA levels were calculated using the $2^{-\Delta\Delta Ct}$ method (*195*) and normalized to *GAPDH* or *HPRT* mRNA levels and are presented in Figure 18 relative to uninfected mESC. We measured the expression levels of *Oct4*, a pluripotency marker, in infected mESC to determine whether transduction with JDββ-based vectors alone pushes mESC to differentiate. Expression of *Oct4* was essentially unaffected in mESC transduced with JDββHE or vββG4Nk compared to mock infected mESC (Ø). *Oct4* mRNA was not detected in the terminally differentiated cells of the adult mouse heart. High levels of human *GATA4* expression were observed in mESC transduced with vββG4Nk but not mock- or JDββHE-infected mESC or mouse heart. Abundant *GATA4* transgene expression was detected only in vββG4Nk-transduced mESC, confirming the species-specificity of our *GATA4* primers. No amplification of human *NKX2.5* cDNA was observed from vββG4Nk-infected mESC although we knew from the earlier Western blot and semi-quantitative PCR data that the gene is expressed (Figure 17). The polymerases used in these two experiments were different, Pfx for semi-quantitative PCR and the proprietary, thermostable polymerase of the SYBRgreen real-time PCR master mix (Life Technologies) for the qRT-PCR reactions, potentially accounting for the discrepancy. *GATA4* is expressed early in cardiac development, and its expression continues in mature cardiomyocytes. Our data shows that endogenous mouse *Gata4* was upregulated in response to vββG4Nk- but not JDββHE-transduction, consistent with published reports that *GATA4* binds to its own promoter to upregulate its expression (*141*). Endogenous *Gata4* expression was greater from vββG4Nk-transduced mESC than mouse heart. A similar upregulation of endogenous *Nkx2.5* in response to vββG4Nk-transduction was not observed although GATA4 can reportedly upregulate NKX2.5 expression (*141*). Contrary to what was suggested by the semi-quantitative PCR data, *cTnI* and *Mlc2a*, mRNAs that encode

cardiomyocyte structural proteins (Table 1), were not detected by qRT-PCR in any of the mESC samples but were present in mouse heart (Figure 18).

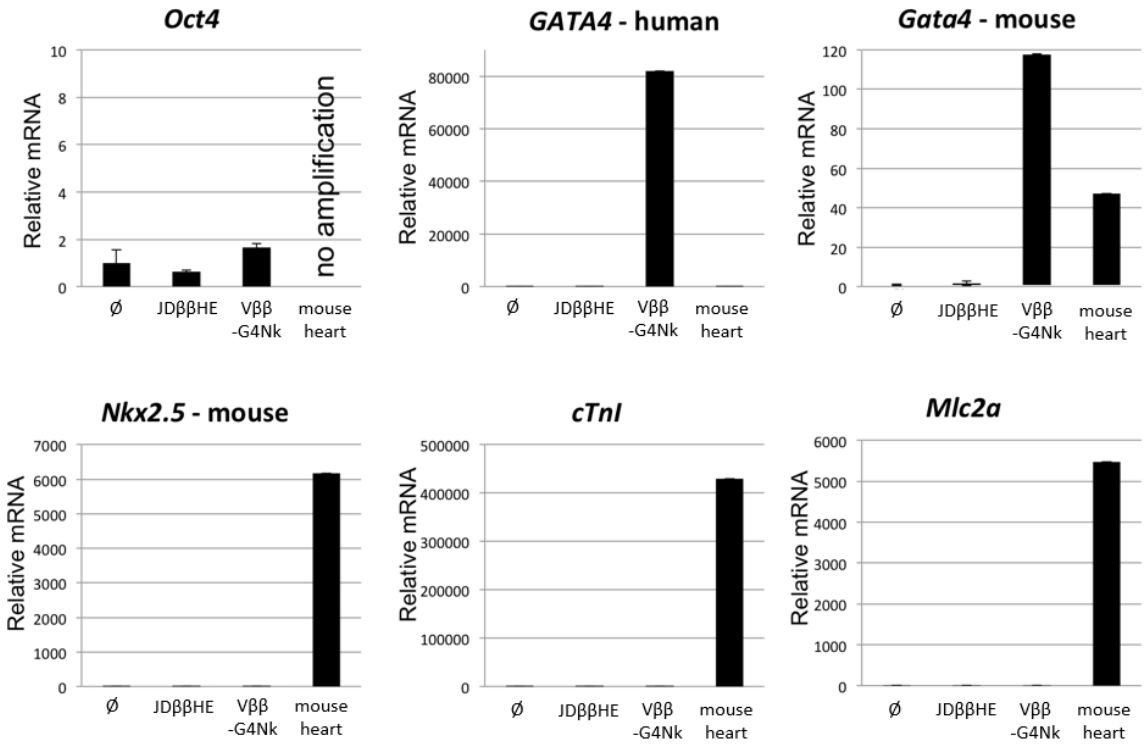

Figure 18. Gene expression in mock-, JDββHE-, and vββG4Nk-infected mESC by qRT-PCR
qRT-PCR data is shown for mESC 48 hpi with JDββHE, vββG4Nk, or mock-infected and mouse heart cDNA. Gene expression is normalized to *HPRT* or *GAPDH* mRNA and fold change is expressed relative to uninfected mESC.

To confirm the specificity of the mouse *Gata4* primers and thereby verify that endogenous *Gata4* is upregulated in mESC in response to infection with vββG4Nk, we completed additional PCR with this primer set on cDNA from vββG4Nk-infected mESC. A prominent product of the expected size (72 bp) was detected by agarose gel electrophoresis (Figure 19A), isolated, and cloned. Sequencing confirmed that the amplified product was derived from the 5' UTR of mouse *Gata4* mRNA that has no sequence homology with its human ortholog (Figure 19B) or with vector vββG4Nk.

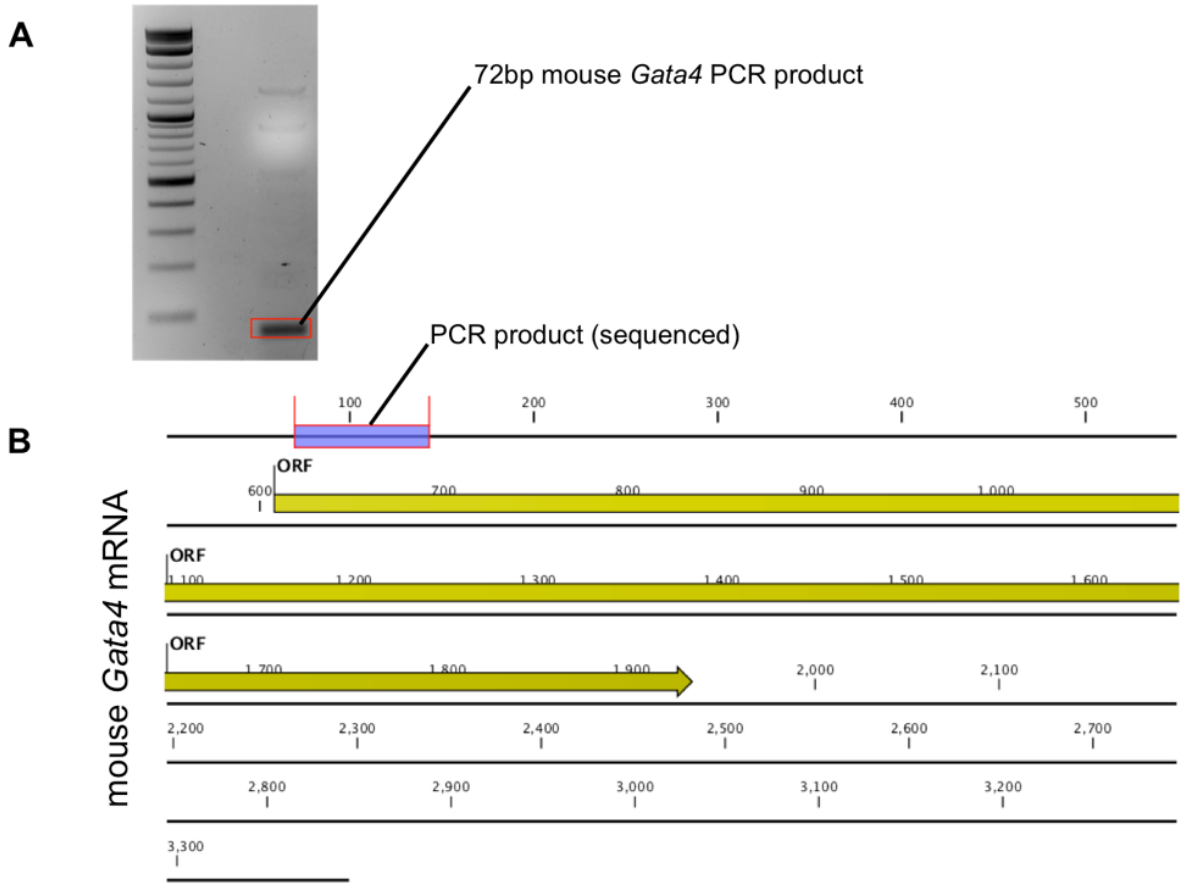

Figure 19. PCR product amplified using mouse *Gata4* primers on cDNA from vββG4Nk-infected mESC

(A) 72 bp PCR product amplified from mESC 48 hpi with vββG4Nk run on a 2% agarose gel. (B) Sequencing results of this product show that it is located in the 5' UTR of mouse *Gata4* mRNA.

To determine whether transduction of mESC with these vectors affects gene expression throughout differentiation, mESC were infected in suspension for 1 h with 1 pfu/cell of vector JDββHE, vββG4Nk, or mock-infected (Ø). The cells were differentiated into EB using the hanging drop method and plated one EB per well in 48 well plates for attachment and outgrowth. RNA was harvested every 3 d for a total of 15 d, and then reverse transcribed. qPCR utilizing TaqMan primers and probes was carried out on the resulting cDNA. All data was normalized to 18S rRNA and is presented in Figure 20 as fold change from time-matched mock-infected EB. Expression of the human *GATA4* and *NKX2.5* transgenes was examined, along with expression of cardiogenic mouse genes that are active throughout differentiation, including *Gata4, Nkx2.5, Mef2c, Tbx5,* and *cTnI* (Table 1). While there was substantial noise in the data, a few important trends were evident from this experiment. Endogenous *Gata4* was upregulated in differentiating EB made from vββG4Nk-infected mESC (vββG4Nk EB) but not in EB from JDββHE-infected mESC (JDββHE EB). Expression of the *GATA4* and *NKX2.5* transgenes was prominent at 3 dpi and remained detectable at 6 dpi (GATA4). Expression of *cTnI*, a protein critical for the contraction of heart muscle, appeared to be upregulated in d15 vββG4Nk EB although the change was small (Figure 20).

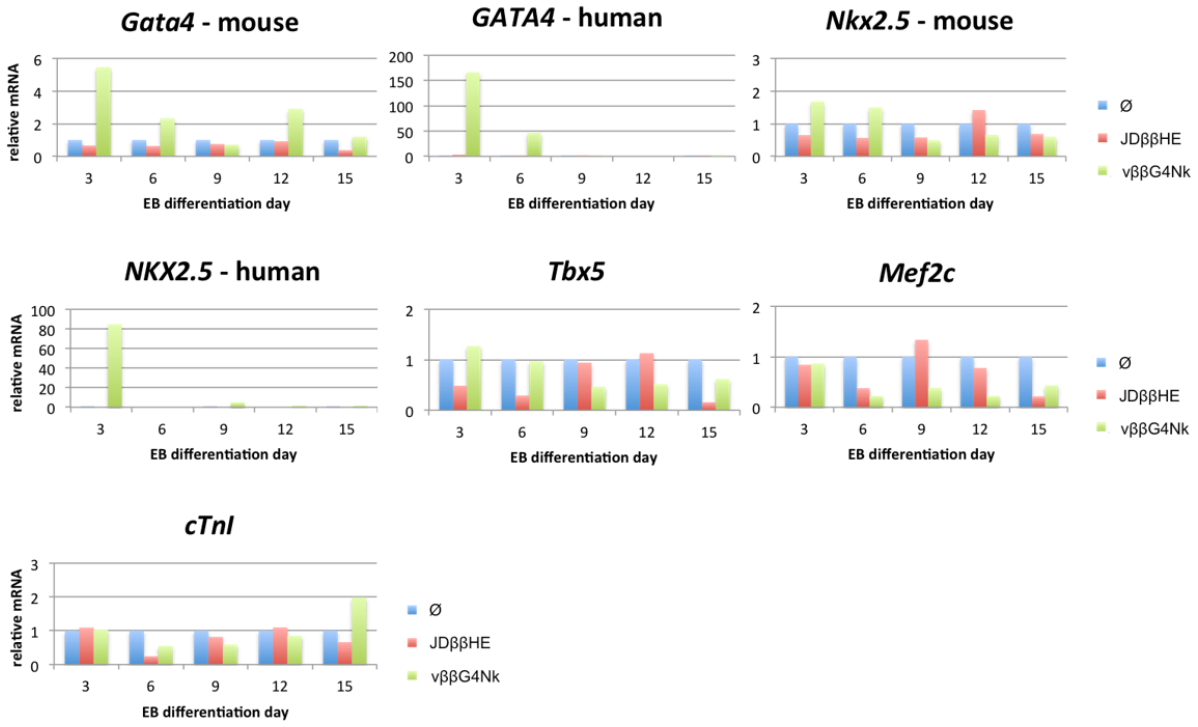

Figure 20. Time course qRT-PCR data from EB from mock-, JDββHE-, and vββG4Nk-infected mESC

Gene expression data was normalized to 18S rRNA and is expressed relative to mock-infected time-matched EB. Fold change in mRNA levels is expressed as the average of three independent wells for each gene and condition at 3, 6, 9, 12, and 15 days after the onset of differentiation.

4.3.5 Transduction of mESC with vββG4Nk prior to differentiation results in a larger population of EB with spontaneously contracting patches

The data described in section 4.4.4 indicated that transduction of mESC with vββG4Nk leads to alterations in cardiac-specific gene expression when compared to Ø- or JDββHE-infected mESC. Specifically, an increase in the expression of endogenous *Gata4*, *Mlca*, and *cTnI* was observed in mESC following transduction with vββG4Nk (Figures 17 and 18). Finally, we examined whether

there were observable physical differences in EB resulting from vββG4Nk transduction. Specifically we were interested in determining whether mESC infected with vββG4Nk and then differentiated into EB contained a higher percentage of spontaneously contracting patches, a phenotype indicative of cardiomyocyte differentiation.

D3 mESC were infected at 1 pfu/cell with JDββHE, vββG4Nk or mock-infected in suspension for 1 h. After infection, cells were diluted in mESC media without LIF, and were allowed to aggregate at the bottom of hanging drops to form EB. The EB were differentiated in hanging drops for 48 h and were then individually pipetted one per well into 48 or 96 well plates for attachment and outgrowth. At least 48 EB from each condition for each experiment were observed under the microscope for 2 weeks after plating. Spontaneously contracting patches of cells appeared between 8 and 14 days after the onset of differentiation. Results were recorded on the day when the most contracting EB were present.

The absolute percentage of EB containing contracting cell patches varied widely between repetitions of the same experiment, likely due to inconsistencies in the mESC used to make EB (passage number, presence of spontaneously differentiated cells, etc.). However there was an obvious and consistent increase in the percentage of vββG4Nk EB that developed spontaneously contracting cells compared to Ø EB or JDββHE EB. This differentiation experiment was repeated five times, and data from each experiment is plotted in Figure 21A. The averages for all of the experiments is shown in Figure 21B. While the absolute percentage of EB with contracting cell patches varied between experiments (Figure 21A), it is clear when all of the data are taken together that vββG4Nk EB consistently contained more spontaneously contracting areas of cardiomyocyte differentiation than Ø EB or JDββHE EB (Figure 21B).

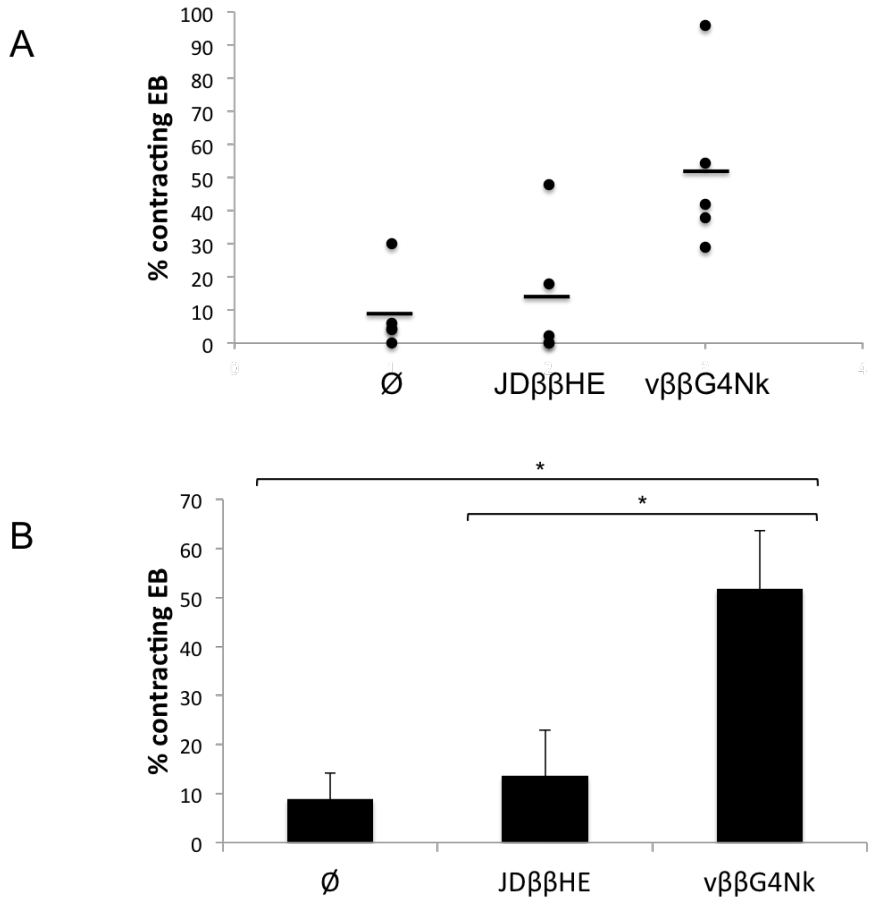

Figure 21. vββG4Nk-infected mESC make a greater percentage of EB containing cardiomyocytes
(A) The percentages of EB containing patches of spontaneously contracting cells are plotted for Ø EB, JDββHE EB, and vββG4Nk EB in 5 independent experiments. (B) The averages of the 5 independent differentiation experiments from (A) are shown. * $p < 0.05$. Data were analyzed using Students *t* test. Error bars indicate SEM.

4.4 DISCUSSION

JDββHE is a replication defective HSV vector that efficiently transduces mESC, is non-toxic, and does not interfere with EB formation or differentiation into the three germ layers (*132*). In this report, we described the engineering of JDββHE-based vector vββG4Nk to express two early cardiac transcription factors, *GATA4* and *NKX2.5*, plus mCherry as a reporter gene, from the U_L41 locus of the HSV genome. These three transgenes are expressed in one cassette from a single CAG promoter with 2A "ribosomal skipping" sequences between the transgenes that enabled translation of three distinct proteins.

GATA4 and *NKX2.5* are cardiac-specific transcription factors that are essential for heart formation (*136, 138*). We expressed these genes from vββG4Nk in mESC to enhance the differentiation of these cells toward a cardiac lineage. qRT-PCR data showed that 48 h after transduction with vββG4Nk, mESC maintained in media with LIF expressed similar levels of *Oct4* to mock-transduced or JDββHE-transduced mESC, indicating that the vector does not interfere with the pluripotency of the cells. vββG4Nk-transduced mESC expressed high levels of endogenous (mouse) *Gata4* compared to mock (Ø)- and JDββHE-transduced controls and also compared to mouse heart cDNA, demonstrating that expression of the human *GATA4* and *NKX2.5* transgenes from this vector successfully induced expression of endogenous cardiac genes. Semi-quantitative RT-PCR indicated that in addition to endogenous *Gata4*, endogenous *Nkx2.5*, *Mlc2a*, and *cTnI* were also upregulated in mESC transduced with vββG4Nk.

vββG4Nk does not express the essential immediate early gene ICP4, and therefore cannot replicate in mESC. Virus genomes are quickly diluted in these rapidly dividing cells and thus we relied on a pulse of transgene expression to set into motion a cascade of cardiac gene expression events that could effect changes in differentiating EB long after mESC transduction. vββG4Nk expresses only low levels of ICP0, mitigating its toxicity while still allowing robust expression of GATA4 and NKX2.5 proteins in mESC. Transgene mRNA could be detected in mESC transduced with 1 pfu/cell for at least 6 dpi in differentiating EB, and upregulation of endogenous cardiac-specific genes continued even after transgene expression could no longer be detected by qRT-PCR. Finally, we found that transduction of mESC with vββG4Nk followed by differentiation in EB significantly increased their cardiac differentiation such that many more vββG4Nk EB contained large clusters of spontaneously contracting cardiomyocytes than Ø EB or JDββHE EB. While the magnitude of the increase varied between experiments, the percentage of contracting vββG4Nk EB was consistently greater than that of control EB in each of the five differentiation experiments, and when averaged clearly showed that approximately 5 times more vββG4Nk EB contained visible cardiomyocyte differentiation than Ø EB or JDββHE EB.

The data reported in this chapter demonstrates that short-term GATA4 and NKX2.5 expression from HSV vector vββG4Nk induces the expression of other cardiac genes in mESC and differentiating EB, and increases the cardiogenic potential of mESC. It also highlights some of the difficulties in culturing and attempting to differentiate pluripotent stem cells into a specific cell lineage. We chose a combination of two genes that are known to be critical for embryonic heart development, engineered them into a single HSV vector that had been proven to efficiently transduce mESC, and attempted to make cardiomyocytes. While we obtained some promising results, we also discovered the pitfalls of intervening in the differentiation process. Pluripotent

stem cells can be maintained in culture nearly indefinitely, but the cells undergo an inherent drift over time, and these changes affect the way they differentiate. Parameters such as passage number, split rhythm, and undefined media components like serum all can alter the cardiac potential of PSC. The method used to initiate differentiation of stem cells also has a profound effect on the lineages produced. Using EB to differentiate mESC, as we did in these experiments, has both advantages and disadvantages. EB provide a three dimensional structure that mimics a developing embryo and fosters cell-cell interactions that are important for certain developmental programs, but the generation of cytokines and other factors within the EB can make experimental interpretation and reproducibility complicated. Lack of reproducibility between repeats of the same experiment was one of the biggest difficulties we encountered in this project. Moving forward, we better understand these complexities and some of the ways in which they can be controlled.

5.0 POLYCISTRONIC JΔNI8 VECTORS FOR THE CARDIAC DIFFERENTIATION OF EMBRYONIC STEM CELLS

5.1 INTRODUCTION

Herpes simplex virus (HSV) is a double stranded DNA virus with a large (~152 kb) genome and a broad host cell range. HSV is readily rendered replication-incompetent by the deletion of essential immediate early genes, and its toxicity to host cells is mitigated through reduction or eradication of expression of other immediate-early viral proteins, particularly ICP0. Because its large genome contains repeated sequences and many genes that are not required for host cell transduction, extensive deletions can be made without significantly inhibiting its infectivity. These deletions allow substantial room for the insertion of large transgenes or polycistronic transgene cassettes, unlike other viral vectors including adeno-associated virus and lentivirus vectors that have a much smaller genome packaging capacity. Unlike typical lentiviral and retroviral vectors, HSV genomes do not integrate into the host cell genome, a feature that is crucial for clinical translation. HSV vectors can efficiently transduce embryonic stem cells, and expression of developmental genes in ESC from HSV vectors has been shown to produce lineage-related alterations in gene expression profiles (*132*).

Red-mediated recombineering in bacteria was used to derive vGFP, vG4Nk, and vGTM from HSV vector JΔNI8GFP, a U_L41-deleted version of JΔNI7GFP previously described by

Miyagawa et al. (*169*). JΔNI8GFP is deleted for the ICP0, ICP4, and ICP27 immediate early (α) genes, the entire internal repeat or joint region, the UL41 gene and the ICP47 promoter and start codon, and the VP-16 binding motifs in the ICP22 gene regulatory region to change its expression kinetics from that of an immediate early gene to that of an early (β) gene. The BAC elements, including a chloramphenicol-resistance gene (cm^R) and β-galactosidase expression cassette, are located between loxP sites in the UL37-UL38 intergenic region (*214*), and the vector contains a hyperactive N/T double mutation in the gB gene to enhance viral entry into cells (*215*). An mCherry expression cassette driven by the ubiquitin C promoter is in the deleted ICP4 locus, and an eGFP expression cassette driven by the CAG promoter is in the LAT locus.

JΔNI8GFP is a highly defective, high capacity, non-toxic HSV vector that is capable of robust transgene expression from the LAT locus not only in neuronal, but also in many non-neuronal cell types, despite the absence of all IE gene expression. We engineered this backbone to express two different polycistronic cardiac cassettes from the LAT locus for cardiomyocyte differentiation/transdifferentiation. vG4Nk expresses *GATA4*, *NKX2.5*, and eGFP, separated by 2A "ribosomal skipping" sequences (*212*), from a single CAG promoter. *GATA4* and *NKX2.5* transgenes were chosen to enhance the cardiac differentiation of embryonic stem cells because they are both vital cardiac transcription factors that are spatiotemporally co-expressed in the precardiac mesoderm. GATA4 and NKX2.5 associate with one another to bind to the promoters of other cardiogenic genes, synergistically inducing their transcription (*141*), and loss of either gene function results in the absence of heart formation and early embryonic lethality (*135*).

vGTM was initially conceived as a vector for the transdifferentiation of fibroblasts into cardiomyocytes. Like vG4Nk, it expresses cardiac transcription factors from a single CAG promoter as one continuous transcript with genes separated by 2A sequences to allow translation

of individual proteins. *GATA4*, *TBX5*, and *MEF2C* are cardiac-specific transcription factors that are vital for embryonic heart development. GATA4 has been shown to physically interact with both TBX5 (*216*) and MEF2C (*217*) to synergistically activate the transcription of other cardiac genes. Expression of the combination of these three transcription factors via retroviral transduction of fibroblasts facilitated the first reported success in achieving the in vitro transdifferentiation of a terminally differentiated cell type into cardiomyocytes (*143*). Soon after, it was reported that the same combination with the addition of *Hand2* could reprogram fibroblasts in vitro with greater efficiency, and also could reprogram fibroblasts into cardiomyocytes in vivo (*145*). Yet another transdifferention cocktail including *MEF2C*, *TBX5*, and *MYOCD* has since been used to reprogram fibroblasts into cardiomyocyte-like cells in vitro (*218*). Qian et al. more recently reported the highly successful in vivo reprogramming of non-myocytes into cardiomyocytes in the adult mouse heart following coronary artery ligation. Retroviruses expressing *GATA4*, *TBX5*, and *MEF2C* were injected directly into the heart, resulting in decreased infarct size and moderate improvements in cardiac function up to three months post MI (*144*).

vG4Nk and vGTM each efficiently transduced mouse embryonic stem cells and robustly expressed GATA4 and NKX2.5 or GATA4, TBX5, and MEF2C proteins, respectively. Expression of these transgenes from vG4Nk and vGTM in mESC induced early but transient upregulation of endogenous cardiac genes in differentiating EB, yet produced an increased number of EB containing spontaneously contracting cells. Our results clearly indicate that infection of a small number of stem cells with vG4Nk or vGTM has far reaching effects on the mESC differentiation program even when the virus genomes have been drastically diluted as the cells continue to rapidly divide over a period of 12 days. These experiments demonstrate that

mESC are responsive to gene induction by cardiac transcription factors delivered from JΔNI8-derived vectors, and indicate that JΔNI8-based vectors can successfully alter the differentiation program of embryonic stem cells.

5.2 MATERIALS AND METHODS

5.2.1 Cells and culture conditions

HSV vectors in which ICP4, ICP27, and ICP0 have been deleted were propagated on U2OS-ICP4/27 cells (*169*), human osteosarcoma cells that contain both ICP4 and ICP27 coding sequences under control of their native promoters, taking advantage of the ICP0 complementation properties of the U2OS cell line (*219*). These cells were cultured in DMEM (Corning) supplemented with 10% FBS (GIBCO), 100 U/ml penicillin (Cellgro), and 100 μg/ml streptomycin (Cellgro). U2OS-ICP4/27 cells were maintained under constant selection with 2 μg/ml puromycin and 10 μg/ml blasticidin (Sigma).

D3 mouse embryonic stem cells (a gift from T.E. Smithgall, University of Pittsburgh) were cultured in DMEM (Corning) supplemented with 15% FBS (GIBCO), 1% non-essential amino acids (GIBCO), 1 mM sodium pyruvate (GIBCO), 100 U/ml penicillin, 100 μg/mL streptomycin (Cellgro), 0.1 mM 2-mercaptoethanol (GIBCO), and 1000 U/ml mouse LIF (Millipore) on 10 cm dishes coated with 0.2% gelatin (Sigma). Media was exchanged daily and cells were passaged with trypsin every 2-3 d to maintain a state of self-renewal and minimize spontaneous differentiation.

5.2.2 G4NkeGFP cassette construction

The pG4NkmCh plasmid described above was modified to contain eGFP instead of mCherry as a reporter gene. The eGFP coding sequence was PCR amplified from the commercially available plasmid pEGFP-N1 (Clontech) using primers F/Xho-E2A-eGFP and R/eGFP-Pme (Table 4), giving a 719 bp fragment that begins with an XhoI restriction site, then the E2A sequence, the eGFP coding sequence, and ends with a PmeI restriction site (XhoI-E2A-eGFP-PmeI). The purified PCR product was then digested with XhoI and PmeI. Plasmid pG4NkmCh was digested with XhoI and PmeI, the 7.2 kb backbone fragment purified from an agarose gel, and then the PCR product was ligated into the plasmid to create pG4NkeGFP.

5.2.3 GTMeGFP cassette construction

cDNAs for human *MEF2C* and *TBX5* were obtained from Open Biosystems and sequenced for verification (Genewiz). The GTMeGFP cassette was built in two steps. First human *GATA4*, *TBX5*, and mCherry cDNAs were PCR amplified with primers to add convenient restriction sites and 2A sequences and ligated into pcDNA-CAGp (described in section 4.3.2) resulting in plasmid pGTMmCh, and then mCherry was replaced with eGFP. Briefly, *GATA4* was amplified with primers F/EcoRI-GATA4 and R/GATA4-T2A and Tbx5 was amplified with primers F/T2A-Tbx5 and R/Tbx5-PspXI. The resulting two PCR products were then amplified together with F/EcoRI-GATA4 and R/Tbx5-PspXI to produce a fragment that begins with an EcoRI restriction site, then a start codon, the *GATA4* coding sequence, the T2A sequence, the *TBX5* coding sequence, and ending with a PspXI restriction site (EcoRI-GATA4-T2A-Tbx5-PspXI) all in the same ORF. Plasmid pcDNA-CAGp and fragment EcoRI-GATA4-T2A-Tbx5-PspXI were

each cut with EcoRI and PspXI and the fragment was ligated into the plasmid backbone to give rise to plasmid pGT. Next *MEF2C* was PCR amplified with primers F/PspXI-E2A-Mef2c and R/Mef2c-F2A and mCherry was PCR amplified from pG4NkmCh with primers F/F2A and R/mCherry-Pme. The resulting two PCR products were amplified together with primers F/PspXI-E2A-Mef2c and R/mCherry-Pme giving a fragment beginning with a PspXI restriction site, the E2A sequence, Mef2c coding sequence, the F2A sequence, mCherry coding sequence, and ending in a PmeI restriction site (PspXI-E2A-Mef2c-F2A-mCherry-PmeI). This fragment and plasmid pGT were digested with PspXI and PmeI and the mCherry fragment was ligated into the plasmid, giving rise to plasmid pGTMmCh, with *GATA4*, *TBX5*, *MEF2C*, and mCherry all in one continuous ORF. Sequences were obtained for all parts of the cassette to verify that no errors occurred during PCR amplification (Genewiz). Next mCherry was replaced in pGTMmCh with eGFP. The eGFP coding sequence was PCR amplified from the commercially available plasmid pEGFP-N1 (Life Technologies) using primers F/F2A-eGFP and R/eGFP-Pme to produce a fragment containing part of the F2A sequence, the eGFP coding sequence, and a PmeI restriction site. Next the plasmid containing the *MEF2C* cDNA (Open Biosystems) was PCR amplified with primers F/PspXI-E2A-Mef2c and R/Mef2c-F2A to produce a fragment containing a PspXI restriction site, the E2A sequence, the MEF2C coding sequence, and part of the F2A sequence. The previous two fragments were PCR amplified together with primers F/PspXI-E2A-Mef2c and R/eGFP-Pme to produce 2.2 kb fragment PspXI-E2A-Mef2c-F2A-eGFP-PmeI. Both this fragment and plasmid pGTMmCh were digested with PspXI and PmeI, and the PspXI-E2A-Mef2c-F2A-eGFP fragment was ligated into the backbone, creating plasmid pGTMeGFP with *GATA4*, *TBX5*, *MEF2C*, and eGFP separated by 2A sequences and all in one continuous ORF.

Sequences were obtained for all parts of the cassette to verify that no errors occurred during PCR amplification (Genewiz).

Table 6. Primer sequences for construction of GTMmCh and GTMeGFP cassettes

F/Xho-E2A-eGFP	CTGAGCCTCGAGGGTCAATGTACTAACTACGCTTTGTTGAAACTCGCTGGC GATGTTGAAAGTAACCCCGGTCCTatggtgagcaagggcgaggagctg
R/eGFP-Pme	CTGTGGGTTTAAACctatcacttgtacagctcgtccatg
F/EcoRI-GATA4	ccacaGAATTCGTAATAGGATAGCGACatgtatcagagcttggccatg
R/GATA4-T2A	*CCTCGACGTCACCGCATGTTAGCAGACTTCCTCTGCCCTC*TCCGGAGCCcgc agtgattatgtccccgtgac
F/T2A-Tbx5	*GAAGTCTGCTAACATGCGGTGACGTCGAGGAGAATCCTGGCCCA*atggccgacg cagacgagggctttg
R/Tbx5-PspXI	CTGTAGACTCGAGCgctattgtcgctccactctgg
F/PspXI-E2A-Mef2c	CTGAGCGCTCGAGTCGGTCAATGTACTAACTACGCTTTGTTGAAACTCGCTGGC GATGTTGAAAGTAACCCCGGTCCTatgggagaaaaaagattcagattac
R/Mef2c-F2A	*CCACGTCTCCCGCCAACTTGAGAAGGTCAAAATTCAAAGTCTGTTTCAC*gccagaa ccttcagaaagtcgcatg
F/F2A	*GAGACGTGGAGTCCAACCCAGGGCCC*
R/mCherry-Pme	CTGTGGGTTTAAACctatcatgggtccttgtacagctcg
R/Mef2c-F2A	*CCACGTCTCCCGCCAACTTGAGAAGGTCAAAATTCAAAGTCTGTTTCAC*gccagaa ccttcagaaagtcgcatg
F/F2A-eGFP	*ACCTTCTCAAGTTGGCGGGAGACGTGGAGTCCAACCCAGGGCCC*atggtgagcaagg gcgaggagctg

Underlined sequences are restriction sites, green designates start codons, blue designates 2A sequences (italics for partial 2A), and red designates stop codons.

5.2.4 JΔNI8 vector engineering

Red-mediated recombineering in bacteria (*220*) was used to create the described HSV-BAC constructs. All HSV-BAC constructs described are derived from the JΔNI8GFP HSV-BAC, generated by Y. Miyagawa (*169*). BAC engineering was performed with pRed/ET (Gene Bridges) and pBAD-I-SceI plasmid (from N. Osterrieder, Free University of Berlin, Germany) with E. coli strain GS1783 (from G. Smith, Northwestern University, Chicago, IL) as described (*221*), see Figure 22. First mCherry was deleted from the ICP4 locus of JΔNI8GFP BAC. The kanamycin resistance gene and I-SceI sequences flanked by sequences surrounding mCherry in the ICP4 locus of JΔNI8GFP BAC were PCR amplified from plasmid pBAD-I-SceI with primers EpKAN-del-mCherry-f1 and EpKAN-del-mCherry-r. The resulting fragment was then amplified with EpKAN-del-mCherry-f2 and EpKAN-del-mCherry-r for Red-mediated recombination into the ICP4 locus to delete mCherry and insert the kanamycin resistance gene, which was then selected for and removed as previously described (*220, 221*). The resulting HSV-BAC was termed JΔNI8GFPΔcherry. Next the kanamycin resistance cassette (kan^R) and I-SceI sites were introduced into the BamHI site of the *GATA4* coding sequence in plasmid pG4NkeGFP and into the Asp718 site of the *MEF2C* site of pGTMeGFP. For pG4NkeGFP, plasmid pBAD-I-SceI was PCR amplified with primers F/Kan-GATA4 and R/Kan-GATA4. This PCR fragment was digested with BamHI and cloned into the BamHI site in pG4NkeGFP. For pGTMeGFP, plasmid pBAD-I-SceI was PCR amplified with primers F/Kan-Mef2c and R/Kan-Mef2c. This PCR fragment was digested with Asp718 and cloned into the Asp718 site in pGTMeGFP. Each gene cassette containing kan^R was recombined into the LAT locus of JΔNI8GFPΔcherry-BAC,

followed by kanamycin selection and then removal of the kanamycin cassette from *GATA4* and *MEF2C* coding sequences to create HSV-BACs JΔNI8G4NkeGFP and JΔNI8GTMeGFP.

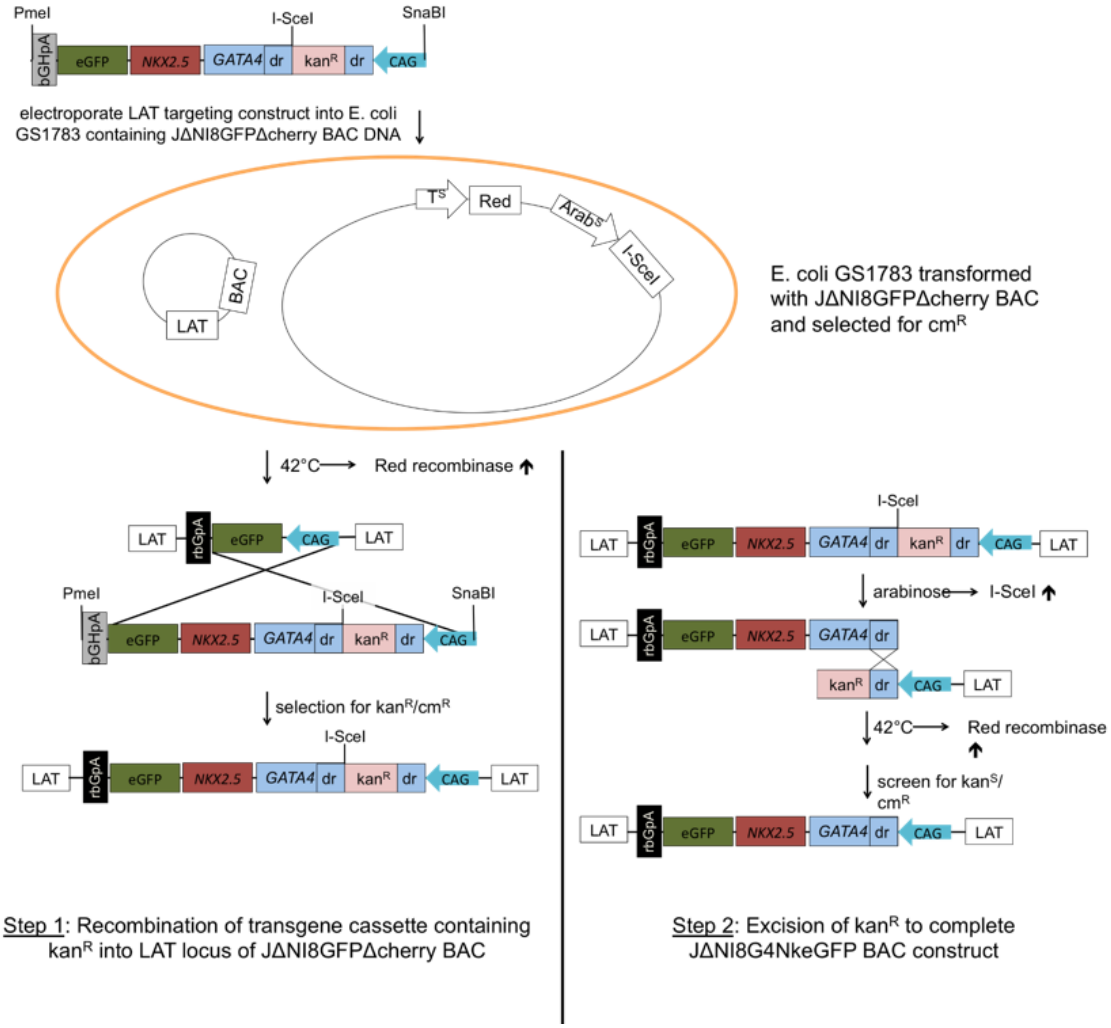

Figure 22. Example schematic of Red/ET recombineering steps

A kan^R cassette consisting of an I-SceI restriction site, kanamycin resistance gene, and 50 bp direct repeat of the target sequence was inserted into the *GATA4* gene in the G4NkeGFP LAT-targeting construct. In step 1, the multigene cassette was electroporated into E. coli strain GS1783 that was transformed with the JΔNI8GFPΔcherry BAC and selected for cm^R. GS1783 contains a temperature inducible (T^S) promoter driving expression of Red recombinase and an arabinose inducible (Arab^S) promoter driving expression of restriction enzyme I-SceI. Production of Red recombinase was induced by culturing the cells at 42°C, allowing the G4NkeGFP cassette to recombine into the LAT locus via homology with the CAG promoter and the eGFP coding sequence present in JΔNI8GFPΔcherry BAC. Recombinants were selected for kan^R/cm^R and confirmed by PCR and FIGE. In step 2, the kan^R cassette is excised. Arabinose was added to the culture to induce the production of I-SceI, which then cut the BAC DNA immediately to the left of the kan^R gene. The cells were cultured at 42°C to produce Red recombinase and thereby promote recombination between the direct repeats inside the *GATA4* gene, seamlessly removing kan^R and leaving the *GATA4* coding sequence intact. Recombinants were screened for kan^S/cm^R and confirmed by PCR and FIGE.

Table 7. Primer sequences for BAC recombineering

EpKAN-del-mCherry-f1	GGCGGGTGCGCCGTGCTCTGTTGGTTTCACCTGTGGCAGCCCGGGCC CCCCGCGGaggatgacgacgataagtagggata
EpKAN-del-mCherry-r	CCGCGGGGGGCCCGGGCTGCCACAGGTGAAACCAACAGAGCACGGC GCACcaaccaattaaccaattctgattag
EpKAN-del-mCherry-f2	CTTGGGGCGGTCCCGCCCGCCGGCCAATGGGGGGGCGGCAAGGCGG GCGGGTGCGCCGTGCTCTGTTGGT
F/Kan-GATA4	GAGGGGATCCAAACCAGAAAACGGAAGCCCAAGAACCTGAATAAATCT AAGACAAGGATGACGATAAGTAGGGATA
R/Kan-GATA4	CACAGGATCCCAACCAATTAACCAATTCTGATTAG
F/Kan-Mef2c	GAGGGGTACCGAGTACTCTCTGAGTAGTGCAGACCTGTCATCTCTGTCT GGGTTAGGATGACGACGATAAGTAGGGATA
R/Kan-Mef2c	CACAGGTACCCAACCAATTAACCAATTCTGATTAG

Underlined sequences represent restriction sites added with primers.

JΔNI8 BAC DNA constructs were confirmed by PCR analysis, FIGE analysis of restriction enzyme digests, and targeted DNA sequencing. JΔNI8GFPΔcherry, JΔNI8G4NkeGFP, and JΔNI8GTMeGFP BACs were converted into infectious viruses (vGFP, vG4Nk, and vGTM, respectively) by transfection into U2OS-ICP4/27 cells. 4 μg BAC DNA in 500 μl OptiMEM (Invitrogen) was incubated with 1 μl Lipofectamine Plus Reagent (Invitrogen) for 5 min at room temperature, then 6.25 μl Lipofectamine LTX (Invitrogen) was added and the mixture incubated at room temperature for 30 min before being added to the cells. The cells in transfection mixture were incubated at 37°C for 6 h, then the media was replaced with serum free

DMEM and the cells were cultured overnight at 37°C. The cells were transferred to 33°C and virus growth was monitored until complete CPE was observed. Supernatant virus was titered and the viruses were amplified through infection of sequentially larger cultures at an MOI of 0.001 pfu/cell. For large scale production, U2OS-ICP4/27 cells were plated in the desired number of T150 flasks and confluent monolayer cells were infected at an MOI of 0.0001 pfu/cell in 10 ml serum free DMEM (Corning) per flask with occasional gentle agitation for 2 h at 37°C. After 2h, 10 ml serum free DMEM was added to each flask, and the infected cells were incubated at 33°C to allow for maximum virus survival without cell overgrowth until the entire flask reached CPE, typically 7-10 days post infection. The media was then collected and the dead cells were spun out in a table top centrifuge at 3000 rpm for 10 min at 4°C. The supernatant containing the virus was filtered through a 0.8 μm then a 0.45 μm Versapor membrane (PALL Corporation), and then concentrated by multiple cycles of high-speed centrifugation at 19,500 rpm for 45 min each cycle. All of the supernatant was spun down into 2 – 4 tubes, and the resulting viral pellets were each gently resuspended in 200 μl PBS with 10% glycerol by slow shaking at 4°C for 24-48 h. The resulting concentrated virus was divided into 5-20 μl aliquots and stored at -80°C.

5.2.5 Genome copy titer of JΔNI8 vectors

Genome copy titer measurements were performed on 5 μl aliquots of all JΔNI8-based vectors. Viral DNA was extracted with the DNeasy Blood & Tissue Kit (Qiagen). Genome copy titers were determined by qPCR for the glycoprotein D (gD) (*222*) with a TaqMan primer and probe set (Invitrogen) using conditions described above. Cellular 18S ribosomal DNA levels were measured with TaqMan Ribosomal RNA control reagents (Invitrogen) and were used to

normalize viral DNA amounts. Absolute genome copy titers were calculated as previously described (*222-224*).

5.2.6 Western blot analysis

GATA4, NKX2.5, TBX5, and MEF2C expression from both pG4NkeGFP and pGTMeGFP were confirmed by transfecting U2OS-ICP4/27 cells with the plasmids using Lipofectamine LTX (Invitrogen) according to the manufacturer's protocol and collecting proteins from the cells 48 h post transfection. GATA4, NKX2.5, TBX5, and MEF2C expression from vG4Nk and vGTM was confirmed by infecting U2OS-ICP4/27 cells, non-complementing U2OS cells, and D3 mouse embryonic stem cells and collecting proteins 24 hpi. Cell lysates were collected in RIPA lysis buffer supplemented with protease inhibitors (Roche). Proteins were separated on a 10% polyacrylamide gel and transferred by semi-dry transfer onto PVDF membranes. The membranes were washed in TBS and blocked for 1 h at room temperature in TBS-T (20 mM Tris, 0.5 M NaCl [pH 7.5] plus 0.5% Tween 20) supplemented with 10% nonfat dry milk. Primary antibodies were diluted in blocking buffer. The diluted antibodies were reacted with the blocked PVDF overnight at 4°C, washed 3 times for 10 min each in TBS-T, and reacted with horseradish peroxidase-conjugated secondary antibodies diluted in blocking buffer for 1 h at room temperature. The bound Igs were revealed by enhanced chemiluminescence (Thermo Scientific). Antibody information can be found in Table 1.

5.2.7 Embryoid body assay

D3 mouse embryonic stem cells were infected in suspension with vGFP, vG4Nk, vGTM, or mock infected in a small volume in Eppendorf tubes at 37°C with continuous rotation for 1-2 h. Infected cells were diluted in mESC media without LIF at a concentration of $4x10^4$ cells/ml. 20 µl drops of cells were pipetted onto the lid of a petri dish, and the lid was inverted over the dish that contained 30 ml sterile water to prevent the drops from evaporating. The cells were incubated at 37°C with 5% CO2 and allowed to aggregate to form embryoid bodies (EB) and differentiate for two days in hanging drops. After 48 h in hanging drops, the EB were pipetted one per well into 48 well plates, each well containing 500 µl mESC media without LIF. EB were observed daily for the appearance of spontaneously contracting cells, and the number of wells containing these cells was recorded each day.

5.2.8 Cytosine β-D-arabinofuranoside (Ara-C) to inhibit cell division

Cytosine β-D-arabinofuranoside (Sigma) was used to inhibit mESC division following transduction with HSV vectors. mESC were treated with 0.3uM Ara-C for 48 hpi after the onset of differentiation in EB. Ara-C was diluted upon plating EB and then completely washed out 24 h later.

5.2.9 RNA extraction and quantitative RT-PCR analysis

Total RNA was extracted from D3 mES cell lines and embryoid bodies using Qiagen RNeasy Plus mini kit (Qiagen) according to the manufacturer's protocol.

Reverse transcription was performed on 1-2 μg RNA in 20 μl final volume using random decamers as first strand primers with Ambion's RETROscript Kit (Ambion), and the resulting cDNA was diluted 1:10 for quantitative RT-PCR analysis.

Primers were obtained from Invitrogen. Primer sequences and references for qPCR are listed in Table 1. qPCR was performed using LightCycler SYBRgreen Master Mix (Roche) or TaqMan Gene Expression Assays (Invitrogen) and a Step One Plus Real-Time PCR System (Applied Biosystems). Cycling conditions were 95°C for 10 min followed by 40 cycles of 95°C for 15 sec and then 60°C for 1 min. Each cDNA was analyzed in triplicate, and the results for the three wells were averaged. Threshold cycle (Ct) values were used to calculate changes in gene expression using the $2^{-\Delta\Delta Ct}$ method (*195*). Expression levels were normalized to *HPRT* mRNA for SYBRgreen or 18S ribosomal RNA levels for TaqMan, and expressed relative to uninfected D3 mESC.

5.3 RESULTS

5.3.1 Assembly and validation of differentiation and trans-differentiation cassettes

Polycistronic cassettes G4NkeGFP and GTMeGFP were assembled in plasmid pcDNA-CAGp (section 4.3.2) to co-express *GATA4*, *NKX2.5*, and eGFP or *GATA4*, *TBX5*, *MEF2C*, and eGFP respectively (Figure 23A and Methods sections 5.3.2 and 5.3.3). Gene expression from each cassette is driven by a single CAG promoter, and genes are separated by 2A "ribosomal skipping" sequences (*212*) to allow for individual translation of each transgene.

The mCherry reporter gene in pG4NkmCh (Chapter 4, Figure 9) was replaced with an eGFP gene to allow for brighter fluorescence in transfected or infected cells. The reporter gene switch was verified by transfecting the constructs pG4NkmCh and pG4NkeGFP into Vero cells and observation of eGFP expression in the pG4NkeGFP-transfected cells (Figure 23B, *upper*).

Plasmid pGTMeGFP was constructed by first creating pGTMmCh through PCR amplification of human *GATA4*, *TBX5*, and *MEF2C* cDNAs with 2A extensions and cloning them into pcDNA-CAGp with mCherry as the final gene in the cassette (described in 5.3.3). Expression of GATA4, TBX5, MEF2C, and mCherry from pGTMmCh was verified by transfecting the plasmid into U2OS-ICP4 cells, collecting cells lysates 48 h post transfection, and Western blotting with antibodies against the transgene products (Figure 23C). mCherry was replaced by eGFP using the same template, primers, and cloning strategy as for pG4NkeGFP to create pGTMeGFP, and the resulting plasmid was transfected into Vero cells to confirm the reporter gene switch (Figure 23B, *lower*).

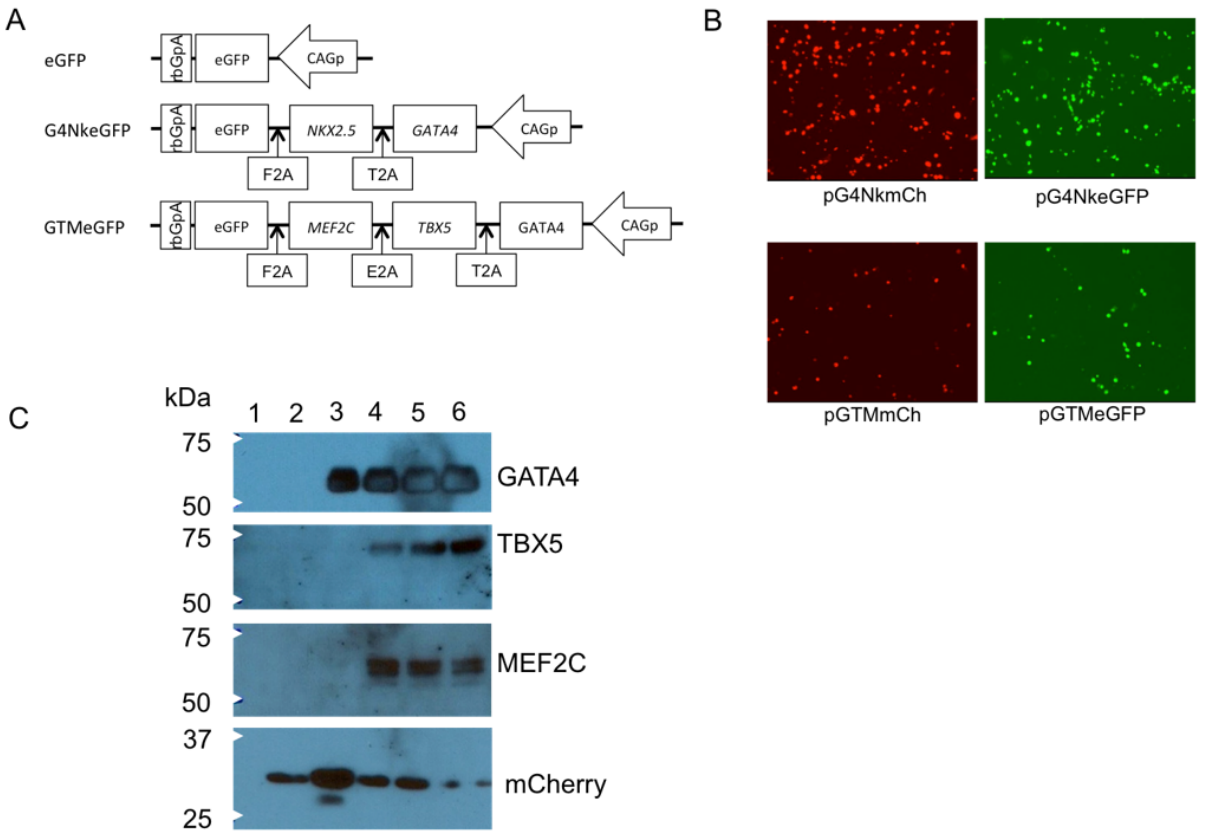

Figure 23. Cassette schematics and verification of gene expression from pG4NkeGFP and pGTMeGFP

(A) Trangene cassettes for the expression of eGFP alone, *GATA4*, *NKX2.5*, and eGFP, and *GATA4*, *TBX5*, *MEF2C*, and eGFP, each from a single CAG promoter. (B) Fluorescence microscopy pictures of Vero cells transfected with parental plasmids pG4NkmCh or pGTMmCh and imaged for mCherry expression or with derivatives pG4NkeGFP or pGTMeGFP and imaged for GFP expression 48 h post transfection. (C) Western blots of lysates collected 48 h post transfection from U2OS-ICP4 cells transfected with various expression plasmids: untransfected cells (lane 1), pcGWmCherry (lane 2), pH41G4NkmCh (lane 3), and 3 clones of pGTMmCh (lanes 4-6).

5.3.2 Deletion of mCherry from JΔNI8GFP BAC

HSV vector JΔNI8GFP was constructed in our lab by Yoshitaka Miyagawa as a U_L41-deleted derivative of JΔNI7GFP described in reference (*169*). To allow for the use of red fluorescent secondary antibodies for immunofluorescence imaging and flow cytometry of transduced cells, mCherry was deleted from the ICP4 locus of JΔNI8GFP BAC so that the resulting HSV vector would contain a single fluorescent reporter gene. Engineering of BAC DNA was performed by Red-mediated recombination in E. coli strain GS1783. This bacterial strain contains a temperature-inducible expression cassette for the phage λ Red proteins Exo, Beta and Gam, and an arabinose-inducible gene for the rare-cutting homing endonuclease *I-SceI* in its chromosomal DNA (*221*). An mCherry deletion construct consisting of the kanamycin resistance gene (kan^R) flanked by homology arms to the ICP4 region surrounding the mCherry cassette in JΔNI8GFP BAC was created by PCR amplification. The construct was electroporated into bacteria containing JΔNI8GFP BAC, and BAC recombinants were selected on chloramphenicol/kanamycin-containing agar plates. Proper recombinants were identified using PCR with primers to amplify the region surrounding the ICP4 locus. The primers were designed to amplify a 2515 bp product containing the mCherry coding sequence in the parent JΔNI8GFP BAC. Upon replacement of the mCherry gene with the kan^R gene, these primers would yield a product of 1300 bp (Figure 24A, *left*). Clones #2 and #6 produced a product of the expected size (Figure 24A, *right*). These products were verified by sequencing. Large BAC DNA preps were produced for the two recombinants and the parental DNA for comparison. The DNAs were digested overnight with BsrGI and the resulting fragments were resolved by field inversion gel

electrophoresis (FIGE). Successful recombination resulted in the elimination of the BsrGI site inside the mCherry coding sequence, causing a shift of the 3.9 kb and 16.5 kb fragments of the parental BAC DNA into a single 19.2 kb fragment (Figure 24B); no other changes from the parental BAC DNA were observed. The recombinants were called JΔNI8GFPΔcherryKan^{R} BAC.

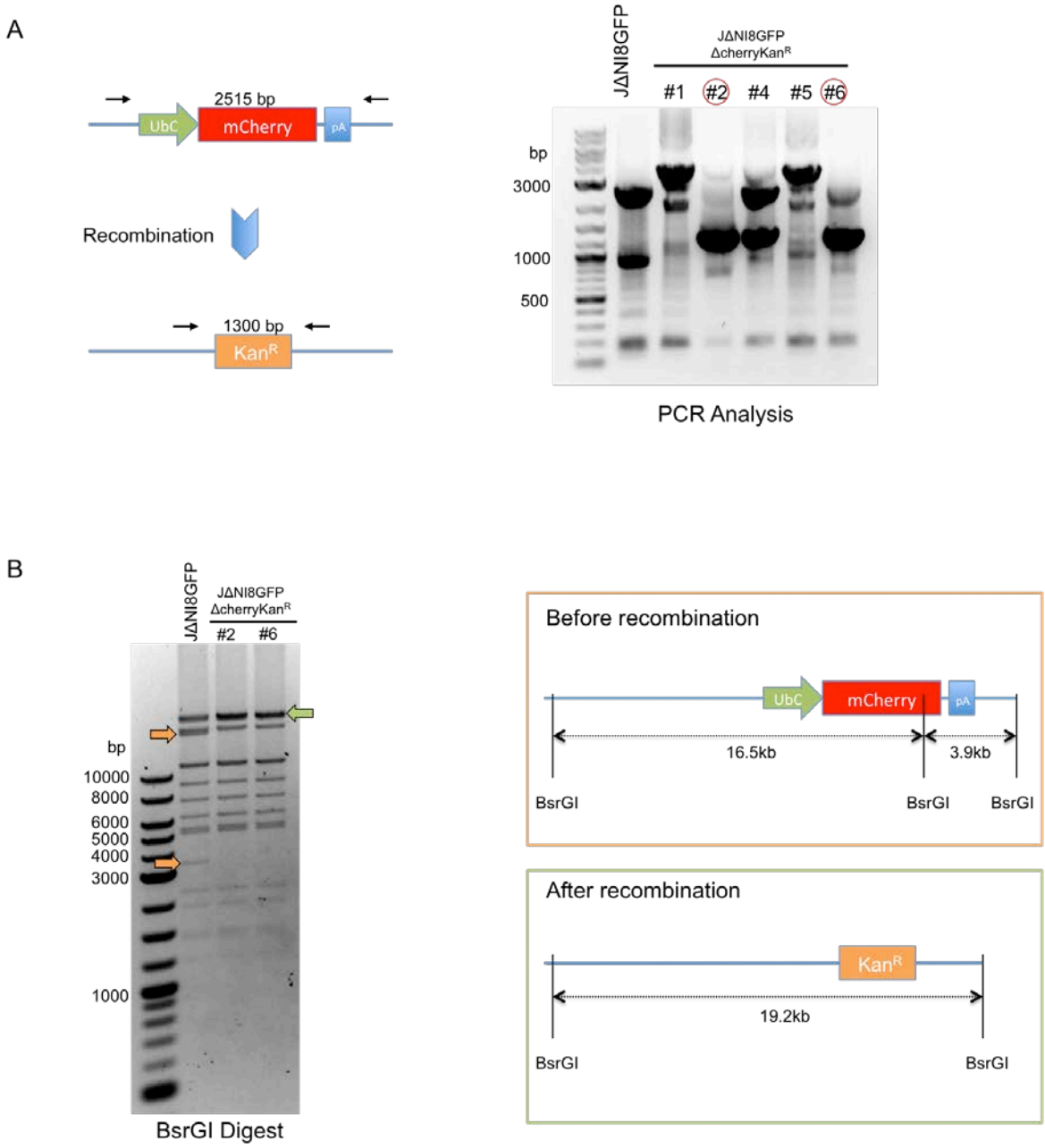

Figure 24. Verification of mCherry deletion/Kan^R insertion into JΔNI8GFP BAC
(A) PCR amplification of the region surrounding the mCherry deletion/Kan^R insertion. The left panel shows a diagram of the area surrounding the ICP4 region before and after recombination. Locations of PCR primers are marked by small black arrows. The right panel shows the results of PCR performed on 5 different JΔNI8GFPΔcherryKan^R BAC clones and parent JΔNI8GFP. (B) FIGE analysis of BsrGI-digested JΔNI8GFP and 2 clones of JΔNI8GFPΔcherryKan^R BAC DNA. The left panel shows the FIGE gel with arrows marking the fragments that change, before (orange) and after (green) recombination. The right panel shows a schematic of the area of recombination and the sizes of the expected fragments upon BsrGI digestion.

The kan^R gene was excised from the ICP4 locus of JΔNI8GFPΔcherryKan^R BAC DNA by arabinose activation of the I-SceI promoter and heat activation (42°C) of the recombinase promoter of the GS1783 host cells. Kanamycin-sensitive/$chloramphenicol^R$ colonies were identified and PCR was used to amplify the region surrounding the anticipated kan^R deletion in both JΔNI8GFPΔcherryKan^R clones. Successful recombination produced a 189 bp product, compared to the 1300 bp kan^R-containing product resulting from PCR with the same primers on JΔNI8GFPΔcherryKan^R DNA (Figure 25A). Several successful recombinants were verified through sequencing. DNA from these recombinants and the parental BAC were digested overnight with EcoRI and the digests were analyzed by FIGE. Deletion of kan^R resulted in a shift of the 21.5 kb fragment to 20.4 kb (Figure 25B). All three of the recombinants that were analyzed showed the correct digestion pattern, indicating that JΔNI8GFPΔcherry BAC was successfully created.

A

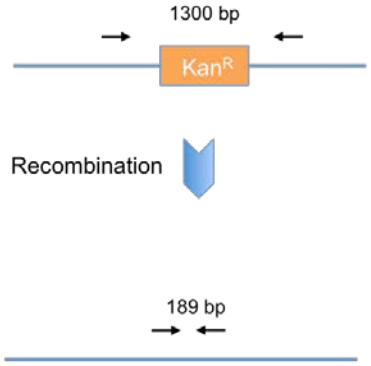
1300 bp
Kan^R
Recombination
189 bp

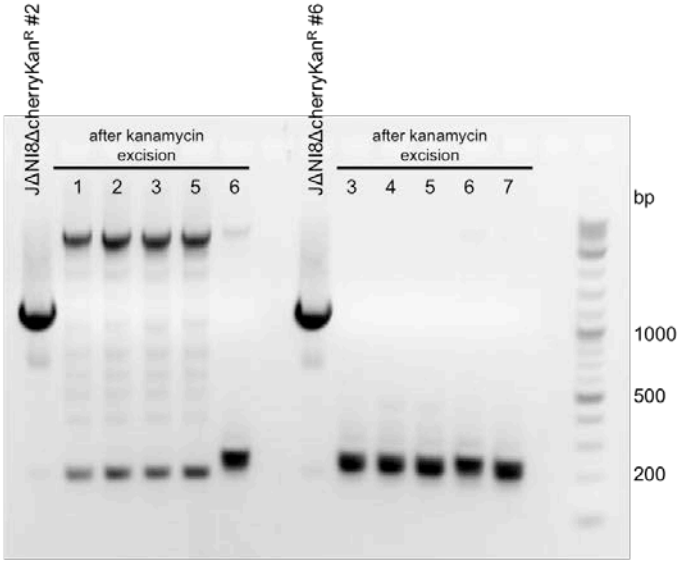
JΔNI8ΔcherryKan^R #2
after kanamycin excision
1 2 3 5 6
JΔNI8ΔcherryKan^R #6
after kanamycin excision
3 4 5 6 7
bp
1000
500
200

B

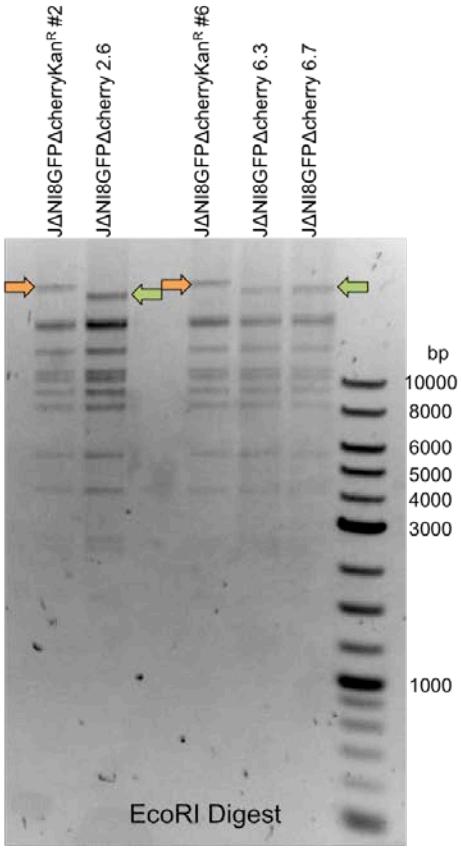
JΔNI8GFPΔcherryKan^R #2
JΔNI8GFPΔcherry 2.6
JΔNI8GFPΔcherryKan^R #6
JΔNI8GFPΔcherry 6.3
JΔNI8GFPΔcherry 6.7
bp
10000
8000
6000
5000
4000
3000
1000
EcoRI Digest

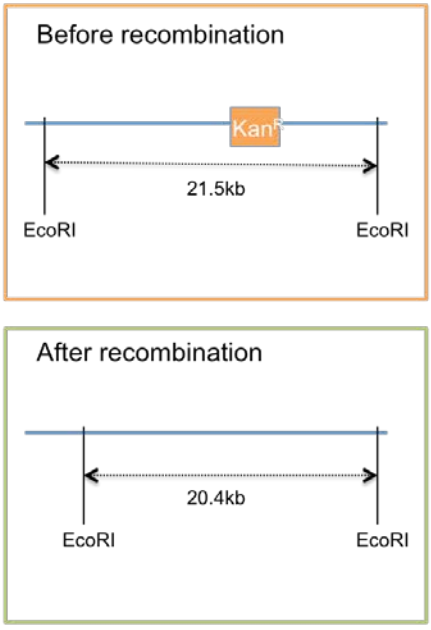
Before recombination
Kan^R
21.5kb
EcoRI
EcoRI
After recombination
20.4kb
EcoRI
EcoRI

Figure 25. Verification of Kan^R deletion from JΔNI8GFPΔcherry BAC
(A) PCR amplification of the region surrounding the kan^R deletion. The left panel shows a diagram of the area surrounding the ICP4 region before and after recombination. Locations of PCR primers are marked by small black arrows. The right panel shows the results of PCR performed on 5 different JΔNI8GFPΔcherry BAC clones and both parent BACs JΔNI8GFPΔcherryKan^R #2 and #6. (B) FIGE analysis of EcoRI-digested JΔNI8GFPΔcherryKan^R and 3 clones of JΔNI8GFPΔcherry BAC DNA. The left panel shows the FIGE gel with arrows marking the fragments that change, before (orange) and after (green) recombination. The right panel shows a schematic of the area of recombination and the sizes of the expected fragments upon EcoRI digestion.

5.3.3 Insertion of a 2A-linked GATA4-NKX2.5 cassette into JΔNI8GFPΔcherry BAC

A unique BamHI site inside the coding sequence of *GATA4* in the plasmid pG4NkeGFP was used to insert the kan^R/I-SceI selection cassette prior to recombination of G4NkeGFP into vGFP. Kan^R was PCR amplified from pBAD-I-SceI with primers to add BamHI sites and a 50 bp direct repeat of *GATA4* coding sequence (Figure 26A). Both the resulting PCR product and pG4NkeGFP were digested with BamHI, the PCR product was ligated into the backbone. Insert orientation was checked with diagnostic restriction digests. Several clones with the correct orientation (kan^R between a 50 bp direct repeat of *GATA4* sequences) were identified and sequenced. One pG4(kan^R)NkeGFP clone with the correct sequence was digested with PmeI and SnaBI to produce a 5597 bp fragment for recombination into the LAT locus of JΔNI8GFPΔcherry BAC DNA (Figure 26B). This fragment had separate regions of homology with the CAG promoter and the eGFP coding sequence present in the LAT locus of vGFP to direct homologous recombination upon electroporation into bacteria containing JΔNI8GFPΔcherry BAC DNA (Figure 26C). Cm^R/kan^R colonies were selected and the 5’ and 3’ recombination regions were PCR amplified and sequenced to verify that no sequence changes had occurred.

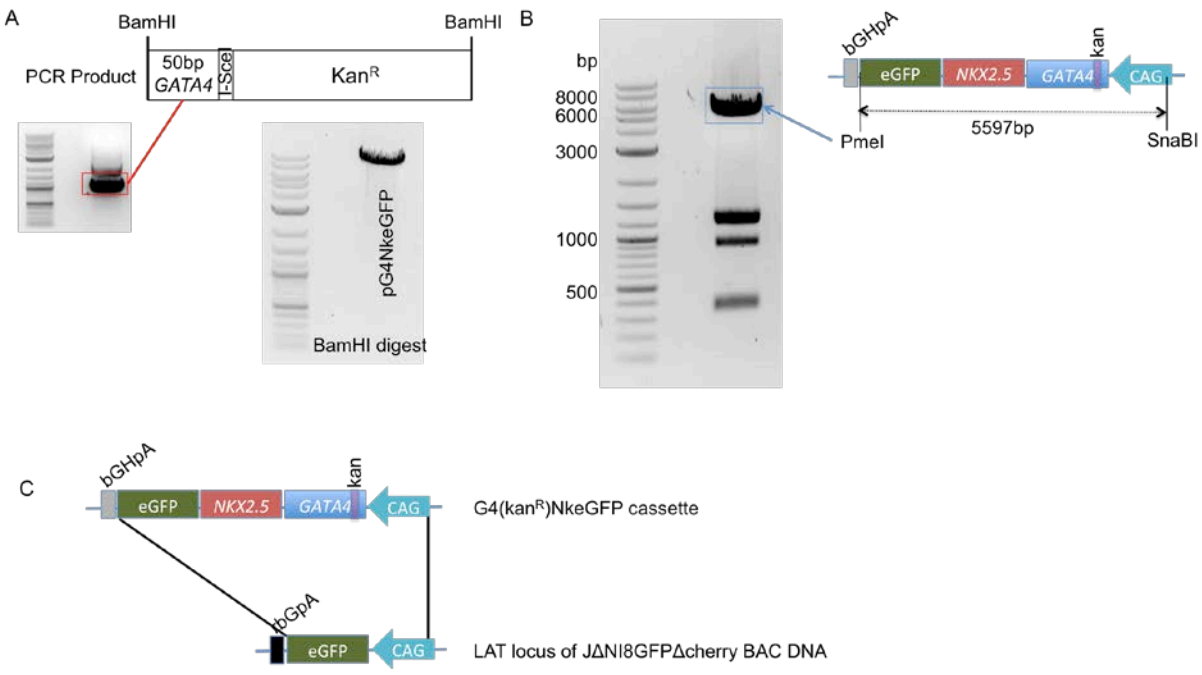

Figure 26. Scheme for introducing kan^R into pG4NkeGFP and digestion for recombination
(A) Diagram and gel of PCR product for insertion of kan^R into a BamHI site inside GATA4 and BamHI digest of pG4NkeGFP. (B) Schematic of G4(kan^R)NkeGFP and digest with PmeI and SnaBI for recombination into JΔNI8GFPΔcherry BAC DNA. (C) Homologous sequences (CAG, eGFP) between the G4(kan^R)NkeGFP cassette and the LAT locus of JΔNI8GFPΔcherry BAC DNA for recombination.

FIGE analysis of MfeI-digested recombinant JΔNI8G4(kan^R)NkeGFP and parental JΔNI8GFPΔcherry BAC DNA confirmed that the G4(kan^R)NkeGFP was successfully recombined into JΔNI8GFPΔcherry BAC DNA in the three clones examined. A 14.9 kb MfeI fragment containing the eGFP expression cassette in the parent BAC increased in size to 17.6 kb following recombination, consistent with acquisition of the GATA4(kan^R)Nkx2.5 sequence (Figure 27).

To generate the final JΔNI8G4NkeGFP BAC construct, the kan^R gene was removed as described above using arabinose-induced I-SceI expression and heat activation of the Red proteins in the BAC-containing GS1783 bacteria. Kan^R excision was first verified by PCR using primers to both sides of the kan^R gene. A 2342 bp product was amplified from the parental BAC. All 5 recombinants tested yielded a 1298 bp product (Figure 28A), consistent with clean deletion of the kan^R gene that was confirmed by DNA sequencing. FIGE analysis of MfeI digested BAC DNA before and after recombination also verified the successful excision of kan^R. The 17.6 kb MfeI fragment that contained kan^R was reduced to 16.5 kb following recombination (Figure 28B). All four clones analyzed showed the expected change, completing the engineering JΔNI8G4NkeGFP BAC.

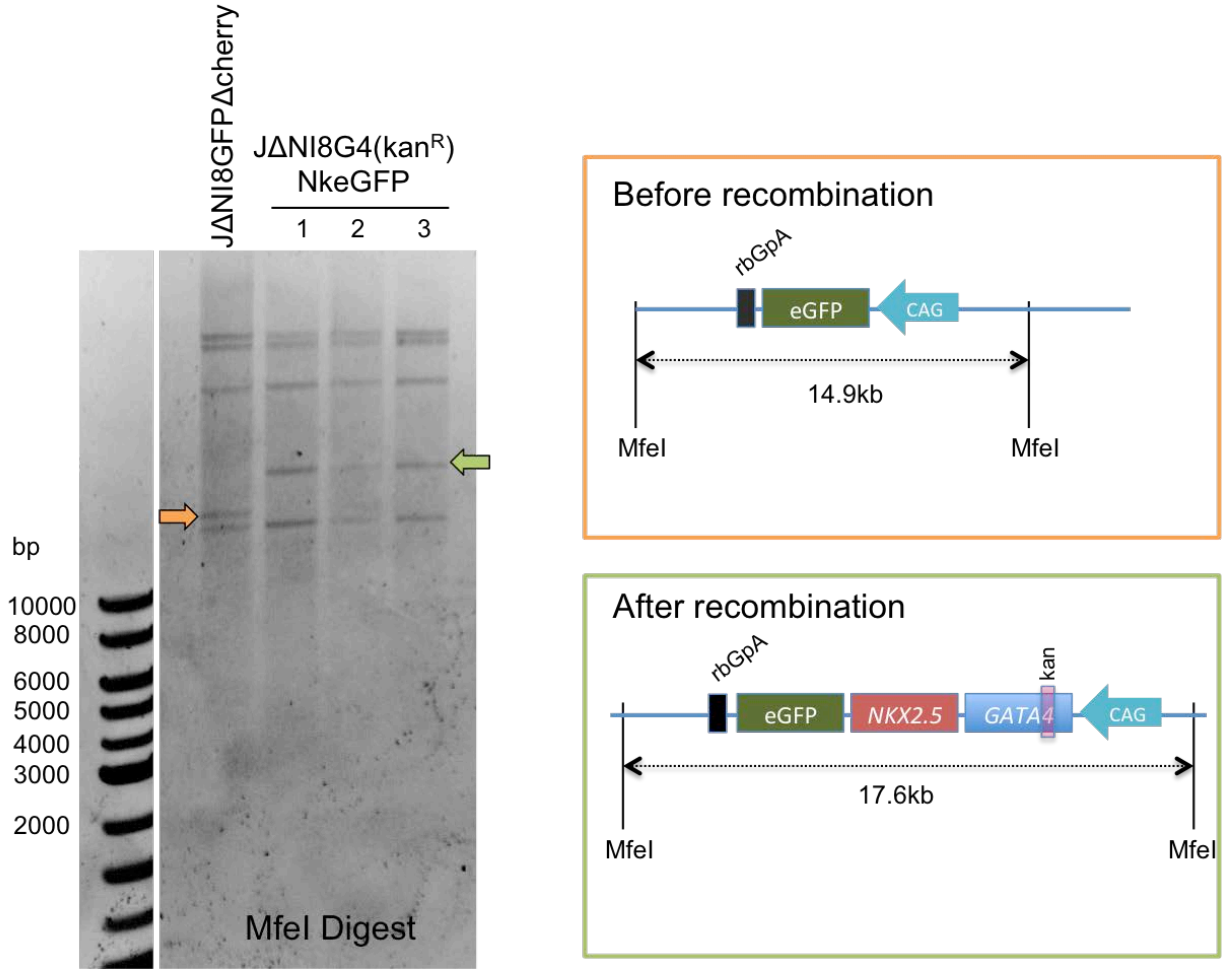

Figure 27. FIGE analysis of MfeI-digested candidate JΔNI8G4(kan^R)NkeGFP BAC isolates
The left panel shows the FIGE gel with arrows marking the fragments that change, before (orange) and after (green) recombination. The right panel shows a schematic of the area of recombination and the sizes of the expected fragments upon MfeI digestion.

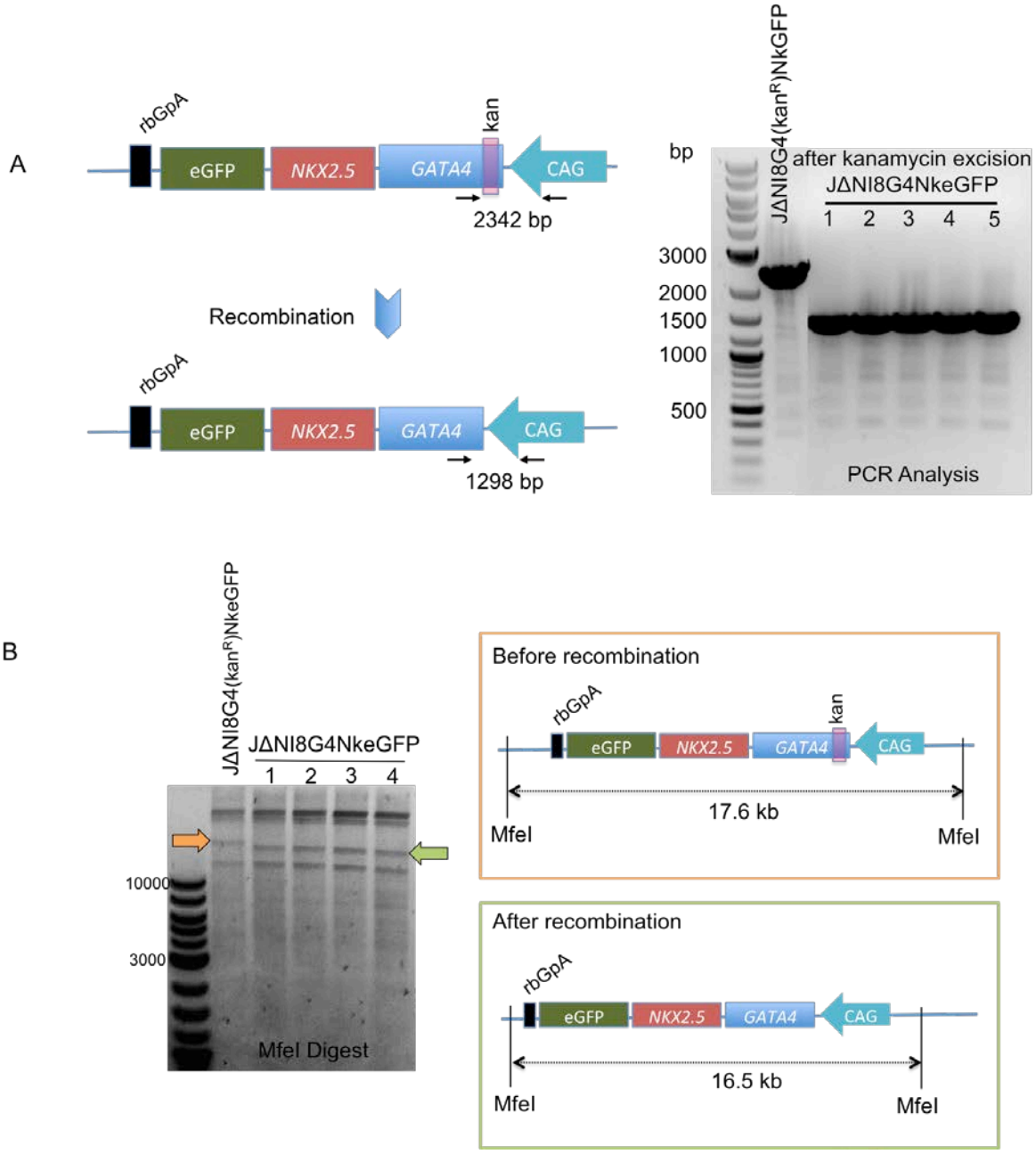

Figure 28. Removal of kan^R from JΔNI8G4(kan^R)NkeGFP
(A) PCR analysis of BAC DNA from 5 kan-sensitive bacterial colonies resulting from Red recombination to delete the kan gene from JΔNI8G4(kan^R)NkeGFP BAC DNA. The left panel shows a diagram of the transgene cassette in the LAT locus before and after recombination. The small black arrows indicate the location of the primers surrounding the deletion with the expected product length indicated underneath. The right panel shows the PCR products. (B) FIGE analysis of MfeI-digested BAC DNA. The right panel shows a diagram of the MfeI fragment that changes length upon recombination. The orange arrow on the FIGE gel in the left panel shows the fragment length before and the green arrow shows the fragment length after kan^R excision.

5.3.4 Construction of a JΔNI8GFPΔcherry BAC derivative for single promoter expression of GATA4, TBX5, and MEF2C

Procedures similar to those described in the previous section were used to generate a BAC construct for HSV-mediated production of the transdifferentiation cocktail *GATA4*, *TBX5* and *MEF2C* along with eGFP from a single transcript. The strategy was to replace the *NKX2.5* gene of JΔNI8G4NkeGFP BAC with 2A-linked *TBX5* and *MEF2C* cDNAs using the *GATA4* and eGFP portions of plasmid pGTMeGFP described in section 5.4.1 as homology arms for Red-mediated recombination.

In the first step, a unique Asp718 (KpnI) site inside the *MEF2C* coding sequence of pGTMeGFP was used to insert the kan^R/I-SceI selection cassette. The kan^R/I-SceI cassette was PCR amplified from pBAD-I-SceI with primers to add Asp718 sites and a 50 bp direct repeat of *MEF2C* coding sequence (Figure 29A). The Asp718-digested PCR product was cloned into the Asp718 site of pGTMeGFP; diagnostic restriction digests were used to identify the desired orientation of the insert and several candidates were confirmed by DNA sequencing. One of these [pGTM(kan^R)eGFP] was digested with PmeI and BamHI to produce a 5328 bp fragment for homology-directed recombination with JΔNI8G4NkeGFP BAC DNA (Figure 29B). The fragment was electroporated into bacteria containing JΔNI8G4NkeGFP BAC DNA and BAC recombinants were identified by selection for chloramphenicol and kanamycin resistance. Candidate BACs were isolated and confirmed by PCR and sequencing through the 5' and 3' recombination sites (data not shown) as well as by FIGE analysis of MfeI-digested BAC DNA [Figure 30, JΔNI8GTM(kan^R)eGFP #1, 4 and 5].

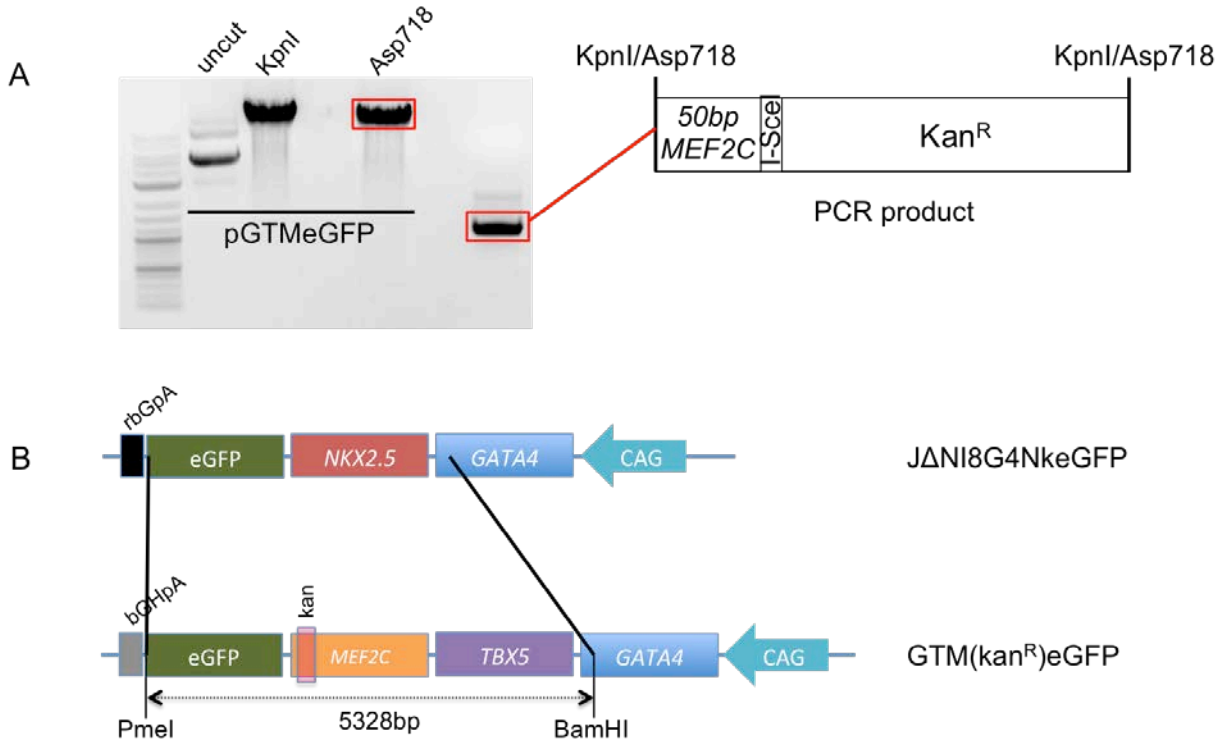

Figure 29. Scheme for introducing kan^R into pGTMeGFP and digestion for recombination
(A) Diagram and gel of PCR product for insertion of kan^R into KpnI/Asp718 site inside *MEF2C* and KpnI and Asp718 digests of pGTMeGFP. (B) Homologous sequences between GTM(kan^R)eGFP cassette and G4NkeGFP cassette in the LAT locus of JΔNI8G4NkeGFP BAC DNA for recombination.

The final product, JΔNI8GTMeGFP BAC, was generated by excision of the kan^R gene from JΔNI8GTM(kan^R)eGFP BAC DNA, essentially as described in the previous section. Kan^R excision was verified by PCR (Figure 31A), FIGE analysis (Figure 31B), and DNA sequencing. The structures of the completed JΔNI8G4NkeGFP and JΔNI8GTMeGFP BAC constructs are illustrated in Figure 32.

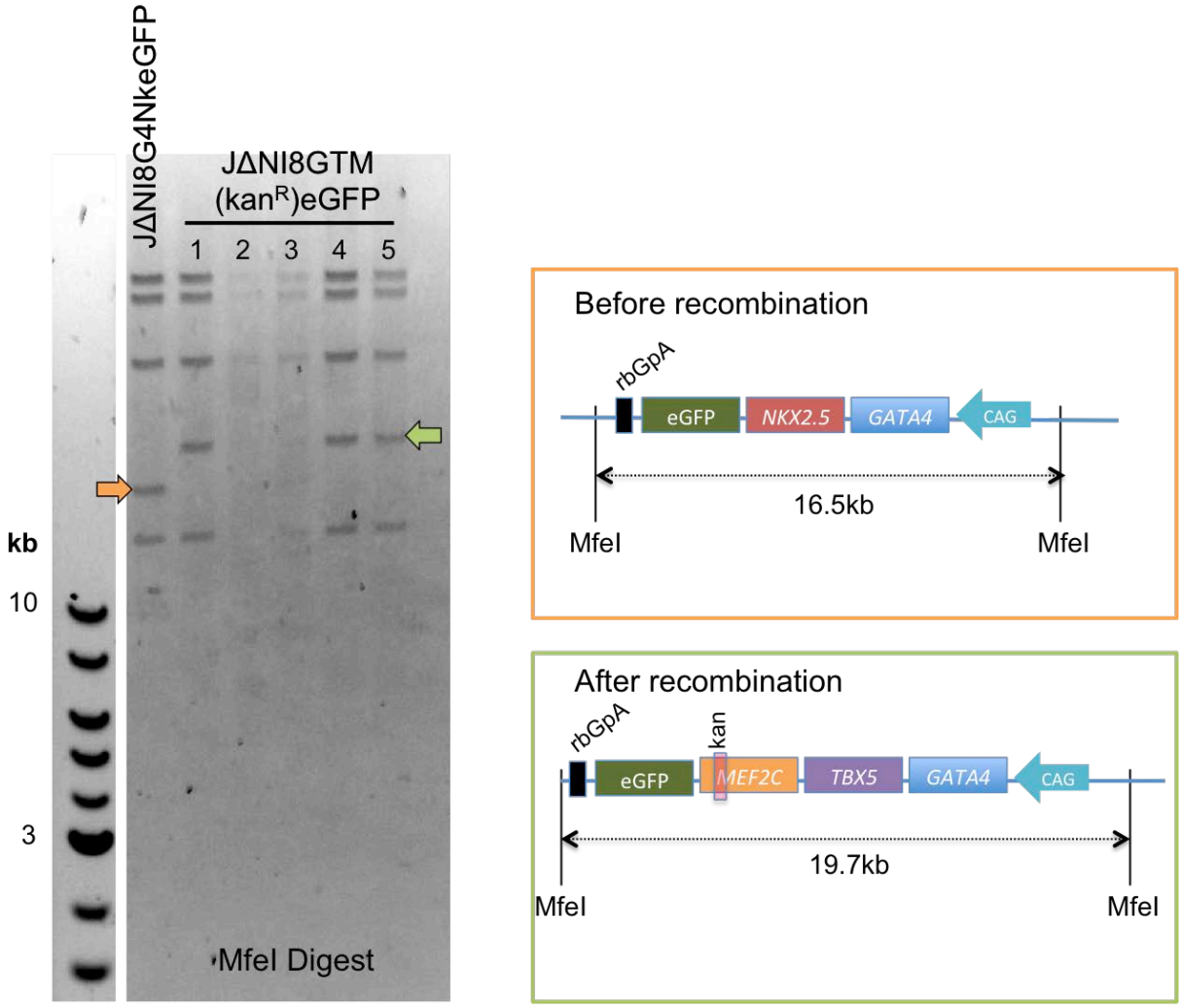

Figure 30. MfeI digest and FIGE analysis of JΔNI8GTM(kan^R)eGFP
The left panel shows the FIGE gel with arrows marking the fragments that change, before (orange) and after (green) recombination. The right panel shows a schematic of the area of recombination and the sizes of the expected fragments upon MfeI digestion.

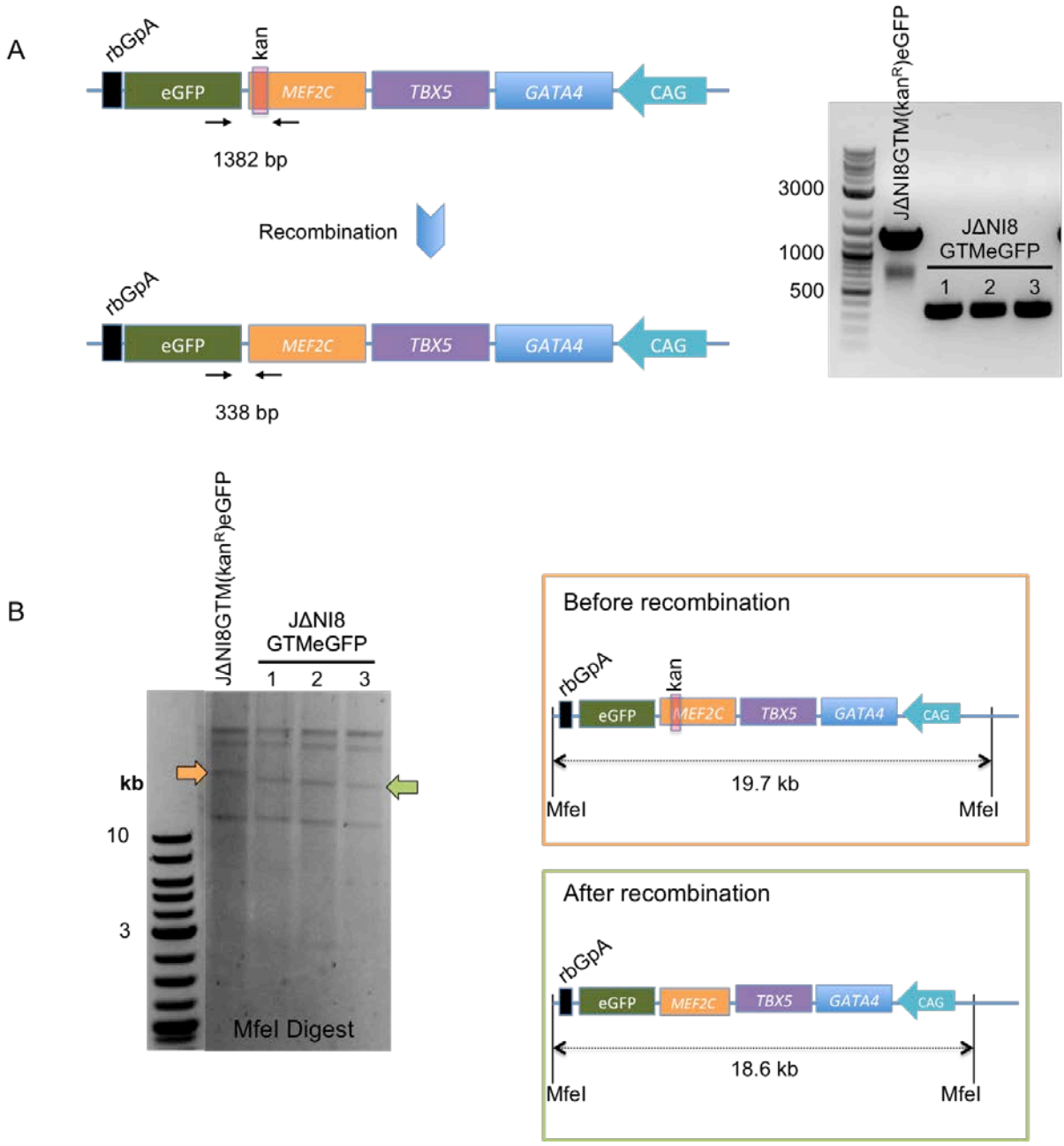

Figure 31. Removal of kan^R from JΔNI8GTM(kan^R)eGFP BAC DNA
(A) PCR analysis of 3 clones selected after kan^R excision from JΔNI8GTM(kan^R)eGFP BAC DNA. The left panel shows a diagram of the transgene cassette in the LAT locus before and after recombination. The small black arrows indicate the location of the primers surrounding the deletion with the expected product lengths shown underneath. The right panel shows the PCR products. (B) FIGE analysis of MfeI-digested BAC DNA. The right panel shows a diagram of the MfeI fragment that changes length upon recombination. The orange arrow on the FIGE gel in the left panel shows the relevant fragment length before and the green arrow shows the fragment length after kan^R excision.

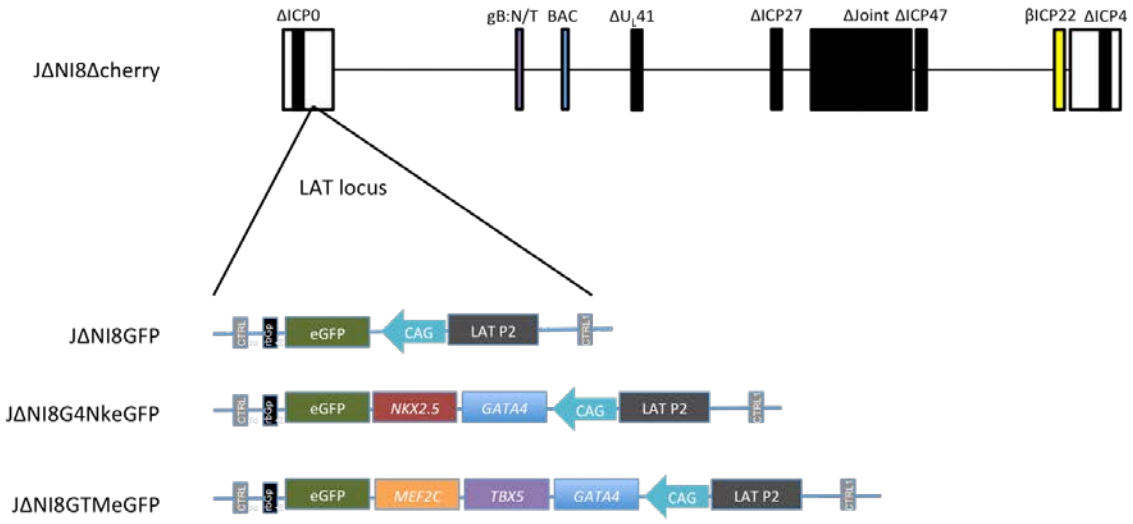

Figure 32. Structure of JΔNI8GFPΔcherry BAC and transgene expression cassettes engineered into the LAT locus
The HSV vector JΔNI8GFP genome is shown schematically with genes labeled at the approximate location in the vector (not to scale). Deletions are depicted in black and the single IE to E gene promoter substitution (β) in yellow (*169*). Transgenes are colored and labeled. The transgene cassettes shown below the vector diagram are located within the LAT 2-kb intron region between LAT elements LAT P2 and CTRL2. The relative position of LAT insulator CTRL1 is also indicated.

5.3.5 Characterization of vectors JΔNI8G4NkeGFP and JΔNI8GTMeGFP

JΔNI8GFPΔcherry, JΔNI8G4NkeGFP, and JΔNI8GTMeGFP BAC DNAs were converted to infectious viruses (vGFP, vG4Nk, and vGTM, respectively) by transfection into ICP4- and ICP27-complementing U2OS cells (U2OS-ICP4/27, (*169*)) that endogenously complement the ICP0 deletion (*225*). The success of the mCherry deletion was visualized by fluorescence microscopy. The parent vector JΔNI8GFP expressed both eGFP and mCherry upon transfection into U2OS-ICP4/27 cells while the mCherry-deleted JΔNI8GFPΔcherry (vGFP) expressed only

eGFP (Figure 33A). Vector production was scaled up to 10 – 20 T150 flasks of cells per vector. Following CPE, the viruses were harvested and concentrated by centrifugation to produce high-titer stocks. Plaque assays and qPCR were used to determine the plaque forming unit (pfu) and genome copy (gc) titers of all three vectors (Figure 33B). Expression of eGFP in non-complementing U2OS cells infected with each virus stock at 1 pfu/cell was readily detectable (Figure 33C).

A

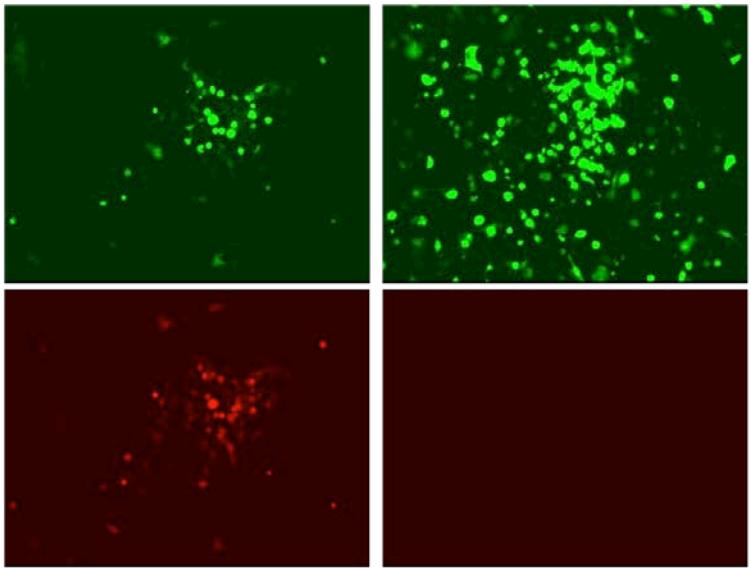

JΔNI8GFP JΔNI8GFPΔcherry

B

Virus	gc/ml	pfu/ml	gc/pfu
vGFP	1.75E+11	4.80E+08	3.64E+02
vG4Nk	2.19E+11	4.80E+08	4.56E+02
vGTM	2.07E+11	2.10E+08	9.84E+02

C

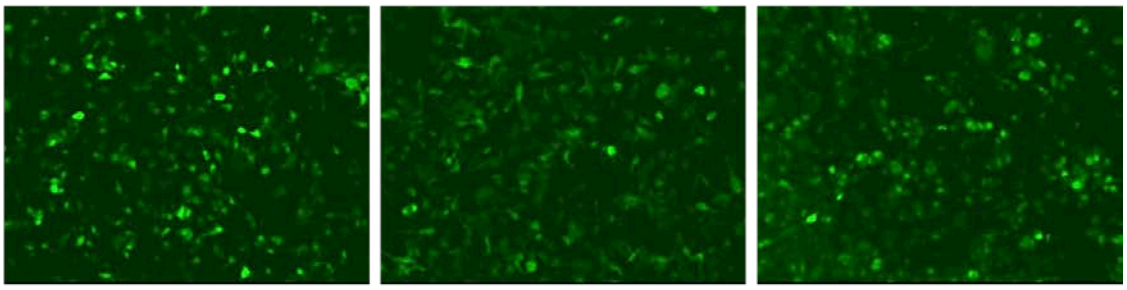

vGFP vG4Nk vGTM

Figure 33. Fluorescent marker expression and titers of JΔNI8 vectors
(A) JΔNI8eGFP and JΔNI8eGFPΔcherry BAC DNA were transfected into U2OS-ICP4/27 cells. Pictures were taken 5 d post transfection. (B) Genome copy (gc) and plaque forming unit (pfu) titers of JΔNI8 vectors. (C) eGFP expression 1 dpi in U2OS cells infected with vGFP, vG4Nk, or vGTM at 1 pfu/cell.

To verify that mESC transduced with vectors vG4Nk and vGTM expressed GATA4 and NKX2.5 or GATA4, TBX5, and MEF2C, respectively, mESC were infected with 1 pfu/cell of each vector. Mock-infected and vGFP-infected mESC were included as controls. Cell lysates were collected 24 hpi and separated by SDS-PAGE. Western blotting demonstrated that mESC infected with vG4Nk robustly expressed GATA4 and NKX2.5 proteins, while mock- and vGFP-infected mESC did not (Figure 34A). Similarly, mESC infected with vGTM robustly expressed GATA4, TBX5, and MEF2C proteins, while mock- and vGFP-infected mESC did not (Figure 34B).

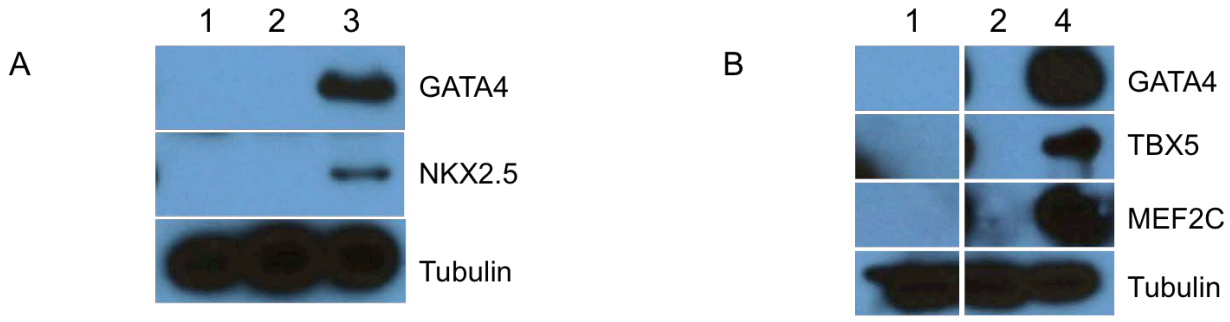

Figure 34. Transgenic protein expression from vG4Nk and vGTM
mESC were infected with 1 pfu/cell in suspension and proteins collected for Western blots 24 hpi. (A) Western blots for GATA4, NKX2.5, and beta tubulin. Lane 1, mock-infected mESC; lane 2, vGFP-infected mESC; lane 3, vG4Nk-infected mESC. (B) Western blots for GATA4, TBX5, MEF2C, and beta tubulin. Lane 1, mock-infected mESC; lane 2, vGFP-infected mESC; lane 4, vGTM-infected mESC.

5.3.6 Transduction of mESC with vG4Nk or vGTM induces cardiac gene expression

In order to examine gene expression changes resulting from transduction with the vG4Nk vector, mESC were mock infected or infected with vGFP or vG4Nk at 2 pfu/cell (roughly 800 gc/cell) for 1.5 h in suspension. Cells were plated in 6 well plates without LIF, and RNA was collected at 0, 24, 48, and 72 hpi and reverse transcribed for qRT-PCR, with mouse heart cDNA as a positive control for expression of mouse cardiac genes. Expression of transgenic (human) and endogenous (mouse) *GATA4* and *NKX2.5* was examined in vG4Nk-infected mESC compared to control vector vGFP-infected mESC. Strong expression of the two human transgenes was detected in vG4Nk-infected cells at 24 hpi. Transgene expression dropped off sharply between 24 and 48 hpi, although *GATA4* and *NKX2.5* transcripts remained detectable through 72 hpi. As expected, expression of the human transgenes was not detected from vGFP-infected mESC (Figure 35A). While expression of human *GATA4* fell dramatically after 24 h from vG4Nk-infected mESC, expression of endogenous *Gata4* increased from 24 h to at least 72 h post mESC infection with vG4Nk, but only barely from vGFP-infected mESC. There was a similar but smaller increase in expression of endogenous *Nkx2.5* from mESC infected with vG4Nk compared to mESC infected with the control vector (Figure 35B).

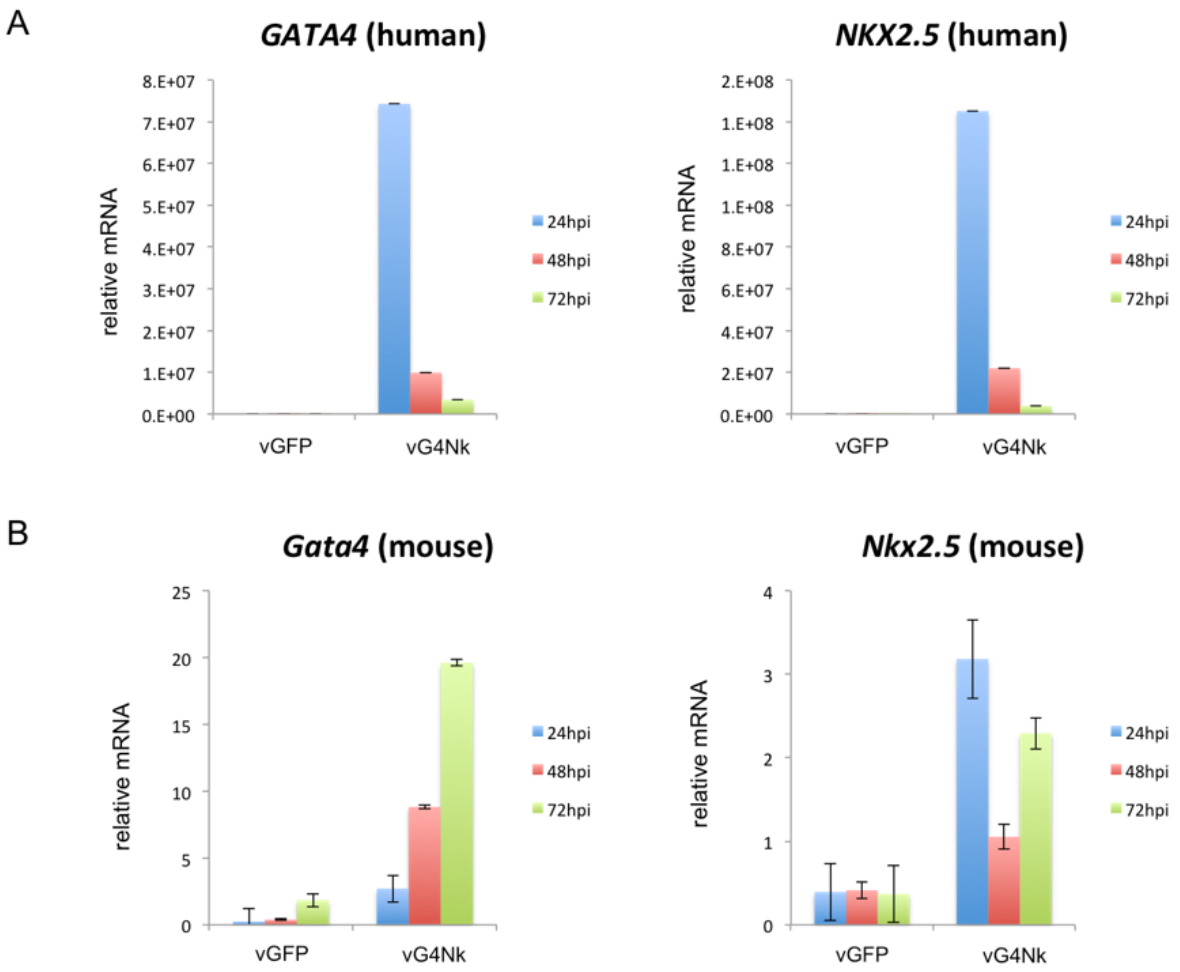

Figure 35. Expression of *GATA4* and *NKX2.5* in vGFP- and vG4Nk-infected mESC as determined by qRT-PCR

mESC were infected with either vGFP or vG4Nk, and qRT-PCR was used to examine expression of human (transgene) (A) and mouse (endogenous) (B) *GATA4* and *NKX2.5* 24, 48, and 72 hpi.

Next we used qRT-PCR to determine the expression levels of GATA4- and NKX2.5-responsive genes typically expressed early in the cardiac differentiation process (Table 1), *Tbx20*, *Gata6*, *Myocd*, and *Foxa2* (*136, 181*), from vG4Nk-infected mESC relative to vGFP- and mock-infected mESC. Of the 4 genes examined, *Gata6* and *Foxa2* showed the greatest response to transduction with vG4Nk. Both *Gata6* and *Foxa2* expression were greater at all three time points from vG4Nk-infected cells than vGFP- or mock-infected cells, and the levels of both transcripts increased continuously over the first 72 hpi (Figure 36). Expression of *Tbx20* was increased 5-fold from vG4Nk-infected mESC at 24 hpi compared to vGFP-infected mESC, and expression of *Myocd* was increased 10-fold. However at 3 dpi, expression of these two genes from the control cells had caught up with that from the experimental vector-infected cells (Figure 36). Together, these results suggested that vector-mediated GATA4 and Nkx2.5 expression increases the induction kinetics of early cardiac-related genes in mESC following LIF withdrawal.

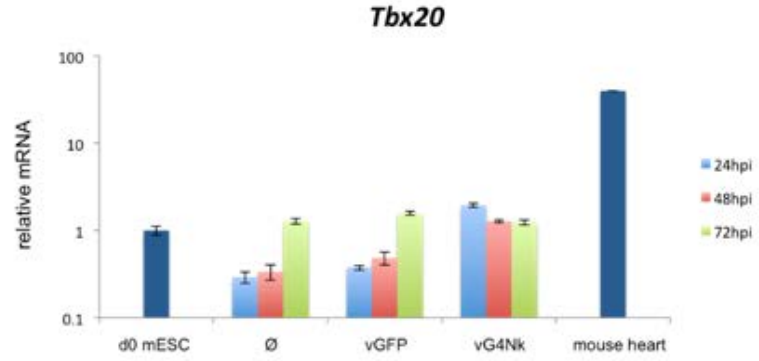
Tbx20
relative mRNA
100
10
1
0.1
d0 mESC
Ø
vGFP
vG4Nk
mouse heart
24hpi
48hpi
72hpi

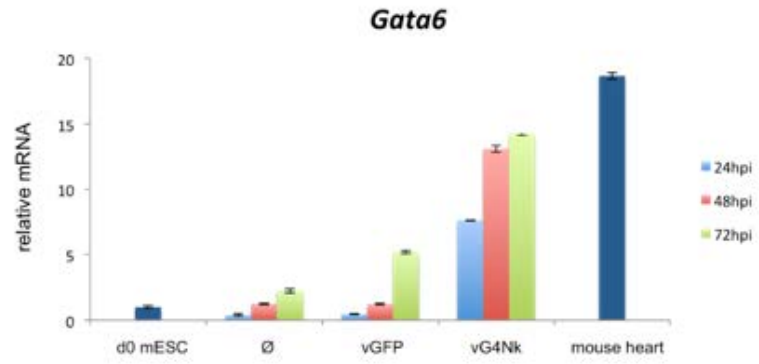
Gata6
relative mRNA
20
15
10
5
0
d0 mESC
Ø
vGFP
vG4Nk
mouse heart
24hpi
48hpi
72hpi

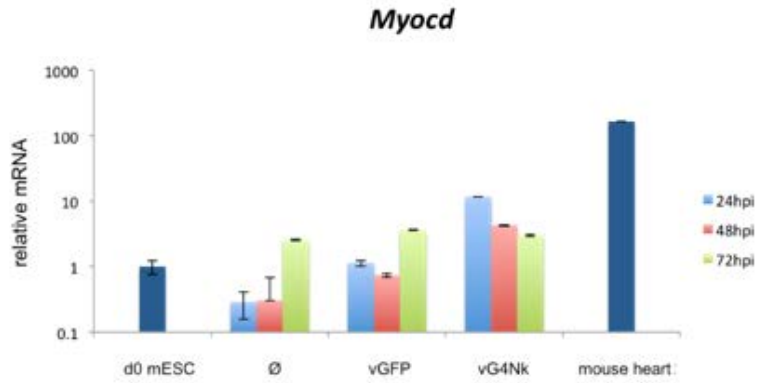
Myocd
relative mRNA
1000
100
10
1
0.1
d0 mESC
Ø
vGFP
vG4Nk
mouse heart
24hpi
48hpi
72hpi

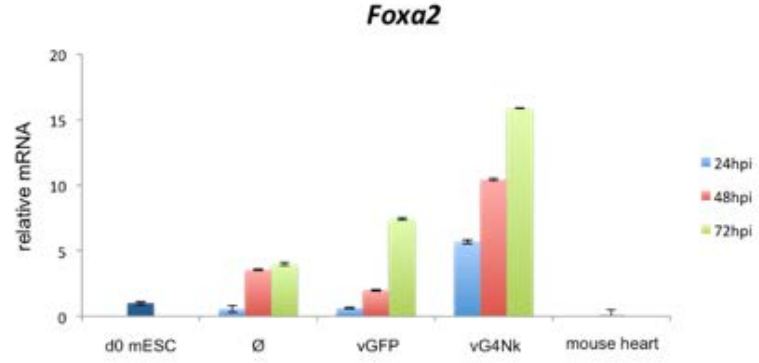
Foxa2
relative mRNA
20
15
10
5
0
d0 mESC
Ø
vGFP
vG4Nk
mouse heart
24hpi
48hpi
72hpi

Figure 36. Expression of GATA4- and NKX2.5-responsive genes in vG4Nk-infected mESC as determined by SYBR Green qRT-PCR
mESC were infected with vGFP, vG4Nk, or mock-infected. qRT-PCR was used to compare the expression of selected GATA4-responsive genes between the three conditions at 24, 48, and 72 hpi. mRNA levels were normalized to 18S rRNA and are expressed relative to day 0 uninfected mESC. Data for *Tbx20* and *Myocd* are displayed on a logarithmic scale while *Gata6* and *Foxa2* are displayed on a linear scale.

We next examined transgene expression and the expression of transgene-responsive endogenous genes in differentiating EB. mESC were infected in suspension with 2 pfu/cell of vGFP, vG4Nk or vGTM, or were mock infected, and the cells were dispensed into hanging drops for EB formation. RNA was collected 24, 48, and 72 hpi and reverse transcribed for qRT-PCR. Similarly to experiments described above, *GATA4* and *NKX2.5* transgenes were expressed robustly at 24 hpi in EB made from vG4Nk-infected mESC (vG4Nk EB), and their mRNAs could be detected for at least 72 h after the onset of differentiation. *GATA4* was expressed at similar levels in EB from vGTM-infected mESC (vGTM EB), and its expression also remained detectable for at least 72 h after infection and the start of differentiation (Figure 37A). Endogenous *Gata4* expression was upregulated for at least 48 hpi from vG4Nk EB, and for at least 72 hpi from vGTM EB compared to EB from mock- (Ø EB) or vGFP-infected mESC (vGFP EB). Interestingly, while endogenous *Nkx2.5* did not appear to be upregulated from vG4Nk EB, its expression from vGTM EB was higher at 72 hpi than at earlier times or from any of the other EB at 72 hpi. *Sox17*, a gene previously shown to be upregulated by GATA4 (*181*), was expressed at increasing levels over the first 72 hpi from both vGTM EB and vG4Nk EB, each greater than in Ø EB or vGFP EB. (Figure 37B).

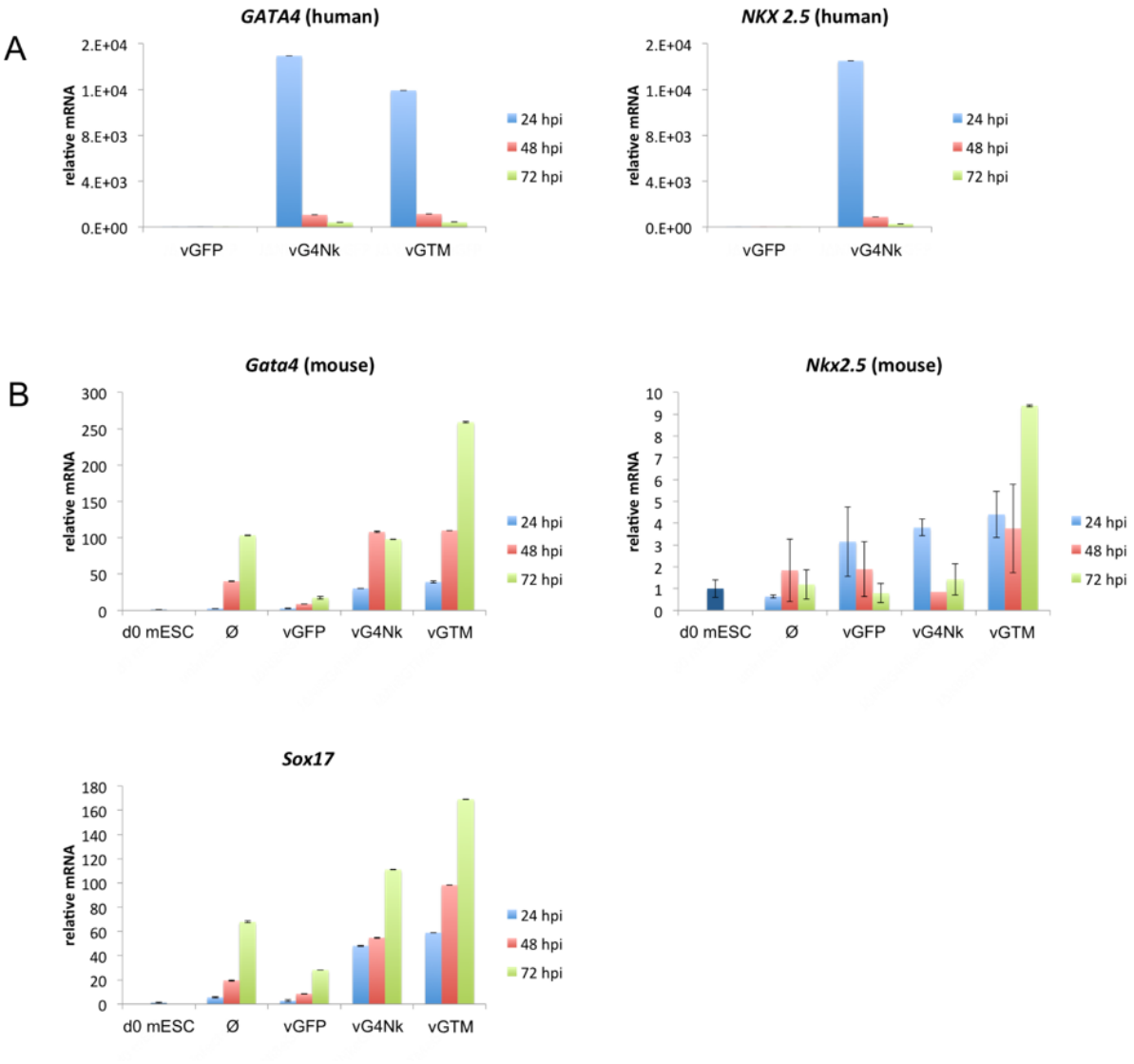

Figure 37. Expression of GATA4 and Nkx2.5 transgenes and endogenous genes in EB determined by TaqMan qRT-PCR

mESC were infected with vGFP, vG4Nk, vGTM or mock-infected. TaqMan qRT-PCR was used to examine expression of transgenes and endogenous genes from EB at 24, 48, and 72 hpi. mRNA levels were normalized to HPRT and are presented relative to the levels in vGFP EB at 24 hpi (A) or uninfected mESC (B). (A) Expression of human *GATA4* in vG4Nk EB or vGTM EB (*left*) and of human *NKX2.5* in vG4Nk EB. (B) Relative expression of endogenous cardiomyogenic genes *Gata4*, *Nkx2.5*, and *Sox17*.

Lastly we sought to examine the effects of transduction with vG4Nk and vGTM on gene expression in differentiating EB at later times post infection. mESC were infected with 3000 gc (~ 5 pfu)/cell of the three JΔNI8 vectors and differentiated by EB formation in hanging drops. RNA was extracted at 3 dpi for the first time point, and the remaining EB were plated in 48 well plates for attachment, outgrowth, further differentiation, and RNA extraction at 6 and 9 dpi. RNA was reverse transcribed and gene expression levels were determined by qRT-PCR. While human *GATA4* transgene RNA was detectable for at least 9 dpi from both vG4Nk EB and vGTM EB, upregulation of endogenous *Gata4* was only seen at 3 dpi. At later time points, endogenous *Gata4* levels were similar to those from Ø EB and vGFP EB. *Gata6* appeared to be slightly upregulated from d3 vG4Nk EB and vGTM EB, but expression levels from Ø EB vGFP EB were higher at both 6 and 9 dpi. Similarly, *Sox17*, *Foxa2*, and *Myo5b* were upregulated on day 3 from vG4Nk EB and vGTM EB, but by 6 dpi these genes were expressed at levels comparable to those from Ø EB and vGFP EB (Figure 38). Taken together, the results from these experiments suggested early but transient upregulation of endogenous cardiac genes by vector-mediated expression of human GATA4 and Nkx2.5. Experiments in the next section were performed to determine whether these early changes might influence the efficiency of cardiomyocyte terminal differentiation.

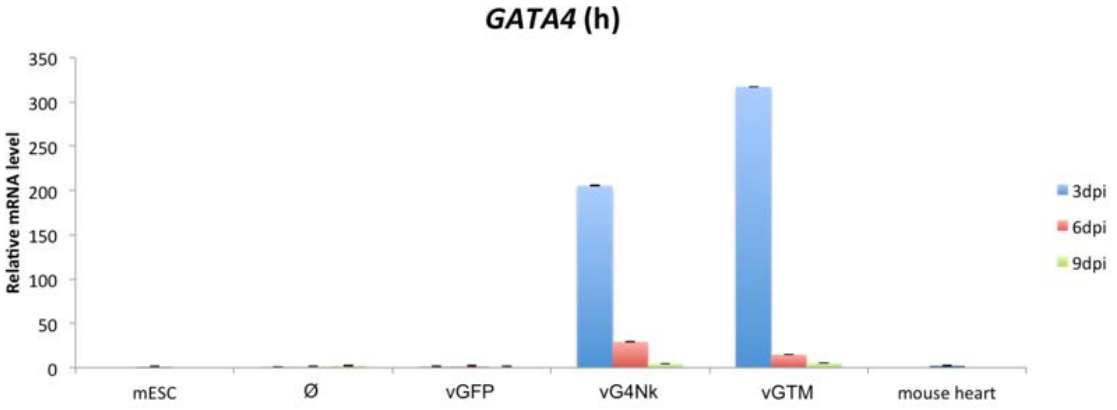
GATA4 (h)
Relative mRNA level
350
300
250
200
150
100
50
0
mESC
Ø
vGFP
vG4Nk
vGTM
mouse heart
3dpi
6dpi
9dpi

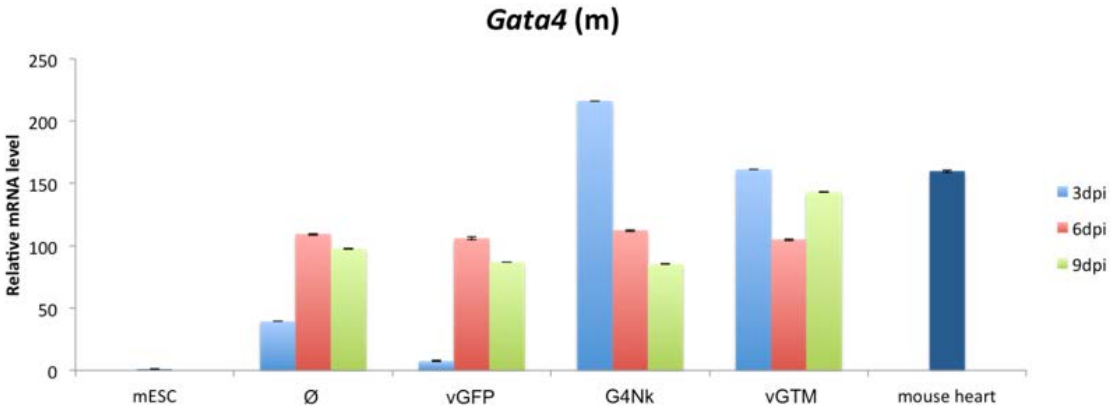
Gata4 (m)
Relative mRNA level
250
200
150
100
50
0
mESC
Ø
vGFP
G4Nk
vGTM
mouse heart
3dpi
6dpi
9dpi

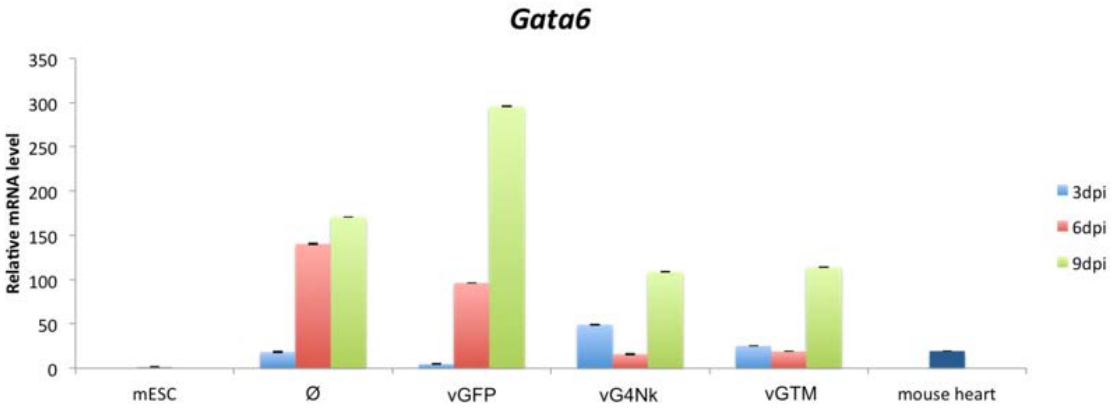
Gata6
Relative mRNA level
350
300
250
200
150
100
50
0
mESC
Ø
vGFP
vG4Nk
vGTM
mouse heart
3dpi
6dpi
9dpi

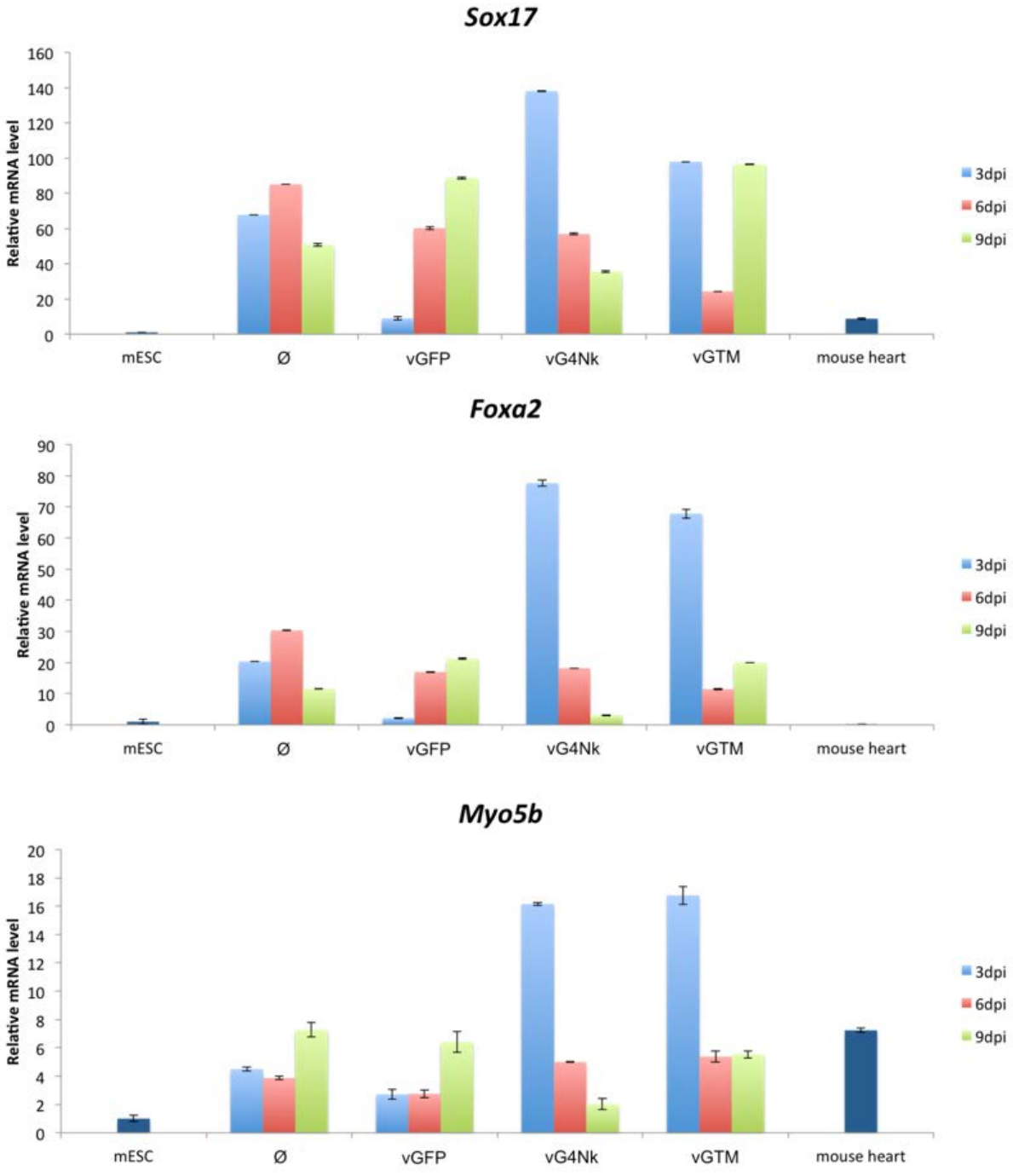

Figure 38. Longer term cardiac gene expression from infected mESC-derived EB
Gene expression at 3, 6, and 9 dpi in EB from mESC transduced with vGFP, vG4Nk, or vGTM, or uninfected mESC as determined by SYBRgreen qRT-PCR. Expression was normalized to 18S rRNA (human and mouse GATA4) or HPRT (Foxa2, GATA6, Myo5b, and Sox17) RNA, and is presented relative to uninfected, undifferentiated mESC.

5.3.7 Transduction of mESC with vG4Nk or vGTM prior to differentiation in combination with temporary inhibition of cell division increases the population of EB showing spontaneously contracting patches

To determine whether vG4Nk infection of mESC prior to the onset of differentiation could increase the percentage of EB with visibly contracting cardiomyocytes, mESC were infected with vGFP or vG4Nk at 2 pfu/cell, or mock-infected. As before, cells were aggregated in hanging drops immediately after infection for differentiation in EB. EB were plated at 3 dpi, one per well in 48 well plates for attachment and outgrowth. EB were examined daily for the appearance of spontaneously contracting cardiomyocytes. Visible cardiomyocytes first appeared 8 d past the onset of differentiation, and initially there was a greater percentage of contracting vG4Nk EB than Ø EB or vGFP EB. However, between days 8 and 10, the percentage of EB containing visible cardiomyocytes became equal between the three conditions (Figure 39A). This differentiation experiment was repeated several times with similar results (data not shown).

In order to prolong the persistence of viral genomes in differentiating EB, we explored the use of cytosine β-D-arabinofuranoside (Ara-C) to temporarily inhibit cell division and diminish the initial rate of HSV genome dilution. To determine the appropriate Ara-C concentration to delay cell division without toxicity, we treated cells with 0 – 10 μM Ara-C, replacing the media and counting cells in duplicate wells each day for 4 d. While 1 μM Ara-C appeared to be toxic to mESC, causing the number of cells to decrease from 0 to 4 d, cell division still occurred with 0.1 μM Ara-C (Figure 39B). We chose an intermediate concentration of 0.3 μM Ara-C for the next differentiation experiment.

A

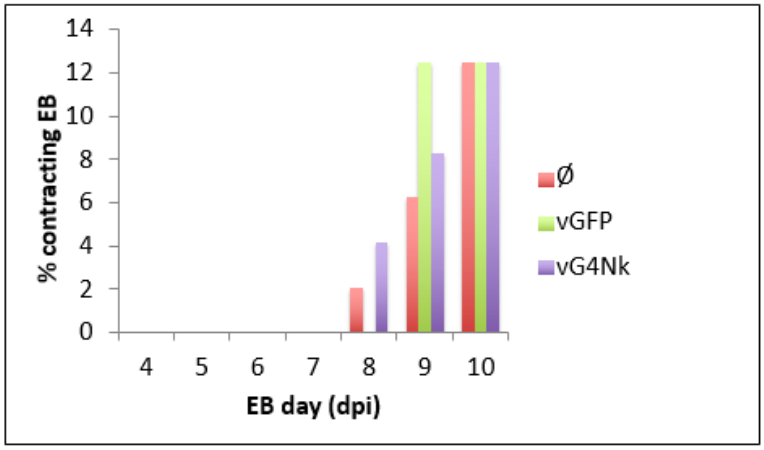

B

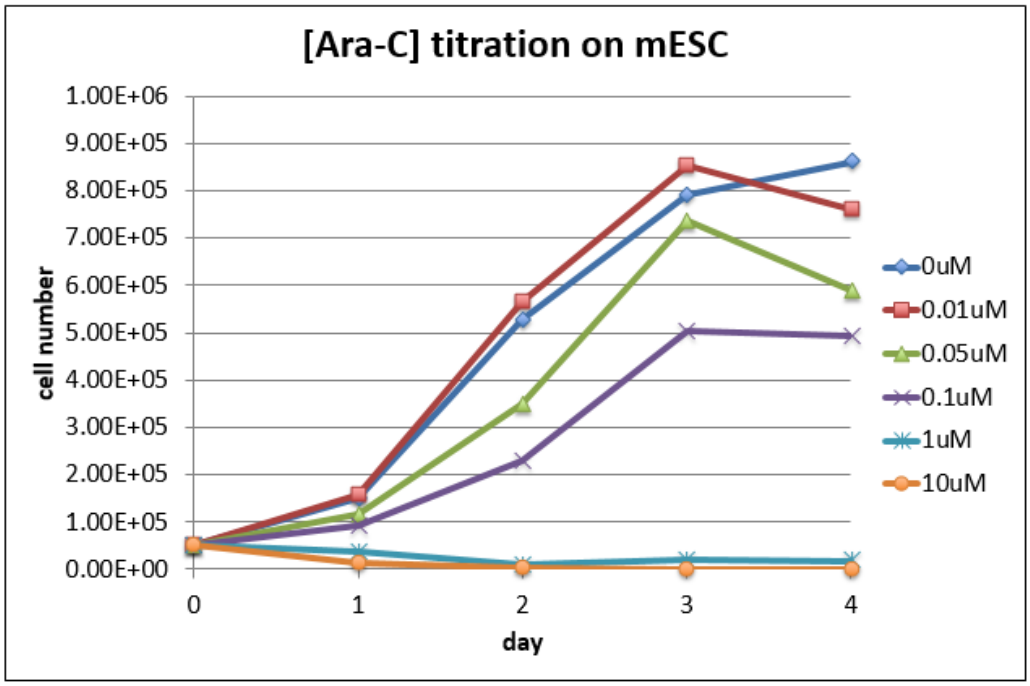

Figure 39. Cardiomyocyte appearance in vG4Nk EB and Ara-C titration on mESC
(A) mESC were infected with vGFP, vG4Nk, or mock, and EB were plated at 3 dpi. The percentage of spontaneously contracting EB was counted each day from 4 – 10 dpi. (B) Ara-C was titrated on mESC with concentrations from 0 – 10 μM and the number of cells was counted each day.

In the next differentiation experiment, we included vGTM to examine its ability to influence cardiomyocyte formation. mESC were infected in suspension with 2000 gc/cell of vGFP, vG4Nk, or vGTM, or were mock-infected. Cells were diluted in media containing 0.3 μM Ara-C and transferred into hanging drops to allow aggregation into EB. Because cell division was inhibited by Ara-C, 4000 cells were dispensed per 30 μl drop instead of the typical 800 cells/20 μl drop. EB were allowed to differentiate in hanging drops for three days, then plated one per well in 48 well plates for attachment and outgrowth. This experiment was repeated three times, and the results for each individual experiment can be seen in Figure 40A. Because of variability in the time to first appearance of visibly contracting cells between the three experiments, as well as differences in the percentages of contracting EB at each data point, the error surrounding the average value for the three experiments combined is high (data not shown). However there is a clear trend that spontaneously contracting cardiomyocytes appeared sooner in Ara-C-treated vG4Nk EB and especially with vGTM EB than in similarly treated Ø EB or vGFP EB. Moreover, the percentage of contracting EB was greater at almost every time point for vG4Nk EB or vGTM EB (Figure 40B). Taken together, these three experiments clearly indicated that infection of a small number of stem cells with vG4Nk or vGTM has long reaching effects on the mESC differentiation program even when the virus genomes have been drastically diluted as the cells divide over a period of 12 days.

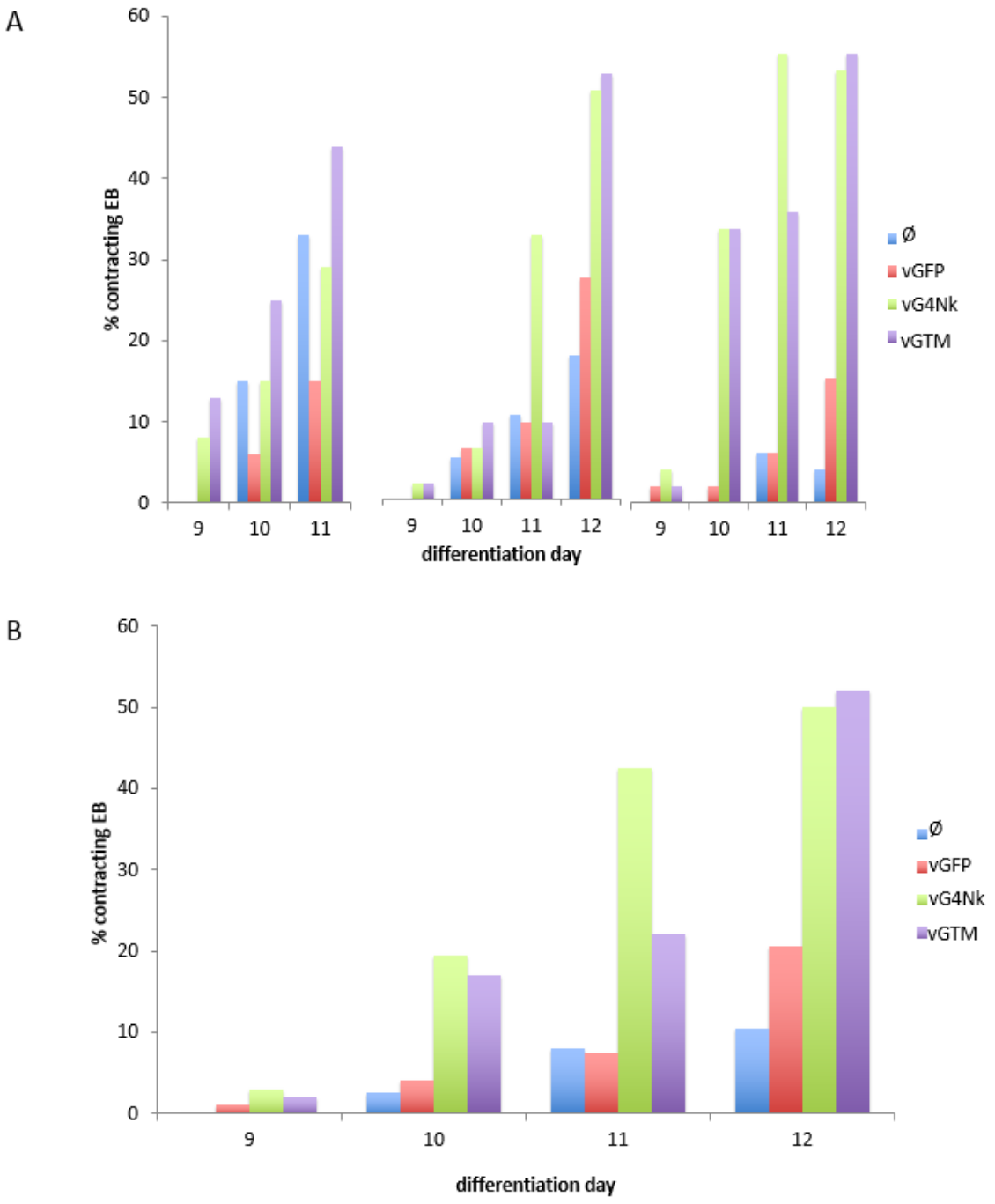

Figure 40. Contracting Ø, vGFP, vG4Nk, and vGTM EB with Ara-C treatment
mESC were infected with vGFP, vG4Nk, vGTM, or mock infected, and treated with 0.3 μM Ara-C for the first 48 h of differentiation in EB. (A) The results of three independent experiments (*left*, *center*, and *right*) showing the percentage of EB containing visible cardiomyocytes. (B) The averages of the independent experiments from (A).

5.4 DISCUSSION

In this chapter, we describe the engineering and use of two JΔNI8-based vectors to influence mESC to differentiate toward a cardiac cell fate. Two highly replication defective HSV vectors, vG4Nk and vGTM, were created through BAC recombineering to express polycistronic transgene cassettes of cardiac-specific transcription factors separated by 2A "ribosomal skipping" sequences. The JΔNI8 backbone contains numerous gene deletions, including ICP4, ICP27, ICP0, ICP47, U_L41, and the entire joint region of the HSV genome; the modified promoter of the remaining IE gene, ICP22, is inactive in the absence ICP4. Transgene cassettes were expressed from the LAT locus in both vG4Nk and vGTM. This region of the HSV genome contains LAP2, which can act as a long-term enhancer element for transgene expression (*173*). The LAT locus is also protected from viral genome silencing during latency by regions rich in CTCF binding sites called CTRLs. Unlike JDβββHE-based vectors, these JΔNI8-based vectors express no ICP0, and the transgenes are expressed from a protected locus, so they are able to efficiently transduce many cell types without detectable toxicity (*169*).

vG4Nk and vGTM are both capable of growing to high titers and efficiently transducing mESC. Both GATA4 and NKX2.5 proteins were detected in vG4Nk-infected D3 mESC by Western blotting. Likewise, GATA4, TBX5, and MEF2C were detected in vGTM-infected mESC by Western blotting. Expression of eGFP was clearly visible in both vG4Nk- and vGTM-transduced mESC and U2OS cells.

qRT-PCR experiments with species-specific primers and probes demonstrated that *GATA4* transgene expression from vG4Nk EB and vGTM EB could be detected for at least 9 dpi. Transduction of mESC with either of these two vectors induced the expression of endogenous genes that play a vital role in cardiogenesis, including *Gata4*, *Sox17*, *Foxa2*, and *Myo5b*, for at

least 3 dpi. While vG4Nk was more efficient than vGTM at inducing endogenous *Gata4* expression in transduced mESC, both vG4Nk and vGTM performed similarly to induce the expression of the other transgenes examined.

Initially, transduction of mESC with neither vG4Nk nor vGTM increased visible cardiomyocyte differentiation in EB. However, when Ara-C was used to inhibit cell division for 48 hpi, significantly more vG4Nk EB and vGTM EB contained spontaneously contracting patches of cardiomyocytes than Ø EB or vGFP EB. As with previous similar experiments, there was significant variability in the absolute percentages of EB with contracting cardiomyocytes between replicates. However, the trend remained consistent that between 4 – 6 times more vG4Nk EB and vGTM EB mESC contained visible cardiomyocytes than Ø EB or GFP EB.

The results in this chapter demonstrate that both vector vG4Nk and vector vGTM efficiently deliver transgenes for cardiac transcription factors to mESC at low MOI and with no overt toxicity. Expression of GATA4 and NKX2.5 or GATA4, TBX5, and MEF2C proteins from these vectors induced expression of target genes involved in cardiomyogenesis. Transduction of mESC with vG4Nk and vGTM followed by EB differentiation of transduced cells had a positive impact on cardiomyocyte differentiation for as long as 12 dpi. These promising results suggest a number of possible future directions. Microarray or RNA-Seq technology could be used to capture a snapshot of how transduction of stem cells with these vectors affects gene expression more globally. As discussed in section 4.5, differentiating mESC in EB has both advantages and disadvantages. EB provide a three dimensional structure that mimics a developing embryo and fosters cell-cell interactions that are important for certain developmental programs, but the generation of cytokines and other factors within the EB can make experimental interpretation and reproducibility difficult. We might want to explore alternative methods to differentiate

mESC that may be more amenable to cardiac development, for example differentiation in a monolayer or differentiation entirely in suspension. It would also be useful to examine expression of cardiac-specific proteins in differentiated cells using flow cytometry and/or immunofluorescence and confocal microscopy to gain a better understanding of the magnitude of the increase in cardiomyocyte differentiation achieved using vectors vG4Nk and vGTM. To this end we engineered a cardiac reporter cell line with the cardiac-specific α-MHC promoter driving expression of eGFP. The reporter construct functioned flawlessly at first, as evidenced by all contracting cells in EB displaying green fluorescence, but after several passages under continuous antibiotic selection, the cells lost their reporter function.

The cardiac transcription factors GATA4, TBX5, and MEF2C in vGTM were originally chosen because this combination was successfully used to transdifferentiate fibroblasts into cardiomyocytes both in vitro (*143*) and even more successfully in vivo (*144*). The in vivo work was completed in the mouse model of MI, and a combination of retroviruses encoding each transcription factor was injected directly into the infarcted area of the heart. Cardiac fibroblasts directly transdifferentiated into cardiomyocytes. Significant improvements in heart function and reduced scarring were observed. However, retroviruses integrate into host cell chromosomes with potential oncogenic effects stemming from insertional mutagenesis. Although beyond the scope of this current work, in vivo use of vGTM for MI repair has great potential without the concerns associated with the use of retroviruses.

6.0 SUMMARY AND CONCLUSIONS

Ischemic heart disease is one of the leading causes of morbidity and mortality worldwide(*22*). The mammalian heart lacks the ability to repair itself (*23*), and drug-based therapies cannot replace functional cardiac tissue. Cell-based therapy is viewed by many as the most promising approach to improve the prognosis of patients suffering from diseases of the heart. In this work, we sought to enrich the population of mature, beating cardiomyocytes derived from PSC in two distinct ways:

1. Creating a mESC line to constitutively overexpress GATA4
2. Using replication defective HSV vectors to deliver combinations of key cardiogenic transcription factors to mESC

GATA4 is a cardiac-specific transcription factor that is vital for cardiomyogenesis and cardiac function from the earliest days of embryonic development through adulthood (*13*). We described the generation of a mESC line to constitutively express high levels of the human GATA4 protein (D3G4). Nucleofection was used to stably transfect D3 mESC with a GATA4 cassette containing the puromycin resistance gene for selection. Multiple clonal lines were generated. One line expressed high levels of GATA4 protein and was dramatically enriched for cardiomyocyte differentiation compared to a control eGFP-expressing cell line. Expression of cardiac-specific genes *Gata4*, *Nkx2.5*, *cTnI*, and *Mlc2a* was increased by up to two orders of magnitude in d12 D3G4 EB compared to d12 eGFP EB. These data suggest that constitutive

GATA4 overexpression is a powerful driver of in vitro cardiac differentiation in mESC. However the use of a stably transfected cell line to overexpress GATA4 is not a clinically viable model for generating cardiomyocytes for transplant. The possibility of undesirable second-site effects and the increased oncogenic potential of cells with permanent chromosomal modifications make them unsafe for therapeutic cell-based treatments in humans.

Next we sought to determine if transient expression of *GATA4* in combination with additional cardiogenic genes *NKX2.5* or *TBX5* and *MEF2C* from non-integrating replication-defective HSV vectors could similarly push mESC toward a cardiac lineage. Cardiac vectors vββG4Nk, vG4Nk, and vGTM were each used to transduce mESC prior to differentiation. EB derived from cells transduced with these vectors demonstrated increased expression of endogenous genes vital for cardiomyogenesis and cardiac function over those transduced with control vectors. At different times post-infection, *Gata4, Nkx2.5, Foxa2, Gata6, Tbx20, Myocardin, Sox17, Mlc2a, Myo5b,* and *cTnI* expression were induced by cardiac vector transduction. Upregulation of several cardiac genes continued after transgene expression could no longer be detected. Transduction of mESC with each of the three cardiac HSV vectors, vββG4Nk, vG4Nk, and vGTM, increased the cardiac potential of the cells upon differentiation in EB. vββG4Nk, vG4Nk, and vGTM EB contained significantly more spontaneously beating cardiomyocytes than EB derived from mESC transduced with control vectors.

The overall findings of this dissertation research suggest that HSV vectors can be a useful tool for producing lineage related changes in differentiating pluripotent stem cells to generate specialized cell types. HSV vectors have many advantages over other gene delivery systems, including a large payload capacity, the ability to express transgenes in many different cell types, and, unlike retro- and lentiviral vectors, viral genomes remain episomal, mitigating concerns

over insertional mutagenesis. Moving forward, in vivo use of vGTM for reprogramming fibroblasts into cardiomyocytes in a study similar to that from Qian et al. would be an exciting next step (*144*). Achieving reprogramming through the use of non-integrating HSV vectors would provide a safe alternative to the original study, and represents a promising potential translational therapy for cardiac ischemia.

BIBLIOGRAPHY

1. G. Auda-Boucher *et al.*, Staging of the commitment of murine cardiac cell progenitors. *Developmental biology* **225**, 214 (Sep 1, 2000).

2. D. G. Wilkinson, S. Bhatt, B. G. Herrmann, Expression pattern of the mouse T gene and its role in mesoderm formation. *Nature* **343**, 657 (Feb 15, 1990).

3. M. Buckingham, S. Meilhac, S. Zaffran, Building the mammalian heart from two sources of myocardial cells. *Nature reviews. Genetics* **6**, 826 (Nov, 2005).

4. K. L. Waldo *et al.*, Conotruncal myocardium arises from a secondary heart field. *Development* **128**, 3179 (Aug, 2001).

5. M. L. Bakker, V. M. Christoffels, A. F. Moorman, The cardiac pacemaker and conduction system develops from embryonic myocardium that retains its primitive phenotype. *Journal of cardiovascular pharmacology* **56**, 6 (Jul, 2010).

6. C. C. Lu, E. J. Robertson, Multiple roles for Nodal in the epiblast of the mouse embryo in the establishment of anterior-posterior patterning. *Developmental biology* **273**, 149 (Sep 1, 2004).

7. T. Schlange, B. Andree, H. H. Arnold, T. Brand, BMP2 is required for early heart development during a distinct time period. *Mechanisms of development* **91**, 259 (Mar 1, 2000).

8. H. Zhang, A. Bradley, Mice deficient for BMP2 are nonviable and have defects in amnion/chorion and cardiac development. *Development* **122**, 2977 (Oct, 1996).

9. M. B. Furtado *et al.*, BMP/SMAD1 signaling sets a threshold for the left/right pathway in lateral plate mesoderm and limits availability of SMAD4. *Genes & development* **22**, 3037 (Nov 1, 2008).

10. K. L. Lee *et al.*, Graded Nodal/Activin signaling titrates conversion of quantitative phospho-Smad2 levels into qualitative embryonic stem cell fate decisions. *PLoS genetics* **7**, e1002130 (Jun, 2011).

11. Y. Liu *et al.*, Sox17 is essential for the specification of cardiac mesoderm in embryonic stem cells. *Proceedings of the National Academy of Sciences of the United States of America* **104**, 3859 (Mar 6, 2007).

12. A. C. Laverriere *et al.*, GATA-4/5/6, a subfamily of three transcription factors transcribed in developing heart and gut. *The Journal of biological chemistry* **269**, 23177 (Sep 16, 1994).

13. J. D. Molkentin, Q. Lin, S. A. Duncan, E. N. Olson, Requirement of the transcription factor GATA4 for heart tube formation and ventral morphogenesis. *Genes & development* **11**, 1061 (Apr 15, 1997).

14. R. J. Arceci, A. A. King, M. C. Simon, S. H. Orkin, D. B. Wilson, Mouse GATA-4: a retinoic acid-inducible GATA-binding transcription factor expressed in endodermally derived tissues and heart. *Molecular and cellular biology* **13**, 2235 (Apr, 1993).

15. C. O. Brown, 3rd *et al.*, The cardiac determination factor, Nkx2-5, is activated by mutual cofactors GATA-4 and Smad1/4 via a novel upstream enhancer. *The Journal of biological chemistry* **279**, 10659 (Mar 12, 2004).

16. Y. Saga *et al.*, MesP1 is expressed in the heart precursor cells and required for the formation of a single heart tube. *Development* **126**, 3437 (Aug, 1999).

17. T. M. Schultheiss, J. B. Burch, A. B. Lassar, A role for bone morphogenetic proteins in the induction of cardiac myogenesis. *Genes & development* **11**, 451 (Feb 15, 1997).

18. F. Reifers, E. C. Walsh, S. Leger, D. Y. Stainier, M. Brand, Induction and differentiation of the zebrafish heart requires fibroblast growth factor 8 (fgf8/acerebellar). *Development* **127**, 225 (Jan, 2000).

19. M. J. Marvin, G. Di Rocco, A. Gardiner, S. M. Bush, A. B. Lassar, Inhibition of Wnt activity induces heart formation from posterior mesoderm. *Genes & development* **15**, 316 (Feb 1, 2001).

20. E. Tzahor, Wnt/beta-catenin signaling and cardiogenesis: timing does matter. *Developmental cell* **13**, 10 (Jul, 2007).

21. C. L. Cai *et al.*, Isl1 identifies a cardiac progenitor population that proliferates prior to differentiation and contributes a majority of cells to the heart. *Developmental cell* **5**, 877 (Dec, 2003).

22. A. S. Go *et al.*, Heart disease and stroke statistics--2014 update: a report from the American Heart Association. *Circulation* **129**, e28 (Jan 21, 2014).

23. M. H. Soonpaa, L. J. Field, Assessment of cardiomyocyte DNA synthesis during hypertrophy in adult mice. *The American journal of physiology* **266**, H1439 (Apr, 1994).

24. C. L. Mummery *et al.*, Differentiation of human embryonic stem cells and induced pluripotent stem cells to cardiomyocytes: a methods overview. *Circulation research* **111**, 344 (Jul 20, 2012).

25. M. A. Pfeffer, E. Braunwald, Ventricular remodeling after myocardial infarction. Experimental observations and clinical implications. *Circulation* **81**, 1161 (Apr, 1990).

26. M. D. Flather *et al.*, Long-term ACE-inhibitor therapy in patients with heart failure or left-ventricular dysfunction: a systematic overview of data from individual patients. ACE-Inhibitor Myocardial Infarction Collaborative Group. *Lancet* **355**, 1575 (May 6, 2000).

27. D. M. Mancini *et al.*, Low incidence of myocardial recovery after left ventricular assist device implantation in patients with chronic heart failure. *Circulation* **98**, 2383 (Dec 1, 1998).

28. M. A. Laflamme *et al.*, Cardiomyocytes derived from human embryonic stem cells in pro-survival factors enhance function of infarcted rat hearts. *Nature biotechnology* **25**, 1015 (Sep, 2007).

29. L. W. van Laake, R. Passier, P. A. Doevendans, C. L. Mummery, Human embryonic stem cell-derived cardiomyocytes and cardiac repair in rodents. *Circulation research* **102**, 1008 (May 9, 2008).

30. C. E. Murry, R. W. Wiseman, S. M. Schwartz, S. D. Hauschka, Skeletal myoblast transplantation for repair of myocardial necrosis. *The Journal of clinical investigation* **98**, 2512 (Dec 1, 1996).

31. J. Leor, M. Patterson, M. J. Quinones, L. H. Kedes, R. A. Kloner, Transplantation of fetal myocardial tissue into the infarcted myocardium of rat. A potential method for repair of infarcted myocardium? *Circulation* **94**, II332 (Nov 1, 1996).

32. G. Ferrari *et al.*, Muscle regeneration by bone marrow-derived myogenic progenitors. *Science* **279**, 1528 (Mar 6, 1998).

33. C. R. Bjornson, R. L. Rietze, B. A. Reynolds, M. C. Magli, A. L. Vescovi, Turning brain into blood: a hematopoietic fate adopted by adult neural stem cells in vivo. *Science* **283**, 534 (Jan 22, 1999).

34. E. Gussoni *et al.*, Dystrophin expression in the mdx mouse restored by stem cell transplantation. *Nature* **401**, 390 (Sep 23, 1999).

35. E. Lagasse *et al.*, Purified hematopoietic stem cells can differentiate into hepatocytes in vivo. *Nature medicine* **6**, 1229 (Nov, 2000).

36. O. N. Koc, H. M. Lazarus, Mesenchymal stem cells: heading into the clinic. *Bone marrow transplantation* **27**, 235 (Feb, 2001).

37. S. Wakitani, T. Saito, A. I. Caplan, Myogenic cells derived from rat bone marrow mesenchymal stem cells exposed to 5-azacytidine. *Muscle & nerve* **18**, 1417 (Dec, 1995).

38. S. Rangappa, J. W. Entwistle, A. S. Wechsler, J. Y. Kresh, Cardiomyocyte-mediated contact programs human mesenchymal stem cells to express cardiogenic phenotype. *The Journal of thoracic and cardiovascular surgery* **126**, 124 (Jul, 2003).

39. X. Li *et al.*, Bone marrow mesenchymal stem cells differentiate into functional cardiac phenotypes by cardiac microenvironment. *Journal of molecular and cellular cardiology* **42**, 295 (Feb, 2007).

40. A. R. Muir, A. H. Kanji, D. Allbrook, The structure of the satellite cells in skeletal muscle. *Journal of anatomy* **99**, 435 (Jul, 1965).

41. A. Rochat, K. Kobayashi, Y. Barrandon, Location of stem cells of human hair follicles by clonal analysis. *Cell* **76**, 1063 (Mar 25, 1994).

42. G. Taylor, M. S. Lehrer, P. J. Jensen, T. T. Sun, R. M. Lavker, Involvement of follicular stem cells in forming not only the follicle but also the epidermis. *Cell* **102**, 451 (Aug 18, 2000).

43. M. Bjerknes, H. Cheng, Clonal analysis of mouse intestinal epithelial progenitors. *Gastroenterology* **116**, 7 (Jan, 1999).

44. K. D. Poss, L. G. Wilson, M. T. Keating, Heart regeneration in zebrafish. *Science* **298**, 2188 (Dec 13, 2002).

45. F. Quaini *et al.*, End-stage cardiac failure in humans is coupled with the induction of proliferating cell nuclear antigen and nuclear mitotic division in ventricular myocytes. *Circulation research* **75**, 1050 (Dec, 1994).

46. J. Kajstura *et al.*, Myocyte proliferation in end-stage cardiac failure in humans. *Proceedings of the National Academy of Sciences of the United States of America* **95**, 8801 (Jul 21, 1998).

47. O. Bergmann *et al.*, Evidence for cardiomyocyte renewal in humans. *Science* **324**, 98 (Apr 3, 2009).

48. J. Kajstura *et al.*, Cardiomyogenesis in the aging and failing human heart. *Circulation* **126**, 1869 (Oct 9, 2012).

49. M. H. Soonpaa, L. J. Field, Assessment of cardiomyocyte DNA synthesis in normal and injured adult mouse hearts. *The American journal of physiology* **272**, H220 (Jan, 1997).

50. M. Mollova *et al.*, Cardiomyocyte proliferation contributes to heart growth in young humans. *Proceedings of the National Academy of Sciences of the United States of America* **110**, 1446 (Jan 22, 2013).

51. A. P. Beltrami *et al.*, Adult cardiac stem cells are multipotent and support myocardial regeneration. *Cell* **114**, 763 (Sep 19, 2003).

52. J. Fransioli *et al.*, Evolution of the c-kit-positive cell response to pathological challenge in the myocardium. *Stem cells* **26**, 1315 (May, 2008).

53. H. Oh *et al.*, Cardiac progenitor cells from adult myocardium: homing, differentiation, and fusion after infarction. *Proceedings of the National Academy of Sciences of the United States of America* **100**, 12313 (Oct 14, 2003).

54. O. Pfister *et al.*, CD31- but Not CD31+ cardiac side population cells exhibit functional cardiomyogenic differentiation. *Circulation research* **97**, 52 (Jul 8, 2005).

55. D. Orlic *et al.*, Bone marrow cells regenerate infarcted myocardium. *Nature* **410**, 701 (Apr 5, 2001).

56. B. E. Strauer *et al.*, [Intracoronary, human autologous stem cell transplantation for myocardial regeneration following myocardial infarction]. *Deutsche medizinische Wochenschrift* **126**, 932 (Aug 24, 2001).

57. C. E. Murry *et al.*, Haematopoietic stem cells do not transdifferentiate into cardiac myocytes in myocardial infarcts. *Nature* **428**, 664 (Apr 8, 2004).

58. L. B. Balsam *et al.*, Haematopoietic stem cells adopt mature haematopoietic fates in ischaemic myocardium. *Nature* **428**, 668 (Apr 8, 2004).

59. A. Abdel-Latif *et al.*, Adult bone marrow-derived cells for cardiac repair: a systematic review and meta-analysis. *Archives of internal medicine* **167**, 989 (May 28, 2007).

60. E. Martin-Rendon *et al.*, Autologous bone marrow stem cells to treat acute myocardial infarction: a systematic review. *European heart journal* **29**, 1807 (Aug, 2008).

61. D. M. Clifford *et al.*, Long-term effects of autologous bone marrow stem cell treatment in acute myocardial infarction: factors that may influence outcomes. *PloS one* **7**, e37373 (2012).

62. J. G. Shake *et al.*, Mesenchymal stem cell implantation in a swine myocardial infarct model: engraftment and functional effects. *The Annals of thoracic surgery* **73**, 1919 (Jun, 2002).

63. K. H. Schuleri *et al.*, Autologous mesenchymal stem cells produce reverse remodelling in chronic ischaemic cardiomyopathy. *European heart journal* **30**, 2722 (Nov, 2009).

64. J. M. Hare *et al.*, A randomized, double-blind, placebo-controlled, dose-escalation study of intravenous adult human mesenchymal stem cells (prochymal) after acute myocardial infarction. *Journal of the American College of Cardiology* **54**, 2277 (Dec 8, 2009).

65. J. M. Hare *et al.*, Comparison of allogeneic vs autologous bone marrow-derived mesenchymal stem cells delivered by transendocardial injection in patients with ischemic cardiomyopathy: the POSEIDON randomized trial. *Jama* **308**, 2369 (Dec 12, 2012).

66. A. R. Williams *et al.*, Intramyocardial stem cell injection in patients with ischemic cardiomyopathy: functional recovery and reverse remodeling. *Circulation research* **108**, 792 (Apr 1, 2011).

67. V. Y. Suncion *et al.*, Does transendocardial injection of mesenchymal stem cells improve myocardial function locally or globally?: An analysis from the Percutaneous Stem Cell Injection Delivery Effects on Neomyogenesis (POSEIDON) randomized trial. *Circulation research* **114**, 1292 (Apr 11, 2014).

68. A. W. Heldman *et al.*, Transendocardial mesenchymal stem cells and mononuclear bone marrow cells for ischemic cardiomyopathy: the TAC-HFT randomized trial. *Jama* **311**, 62 (Jan 1, 2014).

69. V. Karantalis *et al.*, Autologous mesenchymal stem cells produce concordant improvements in regional function, tissue perfusion, and fibrotic burden when administered to patients undergoing coronary artery bypass grafting: The Prospective Randomized Study of Mesenchymal Stem Cell Therapy in Patients Undergoing Cardiac Surgery (PROMETHEUS) trial. *Circulation research* **114**, 1302 (Apr 11, 2014).

70. J. Bartunek *et al.*, Cardiopoietic stem cell therapy in heart failure: the C-CURE (Cardiopoietic stem Cell therapy in heart failURE) multicenter randomized trial with lineage-specified biologics. *Journal of the American College of Cardiology* **61**, 2329 (Jun 11, 2013).

71. A. R. Williams *et al.*, Enhanced effect of combining human cardiac stem cells and bone marrow mesenchymal stem cells to reduce infarct size and to restore cardiac function after myocardial infarction. *Circulation* **127**, 213 (Jan 15, 2013).

72. H. Li *et al.*, Paracrine factors released by GATA-4 overexpressed mesenchymal stem cells increase angiogenesis and cell survival. *American journal of physiology. Heart and circulatory physiology* **299**, H1772 (Dec, 2010).

73. C. E. Eckfeldt, E. M. Mendenhall, C. M. Verfaillie, The molecular repertoire of the 'almighty' stem cell. *Nature reviews. Molecular cell biology* **6**, 726 (Sep, 2005).

74. M. J. Evans, M. H. Kaufman, Establishment in culture of pluripotential cells from mouse embryos. *Nature* **292**, 154 (Jul 9, 1981).

75. G. R. Martin, Isolation of a pluripotent cell line from early mouse embryos cultured in medium conditioned by teratocarcinoma stem cells. *Proceedings of the National Academy of Sciences of the United States of America* **78**, 7634 (Dec, 1981).

76. J. A. Thomson *et al.*, Embryonic stem cell lines derived from human blastocysts. *Science* **282**, 1145 (Nov 6, 1998).

77. K. Takahashi, S. Yamanaka, Induction of pluripotent stem cells from mouse embryonic and adult fibroblast cultures by defined factors. *Cell* **126**, 663 (Aug 25, 2006).

78. N. Maherali *et al.*, Directly reprogrammed fibroblasts show global epigenetic remodeling and widespread tissue contribution. *Cell stem cell* **1**, 55 (Jun 7, 2007).

79. K. Okita, T. Ichisaka, S. Yamanaka, Generation of germline-competent induced pluripotent stem cells. *Nature* **448**, 313 (Jul 19, 2007).

80. M. Wernig *et al.*, In vitro reprogramming of fibroblasts into a pluripotent ES-cell-like state. *Nature* **448**, 318 (Jul 19, 2007).

81. K. Takahashi *et al.*, Induction of pluripotent stem cells from adult human fibroblasts by defined factors. *Cell* **131**, 861 (Nov 30, 2007).

82. T. Tanaka *et al.*, In vitro pharmacologic testing using human induced pluripotent stem cell-derived cardiomyocytes. *Biochemical and biophysical research communications* **385**, 497 (Aug 7, 2009).

83. W. Zhong *et al.*, Hypertrophic growth in cardiac myocytes is mediated by Myc through a Cyclin D2-dependent pathway. *The EMBO journal* **25**, 3869 (Aug 23, 2006).

84. M. Nakagawa *et al.*, Generation of induced pluripotent stem cells without Myc from mouse and human fibroblasts. *Nature biotechnology* **26**, 101 (Jan, 2008).

85. L. Cheng *et al.*, Low incidence of DNA sequence variation in human induced pluripotent stem cells generated by nonintegrating plasmid expression. *Cell stem cell* **10**, 337 (Mar 2, 2012).

86. M. Stadtfeld, M. Nagaya, J. Utikal, G. Weir, K. Hochedlinger, Induced pluripotent stem cells generated without viral integration. *Science* **322**, 945 (Nov 7, 2008).

87. L. Warren *et al.*, Highly efficient reprogramming to pluripotency and directed differentiation of human cells with synthetic modified mRNA. *Cell stem cell* **7**, 618 (Nov 5, 2010).

88. J. Yu *et al.*, Human induced pluripotent stem cells free of vector and transgene sequences. *Science* **324**, 797 (May 8, 2009).

89. M. Amit, J. Itskovitz-Eldor, Derivation and spontaneous differentiation of human embryonic stem cells. *Journal of anatomy* **200**, 225 (Mar, 2002).

90. N. Heins *et al.*, Derivation, characterization, and differentiation of human embryonic stem cells. *Stem cells* **22**, 367 (2004).

91. L. A. Boyer *et al.*, Core transcriptional regulatory circuitry in human embryonic stem cells. *Cell* **122**, 947 (Sep 23, 2005).

92. Y. H. Loh *et al.*, The Oct4 and Nanog transcription network regulates pluripotency in mouse embryonic stem cells. *Nature genetics* **38**, 431 (Apr, 2006).

93. J. Nichols *et al.*, Formation of pluripotent stem cells in the mammalian embryo depends on the POU transcription factor Oct4. *Cell* **95**, 379 (Oct 30, 1998).

94. M. Boiani *et al.*, Variable reprogramming of the pluripotent stem cell marker Oct4 in mouse clones: distinct developmental potentials in different culture environments. *Stem cells* **23**, 1089 (Sep, 2005).

95. J. L. Chew *et al.*, Reciprocal transcriptional regulation of Pou5f1 and Sox2 via the Oct4/Sox2 complex in embryonic stem cells. *Molecular and cellular biology* **25**, 6031 (Jul, 2005).

96. A. Watanabe, Y. Yamada, S. Yamanaka, Epigenetic regulation in pluripotent stem cells: a key to breaking the epigenetic barrier. *Philosophical transactions of the Royal Society of London. Series B, Biological sciences* **368**, 20120292 (Jan 5, 2013).

97. R. L. Williams *et al.*, Myeloid leukaemia inhibitory factor maintains the developmental potential of embryonic stem cells. *Nature* **336**, 684 (Dec 15, 1988).

98. S. Davis *et al.*, LIFR beta and gp130 as heterodimerizing signal transducers of the tripartite CNTF receptor. *Science* **260**, 1805 (Jun 18, 1993).

99. H. Niwa, T. Burdon, I. Chambers, A. Smith, Self-renewal of pluripotent embryonic stem cells is mediated via activation of STAT3. *Genes & development* **12**, 2048 (Jul 1, 1998).

100. Q. L. Ying, J. Nichols, I. Chambers, A. Smith, BMP induction of Id proteins suppresses differentiation and sustains embryonic stem cell self-renewal in collaboration with STAT3. *Cell* **115**, 281 (Oct 31, 2003).

101. V. Akopian *et al.*, Comparison of defined culture systems for feeder cell free propagation of human embryonic stem cells. *In vitro cellular & developmental biology. Animal* **46**, 247 (Apr, 2010).

102. M. Amit *et al.*, Clonally derived human embryonic stem cell lines maintain pluripotency and proliferative potential for prolonged periods of culture. *Developmental biology* **227**, 271 (Nov 15, 2000).

103. R. H. Xu *et al.*, BMP4 initiates human embryonic stem cell differentiation to trophoblast. *Nature biotechnology* **20**, 1261 (Dec, 2002).

104. R. H. Xu *et al.*, Basic FGF and suppression of BMP signaling sustain undifferentiated proliferation of human ES cells. *Nature methods* **2**, 185 (Mar, 2005).

105. K. E. Wagner, M. C. Vemuri, Serum-free and feeder-free culture expansion of human embryonic stem cells. *Methods in molecular biology* **584**, 109 (2010).

106. M. C. Vemuri, T. Schimmel, P. Colls, S. Munne, J. Cohen, Derivation of human embryonic stem cells in xeno-free conditions. *Methods in molecular biology* **407**, 1 (2007).

107. G. Chen *et al.*, Chemically defined conditions for human iPSC derivation and culture. *Nature methods* **8**, 424 (May, 2011).

108. A. Tomescot *et al.*, Differentiation in vivo of cardiac committed human embryonic stem cells in postmyocardial infarcted rats. *Stem cells* **25**, 2200 (Sep, 2007).

109. J. M. Lehman, Studies of teratomas in mice: possibilities for the future production of animal models. *The American journal of pathology* **101**, S33 (Dec, 1980).

110. J. Nussbaum *et al.*, Transplantation of undifferentiated murine embryonic stem cells in the heart: teratoma formation and immune response. *FASEB journal : official publication of the Federation of American Societies for Experimental Biology* **21**, 1345 (May, 2007).

111. T. J. Nelson *et al.*, Improved cardiac function in infarcted mice after treatment with pluripotent embryonic stem cells. *The anatomical record. Part A, Discoveries in molecular, cellular, and evolutionary biology* **288**, 1216 (Nov, 2006).

112. I. Kehat *et al.*, Human embryonic stem cells can differentiate into myocytes with structural and functional properties of cardiomyocytes. *The Journal of clinical investigation* **108**, 407 (Aug, 2001).

113. C. Mummery *et al.*, Cardiomyocyte differentiation of mouse and human embryonic stem cells. *Journal of anatomy* **200**, 233 (Mar, 2002).

114. C. Xu, S. Police, N. Rao, M. K. Carpenter, Characterization and enrichment of cardiomyocytes derived from human embryonic stem cells. *Circulation research* **91**, 501 (Sep 20, 2002).

115. C. Mummery *et al.*, Differentiation of human embryonic stem cells to cardiomyocytes: role of coculture with visceral endoderm-like cells. *Circulation* **107**, 2733 (Jun 3, 2003).

116. T. C. Doetschman, H. Eistetter, M. Katz, W. Schmidt, R. Kemler, The in vitro development of blastocyst-derived embryonic stem cell lines: formation of visceral yolk sac, blood islands and myocardium. *Journal of embryology and experimental morphology* **87**, 27 (Jun, 1985).

117. A. G. Smith, Embryo-derived stem cells: of mice and men. *Annual review of cell and developmental biology* **17**, 435 (2001).

118. A. G. Smith, M. L. Hooper, Buffalo rat liver cells produce a diffusible activity which inhibits the differentiation of murine embryonal carcinoma and embryonic stem cells. *Developmental biology* **121**, 1 (May, 1987).

119. V. Kouskoff, G. Lacaud, S. Schwantz, H. J. Fehling, G. Keller, Sequential development of hematopoietic and cardiac mesoderm during embryonic stem cell differentiation. *Proceedings of the National Academy of Sciences of the United States of America* **102**, 13170 (Sep 13, 2005).

120. U. Technau, Brachyury, the blastopore and the evolution of the mesoderm. *BioEssays : news and reviews in molecular, cellular and developmental biology* **23**, 788 (Sep, 2001).

121. T. Motoike, D. W. Markham, J. Rossant, T. N. Sato, Evidence for novel fate of Flk1+ progenitor: contribution to muscle lineage. *Genesis* **35**, 153 (Mar, 2003).

122. S. J. Kattman, T. L. Huber, G. M. Keller, Multipotent flk-1+ cardiovascular progenitor cells give rise to the cardiomyocyte, endothelial, and vascular smooth muscle lineages. *Developmental cell* **11**, 723 (Nov, 2006).

123. V. C. Chen, R. Stull, D. Joo, X. Cheng, G. Keller, Notch signaling respecifies the hemangioblast to a cardiac fate. *Nature biotechnology* **26**, 1169 (Oct, 2008).

124. T. J. Nelson *et al.*, CXCR4+/FLK-1+ biomarkers select a cardiopoietic lineage from embryonic stem cells. *Stem cells* **26**, 1464 (Jun, 2008).

125. Y. Chen *et al.*, Vascular endothelial growth factor promotes cardiomyocyte differentiation of embryonic stem cells. *American journal of physiology. Heart and circulatory physiology* **291**, H1653 (Oct, 2006).

126. S. Yuasa *et al.*, Transient inhibition of BMP signaling by Noggin induces cardiomyocyte differentiation of mouse embryonic stem cells. *Nature biotechnology* **23**, 607 (May, 2005).

127. J. Hao *et al.*, Dorsomorphin, a selective small molecule inhibitor of BMP signaling, promotes cardiomyogenesis in embryonic stem cells. *PloS one* **3**, e2904 (2008).

128. P. B. Yu *et al.*, Dorsomorphin inhibits BMP signals required for embryogenesis and iron metabolism. *Nature chemical biology* **4**, 33 (Jan, 2008).

129. A. Ao, J. Hao, C. R. Hopkins, C. C. Hong, DMH1, a novel BMP small molecule inhibitor, increases cardiomyocyte progenitors and promotes cardiac differentiation in mouse embryonic stem cells. *PloS one* **7**, e41627 (2012).

130. C. Mauritz *et al.*, Generation of functional murine cardiac myocytes from induced pluripotent stem cells. *Circulation* **118**, 507 (Jul 29, 2008).

131. A. Martinez-Fernandez *et al.*, iPS programmed without c-MYC yield proficient cardiogenesis for functional heart chimerism. *Circulation research* **105**, 648 (Sep 25, 2009).

132. A. M. Craft *et al.*, Herpes simplex virus-mediated expression of Pax3 and MyoD in embryoid bodies results in lineage-Related alterations in gene expression profiles. *Stem cells* **26**, 3119 (Dec, 2008).

133. F. Charron, M. Nemer, GATA transcription factors and cardiac development. *Seminars in cell & developmental biology* **10**, 85 (Feb, 1999).

134. L. Zhou, Y. Liu, L. Lu, X. Lu, R. A. Dixon, Cardiac gene activation analysis in mammalian non-myoblasic cells by Nkx2-5, Tbx5, Gata4 and Myocd. *PloS one* **7**, e48028 (2012).

135. M. S. Parmacek, Myocardin-related transcription factors: critical coactivators regulating cardiovascular development and adaptation. *Circulation research* **100**, 633 (Mar 16, 2007).

136. H. Akazawa, I. Komuro, Cardiac transcription factor Csx/Nkx2-5: Its role in cardiac development and diseases. *Pharmacology & therapeutics* **107**, 252 (Aug, 2005).

137. J. Huang *et al.*, Myocardin is required for cardiomyocyte survival and maintenance of heart function. *Proceedings of the National Academy of Sciences of the United States of America* **106**, 18734 (Nov 3, 2009).

138. R. K. Patient, J. D. McGhee, The GATA family (vertebrates and invertebrates). *Current opinion in genetics & development* **12**, 416 (Aug, 2002).

139. F. A. Stennard, R. P. Harvey, T-box transcription factors and their roles in regulatory hierarchies in the developing heart. *Development* **132**, 4897 (Nov, 2005).

140. D. Wang *et al.*, Activation of cardiac gene expression by myocardin, a transcriptional cofactor for serum response factor. *Cell* **105**, 851 (Jun 29, 2001).

141. Y. Lee *et al.*, The cardiac tissue-restricted homeobox protein Csx/Nkx2.5 physically associates with the zinc finger protein GATA4 and cooperatively activates atrial natriuretic factor gene expression. *Molecular and cellular biology* **18**, 3120 (Jun, 1998).

142. Y. Yamada, K. Sakurada, Y. Takeda, S. Gojo, A. Umezawa, Single-cell-derived mesenchymal stem cells overexpressing Csx/Nkx2.5 and GATA4 undergo the stochastic cardiomyogenic fate and behave like transient amplifying cells. *Experimental cell research* **313**, 698 (Feb 15, 2007).

143. M. Ieda *et al.*, Direct reprogramming of fibroblasts into functional cardiomyocytes by defined factors. *Cell* **142**, 375 (Aug 6, 2010).

144. L. Qian *et al.*, In vivo reprogramming of murine cardiac fibroblasts into induced cardiomyocytes. *Nature* **485**, 593 (May 31, 2012).

145. K. Song *et al.*, Heart repair by reprogramming non-myocytes with cardiac transcription factors. *Nature* **485**, 599 (May 31, 2012).

146. J. X. Chen *et al.*, Inefficient reprogramming of fibroblasts into cardiomyocytes using Gata4, Mef2c, and Tbx5. *Circulation research* **111**, 50 (Jun 22, 2012).

147. R. C. Addis, J. A. Epstein, Induced regeneration--the progress and promise of direct reprogramming for heart repair. *Nature medicine* **19**, 829 (Jul, 2013).

148. C. Ménard *et al.*, Transplantation of cardiac-committed mouse embryonic stem cells to infarcted sheep myocardium: a preclinical study. *The Lancet* **366**, 1005 (2005).

149. M. A. Laflamme *et al.*, Formation of human myocardium in the rat heart from human embryonic stem cells. *The American journal of pathology* **167**, 663 (Sep, 2005).

150. I. Kehat *et al.*, Electromechanical integration of cardiomyocytes derived from human embryonic stem cells. *Nature biotechnology* **22**, 1282 (Oct, 2004).

151. T. Xue *et al.*, Functional integration of electrically active cardiac derivatives from genetically engineered human embryonic stem cells with quiescent recipient ventricular cardiomyocytes: insights into the development of cell-based pacemakers. *Circulation* **111**, 11 (Jan 4, 2005).

152. E. Kolossov *et al.*, Engraftment of engineered ES cell-derived cardiomyocytes but not BM cells restores contractile function to the infarcted myocardium. *The Journal of experimental medicine* **203**, 2315 (Oct 2, 2006).

153. J. Y. Min *et al.*, Transplantation of embryonic stem cells improves cardiac function in postinfarcted rats. *Journal of applied physiology* **92**, 288 (Jan, 2002).

154. J. J. Chong *et al.*, Human embryonic-stem-cell-derived cardiomyocytes regenerate non-human primate hearts. *Nature* **510**, 273 (Jun 12, 2014).

155. P. A. Lalit, D. J. Hei, A. N. Raval, T. J. Kamp, Induced pluripotent stem cells for post-myocardial infarction repair: remarkable opportunities and challenges. *Circulation research* **114**, 1328 (Apr 11, 2014).

156. C. Tang *et al.*, An antibody against SSEA-5 glycan on human pluripotent stem cells enables removal of teratoma-forming cells. *Nature biotechnology* **29**, 829 (Sep, 2011).

157. Y. C. Wang *et al.*, Specific lectin biomarkers for isolation of human pluripotent stem cells identified through array-based glycomic analysis. *Cell research* **21**, 1551 (Nov, 2011).

158. Y. Farouz, Y. Chen, A. Terzic, P. Menasche, Growing hearts in the right place: on the design of biomimetic materials for cardiac stem cell differentiation. *Stem cells*, (Dec 24, 2014).

159. J. P. Vallee *et al.*, Embryonic stem cell-based cardiopatches improve cardiac function in infarcted rats. *Stem cells translational medicine* **1**, 248 (Mar, 2012).

160. R. W. H. a. B. Roizman, Regulation of Herpesvirus Macromolecular Synthesis I. Cascade Regulation of the Synthesis of Three Groups of Viral Proteins. *Journal of Virology* **14**, 8 (1974).

161. M. E. Campbell, J. W. Palfreyman, C. M. Preston, Identification of herpes simplex virus DNA sequences which encode a trans-acting polypeptide responsible for stimulation of immediate early transcription. *Journal of molecular biology* **180**, 1 (Nov 25, 1984).

162. R. J. Watson, J. B. Clements, A herpes simplex virus type 1 function continuously required for early and late virus RNA synthesis. *Nature* **285**, 329 (May 29, 1980).

163. R. D. Everett, Trans activation of transcription by herpes virus products: requirement for two HSV-1 immediate-early polypeptides for maximum activity. *The EMBO journal* **3**, 3135 (Dec 20, 1984).

164. P. Marconi *et al.*, Replication-defective herpes simplex virus vectors for gene transfer in vivo. *Proceedings of the National Academy of Sciences of the United States of America* **93**, 11319 (Oct 15, 1996).

165. P. A. Johnson, A. Miyanohara, F. Levine, T. Cahill, T. Friedmann, Cytotoxicity of a replication-defective mutant of herpes simplex virus type 1. *J Virol* **66**, 2952 (May, 1992).

166. N. Wu, S. C. Watkins, P. A. Schaffer, N. A. DeLuca, Prolonged gene expression and cell survival after infection by a herpes simplex virus mutant defective in the immediate-early genes encoding ICP4, ICP27, and ICP22. *J Virol* **70**, 6358 (Sep, 1996).

167. L. A. Samaniego, L. Neiderhiser, N. A. DeLuca, Persistence and expression of the herpes simplex virus genome in the absence of immediate-early proteins. *J Virol* **72**, 3307 (Apr, 1998).

168. J. Chen, S. Silverstein, Herpes simplex viruses with mutations in the gene encoding ICP0 are defective in gene expression. *J Virol* **66**, 2916 (May, 1992).

169. Y. Miyagawa *et al.*, Herpes simplex viral vector design for efficient transduction of non-neuronal cells without cytotoxicity. *Proceedings of the National Academy of Sciences of the United States of America*, (Mar 16, 2015).

170. D. M. Krisky *et al.*, Deletion of multiple immediate-early genes from herpes simplex virus reduces cytotoxicity and permits long-term gene expression in neurons. *Gene therapy* **5**, 1593 (Dec, 1998).

171. J. R. Smiley, M. M. Elgadi, H. A. Saffran, Herpes simplex virus vhs protein. *Methods in enzymology* **342**, 440 (2001).

172. L. A. Samaniego, N. Wu, N. A. DeLuca, The herpes simplex virus immediate-early protein ICP0 affects transcription from the viral genome and infected-cell survival in the absence of ICP4 and ICP27. *J Virol* **71**, 4614 (Jun, 1997).

173. W. F. Goins *et al.*, A novel latency-active promoter is contained within the herpes simplex virus type 1 UL flanking repeats. *J Virol* **68**, 2239 (Apr, 1994).

174. J. C. Zwaagstra, H. Ghiasi, A. B. Nesburn, S. L. Wechsler, Identification of a major regulatory sequence in the latency associated transcript (LAT) promoter of herpes simplex virus type 1 (HSV-1). *Virology* **182**, 287 (May, 1991).

175. J. A. Palmer *et al.*, Development and optimization of herpes simplex virus vectors for multiple long-term gene delivery to the peripheral nervous system. *J Virol* **74**, 5604 (Jun, 2000).

176. D. C. Bloom, N. V. Giordani, D. L. Kwiatkowski, Epigenetic regulation of latent HSV-1 gene expression. *Biochimica et biophysica acta* **1799**, 246 (Mar-Apr, 2010).

177. W. Rosamond *et al.*, Heart disease and stroke statistics--2008 update: a report from the American Heart Association Statistics Committee and Stroke Statistics Subcommittee. *Circulation* **117**, e25 (Jan 29, 2008).

178. J. L. Jefferies *et al.*, Genetic predictors and remodeling of dilated cardiomyopathy in muscular dystrophy. *Circulation* **112**, 2799 (Nov 1, 2005).

179. J. C. Moore *et al.*, Human embryonic stem cells: genetic manipulation on the way to cardiac cell therapies. *Reproductive toxicology* **20**, 377 (Sep-Oct, 2005).

180. L. Howard *et al.*, Profiling of transcriptional and epigenetic changes during directed endothelial differentiation of human embryonic stem cells identifies FOXA2 as a marker of early mesoderm commitment. *Stem cell research & therapy* **4**, 36 (2013).

181. M. Oda *et al.*, DNA methylation restricts lineage-specific functions of transcription factor Gata4 during embryonic stem cell differentiation. *PLoS genetics* **9**, e1003574 (Jun, 2013).

182. C. S. Chao *et al.*, Novel GATA6 Mutations in Patients with Pancreatic Agenesis and Congenital Heart Malformations. *PloS one* **10**, e0118449 (2015).

183. J. H. van Berlo, B. J. Aronow, J. D. Molkentin, Parsing the roles of the transcription factors GATA-4 and GATA-6 in the adult cardiac hypertrophic response. *PloS one* **8**, e84591 (2013).

184. J. D. Molkentin *et al.*, Direct activation of a GATA6 cardiac enhancer by Nkx2.5: evidence for a reinforcing regulatory network of Nkx2.5 and GATA transcription factors in the developing heart. *Developmental biology* **217**, 301 (Jan 15, 2000).

185. C. L. Cai *et al.*, T-box genes coordinate regional rates of proliferation and regional specification during cardiogenesis. *Development* **132**, 2475 (May, 2005).

186. M. K. Singh *et al.*, Tbx20 is essential for cardiac chamber differentiation and repression of Tbx2. *Development* **132**, 2697 (Jun, 2005).

187. F. A. Stennard *et al.*, Murine T-box transcription factor Tbx20 acts as a repressor during heart development, and is essential for adult heart integrity, function and adaptation. *Development* **132**, 2451 (May, 2005).

188. E. E. Creemers, L. B. Sutherland, J. McAnally, J. A. Richardson, E. N. Olson, Myocardin is a direct transcriptional target of Mef2, Tead and Foxo proteins during cardiovascular development. *Development* **133**, 4245 (Nov, 2006).

189. S. Pfister *et al.*, Sox17-dependent gene expression and early heart and gut development in Sox17-deficient mouse embryos. *The International journal of developmental biology* **55**, 45 (2011).

190. S. W. Kubalak, W. C. Miller-Hance, T. X. O'Brien, E. Dyson, K. R. Chien, Chamber specification of atrial myosin light chain-2 expression precedes septation during murine cardiogenesis. *The Journal of biological chemistry* **269**, 16961 (Jun 17, 1994).

191. S. M. Schumacher-Bass *et al.*, Role for myosin-V motor proteins in the selective delivery of Kv channel isoforms to the membrane surface of cardiac myocytes. *Circulation research* **114**, 982 (Mar 14, 2014).

192. A. Kimura *et al.*, Mutations in the cardiac troponin I gene associated with hypertrophic cardiomyopathy. *Nature genetics* **16**, 379 (Aug, 1997).

193. T. Fujiwara *et al.*, Discovering hematopoietic mechanisms through genome-wide analysis of GATA factor chromatin occupancy. *Molecular cell* **36**, 667 (Nov 25, 2009).

194. P. E. Pertel, A. Fridberg, M. L. Parish, P. G. Spear, Cell fusion induced by herpes simplex virus glycoproteins gB, gD, and gH-gL requires a gD receptor but not necessarily heparan sulfate. *Virology* **279**, 313 (Jan 5, 2001).

195. K. J. Livak, T. D. Schmittgen, Analysis of relative gene expression data using real-time quantitative PCR and the 2(-Delta Delta C(T)) Method. *Methods* **25**, 402 (Dec, 2001).

196. M. X. Zhu, J. Y. Zhao, G. A. Chen, L. Guan, Early embryonic sensitivity to cyclophosphamide in cardiac differentiation from human embryonic stem cells. *Cell biology international* **35**, 927 (Sep, 2011).

197. K. H. So *et al.*, Generation of functional cardiomyocytes from mouse induced pluripotent stem cells. *International journal of cardiology* **153**, 277 (Dec 15, 2011).

198. U. Lakshmipathy *et al.*, Efficient transfection of embryonic and adult stem cells. *Stem cells* **22**, 531 (2004).

199. J. K. Yamashita *et al.*, Prospective identification of cardiac progenitors by a novel single cell-based cardiomyocyte induction. *FASEB journal : official publication of the Federation of American Societies for Experimental Biology* **19**, 1534 (Sep, 2005).

200. R. Anton, H. A. Kestler, M. Kuhl, Beta-catenin signaling contributes to stemness and regulates early differentiation in murine embryonic stem cells. *FEBS letters* **581**, 5247 (Nov 13, 2007).

201. B. Greber *et al.*, Conserved and divergent roles of FGF signaling in mouse epiblast stem cells and human embryonic stem cells. *Cell stem cell* **6**, 215 (Mar 5, 2010).

202. A. Untergasser *et al.*, Primer3--new capabilities and interfaces. *Nucleic acids research* **40**, e115 (Aug, 2012).

203. P. Van Vliet, S. M. Wu, S. Zaffran, M. Puceat, Early cardiac development: a view from stem cells to embryos. *Cardiovascular research* **96**, 352 (Dec 1, 2012).

204. D. M. Tompers, P. A. Labosky, Electroporation of murine embryonic stem cells: a step-by-step guide. *Stem cells* **22**, 243 (2004).

205. P. Lorenz, U. Harnack, R. Morgenstern, Efficient gene transfer into murine embryonic stem cells by nucleofection. *Biotechnology letters* **26**, 1589 (Oct, 2004).

206. Y. Kosaka *et al.*, Lentivirus-based gene delivery in mouse embryonic stem cells. *Artificial organs* **28**, 271 (Mar, 2004).

207. S. R. Cherry, D. Biniszkiewicz, L. van Parijs, D. Baltimore, R. Jaenisch, Retroviral expression in embryonic stem cells and hematopoietic stem cells. *Molecular and cellular biology* **20**, 7419 (Oct, 2000).

208. K. Kawabata, F. Sakurai, N. Koizumi, T. Hayakawa, H. Mizuguchi, Adenovirus vector-mediated gene transfer into stem cells. *Molecular pharmaceutics* **3**, 95 (Mar-Apr, 2006).

209. A. Srivastava, Adeno-associated virus-mediated gene transfer. *Journal of cellular biochemistry* **105**, 17 (Sep 1, 2008).

210. D. M. Krisky *et al.*, Rapid method for construction of recombinant HSV gene transfer vectors. *Gene therapy* **4**, 1120 (Oct, 1997).

211. M. D. Ryan, J. Drew, Foot-and-mouth disease virus 2A oligopeptide mediated cleavage of an artificial polyprotein. *The EMBO journal* **13**, 928 (Feb 15, 1994).

212. M. L. Donnelly *et al.*, Analysis of the aphthovirus 2A/2B polyprotein 'cleavage' mechanism indicates not a proteolytic reaction, but a novel translational effect: a putative ribosomal 'skip'. *The Journal of general virology* **82**, 1013 (May, 2001).

213. W. F. Goins *et al.*, Generation of replication-competent and -defective HSV vectors. *Cold Spring Harbor protocols* **2011**, pdb prot5615 (May, 2011).

214. W. W. Gierasch *et al.*, Construction and characterization of bacterial artificial chromosomes containing HSV-1 strains 17 and KOS. *Journal of virological methods* **135**, 197 (Aug, 2006).

215. H. Uchida *et al.*, A double mutation in glycoprotein gB compensates for ineffective gD-dependent initiation of herpes simplex virus type 1 infection. *J Virol* **84**, 12200 (Dec, 2010).

216. V. Garg *et al.*, GATA4 mutations cause human congenital heart defects and reveal an interaction with TBX5. *Nature* **424**, 443 (Jul 24, 2003).

217. S. Morin, F. Charron, L. Robitaille, M. Nemer, GATA-dependent recruitment of MEF2 proteins to target promoters. *The EMBO journal* **19**, 2046 (May 2, 2000).

218. S. Protze *et al.*, A new approach to transcription factor screening for reprogramming of fibroblasts to cardiomyocyte-like cells. *Journal of molecular and cellular cardiology* **53**, 323 (Sep, 2012).

219. P. Sze, R. C. Herman, The herpes simplex virus type 1 ICP6 gene is regulated by a 'leaky' early promoter. *Virus research* **26**, 141 (Nov, 1992).

220. B. K. Tischer, J. von Einem, B. Kaufer, N. Osterrieder, Two-step red-mediated recombination for versatile high-efficiency markerless DNA manipulation in Escherichia coli. *BioTechniques* **40**, 191 (Feb, 2006).

221. B. K. Tischer, G. A. Smith, N. Osterrieder, En passant mutagenesis: a two step markerless red recombination system. *Methods in molecular biology* **634**, 421 (2010).

222. L. Mazzacurati *et al.*, Use of miRNA Response Sequences to Block Off-target Replication and Increase the Safety of an Unattenuated, Glioblastoma-targeted Oncolytic HSV. *Molecular therapy : the journal of the American Society of Gene Therapy* **23**, 99 (Jan, 2015).

223. H. Uchida *et al.*, Effective treatment of an orthotopic xenograft model of human glioblastoma using an EGFR-retargeted oncolytic herpes simplex virus. *Molecular therapy : the journal of the American Society of Gene Therapy* **21**, 561 (Mar, 2013).

224. M. Tsvitov *et al.*, Characterization of soluble glycoprotein D-mediated herpes simplex virus type 1 infection. *Virology* **360**, 477 (Apr 10, 2007).

225. F. Yao, P. A. Schaffer, An activity specified by the osteosarcoma line U2OS can substitute functionally for ICP0, a major regulatory protein of herpes simplex virus type 1. *J Virol* **69**, 6249 (Oct, 1995).